Development of an Analytical Method for the Detection and Quantitation of Nitrite as a Biomarker of Nitric Oxide and Reactive Nitrogen Species in Biological Samples

By

Sean Dustin Willis
B.S., Rockhurst University, Kansas City, MO, 2008

Submitted to the Department of Chemistry and the Graduate Faculty of the University of Kansas in partial fulfillment of the requirements for the degree of Master of Science.

_____

Chairperson Craig E. Lunte, Ph.D.

_____

Susan M. Lunte, Ph.D.

_____

Jane V. Aldrich, Ph.D.

Date Defended: December 13, 2012

The Thesis Committee for Sean D. Willis
certifies that this is the approved version of the following thesis:

Development of an Analytical Method for the Detection and Quantitation of Nitrite as a Biomarker of Nitric Oxide and Reactive Nitrogen Species in Biological Samples

_____
Chairperson Craig E. Lunte, Ph.D.

Date approved: April 12, 2013

ABSTRACT

Sean D. Willis, MS
Department of Chemistry, December 2012
University of Kansas

The brain is a complex organ, consisting of blood vessels, neurons, neuronal support cells, and meninges. The extracellular space surrounding the neurons is a very complex microenvironment, containing proteins, growth factors, neurotransmitters, and other small molecules. Microdialysis has been extensively used for sampling analytes from extracellular spaces in tissues. The microdialysis membrane excludes large molecules, making it possible to obtain protein free samples from this space that do not require any cleanup steps. The use of microdialysis allows the sampling of multiple analytes in extracellular spaces from multiple regions, making it possible to obtain a temporal profile over the time course of an experiment.

High performance liquid chromatography (LC) coupled with ultraviolet (UV) and electrochemical (EC) detection makes it possible to analyze samples collected via microdialysis with high throughput. Our lab has developed an LC UV-EC based separation and detection method that is capable of the high throughput needed to analyze small sample volumes directly from animal studies to study changes in nitric oxide synthase (NOS) activity and reactive nitrogen species formation in the brain and other tissues with high temporal resolution.

In this thesis, an LC based ion-pair chromatography method is described in conjunction with EC and UV detection methods for the determination of primary and

secondary products of nitric oxide metabolism (nitrite and nitrate) in the microdialysate. The development of an ion-pair based separation and combined UV-EC detection of nitrite and nitrate were the fundamental steps for the optimization of separation of nitrite and nitrate present in microdialysates. Detection optimization for nitrite and nitrate was carried out in the same matrix as that of perfusate used in animal experiments. Separation conditions consisted of 1 mM tetrabutylammonium hydroxide (TBAOH), 15 mM sulfate at pH 4.0, a flow rate of 0.1 mL/min, using a C-18 4 μM 1x150 mm column as the stationary phase. Microdialysis samples were then injected, separated, and detected using LC with UV-EC detection.

The first application of this method involved monitoring changes in nitrite and nitrate concentrations in the rat hippocampus region as a result of chemically-induced excitotoxicity. 3-Mercaptopropionic acid (MPA) was perfused through a microdialysis probe into the hippocampus brain region of a rat, as had occurred in past studies of our research group. In contrast to the elevation of other biomarkers seen by the administration of this compound, this method was unable to detect changes in the concentration of nitrite, and the changes found for nitrate appeared to be random.

The last application of this method involved monitoring changes in nitrite levels in a freely moving sheep administered nitroglycerin through infusion and topical application to the skin, and histamine injection into the skin. This study served to further validate the developed method for wider application beyond rat brain studies and to compare it to a microchip-based amperometric nitrite detection method developed by

the S. Lunte research group. Nitroglycerin infusion produced a response in time course experiments that is in agreement by both methods. Limits of detection, quantitation, and sensitivity were higher with this developed method in comparison to the method under development by the S. Lunte group. Furthermore, because this developed method was capable of determining nitrite concentrations in microdialysis samples, it was used to quantitatively measure nitrite generated during several nitroglycerin infusion experiments. Insufficient response was observed with either nitroglycerin topical application, or histamine injection and infusion to warrant further study of nitrite production under these conditions.

ACKNOWLEDGEMENTS

I would like to thank my grandparents, Archie and Donna Willis, for helping raise me and for believing in me. I would like to thank my dad, Stephen Willis, who worked incredibly hard to give me the best opportunity to succeed.

I would like to thank my research advisor, Craig Lunte, for helping guide my research and this thesis to become a reality. Thank you for your patience, Craig. I would like to also thank Carl Cooley, Sara Thomas, and Megan Dorris. The knowledge of Carl in separations, Sara in animal studies, and Megan in electrochemistry is immense. I feel that that I owe so much to these individuals.

I would like to thank David Scott for his contribution to the collaboration in the last section of this thesis and for being a good friend. I would also like to thank Dr. Susan Lunte for her guidance in this collaboration and the willingness to answer the many questions I had surrounding it. I would like to finally thank Thomas Linz for his help and willingness to answer the many questions I've come to ask.

TABLE OF CONTENTS

CHAPTER 3: ANIMAL METHODS AND 3-MPA RAT MICRODIALYSIS STUDIES

CHAPTER 4: SHEEP STUDIES

LIST OF FIGURES

1.1 Introduction

1.1.1 Oxidative Stress

Nitric oxide is an important biomolecule that has a multi-pronged role in the central nervous system. It may function as a neurotransmitter, a vasodilatator, or react with superoxide under conditions of oxidative stress to form reactive nitrogen species (RNS) [1]. Oxidative stress is defined as an imbalance between the production and action of reactive oxygen species and the ability of the body to easily detoxify reactive intermediates formed or repair the damage resulting from these intermediates [2]. Nitric oxide has been found in elevated levels under conditions of oxidative stress, such as those of ischemia [3]. Studies have shown that under *in vitro* conditions, nitric oxide reacts with reactive oxygen species such as superoxide to form peroxynitrite [4, 5]. Peroxynitrite can react with a variety of biological molecules such as DNA bases, lipids, and thiols, causing damage to these essential biomolecules. Because peroxynitrite also reacts with proteins containing transition metal centers, oxidizing those metals, iron-containing molecules such as hemoglobin, myoglobin and cytochrome P450's may be altered in structure and function [4, 6]. Reaction with amino acids, such as the nitration of tyrosine and the oxidation of cysteine, can result from peroxynitrite intervention. These changes can lead to enzyme impairment, changes in cytoskeletal structure, and reduced capability of cellular signaling [4]. In addition, peroxynitrite is protonated to form peroxynitrous acid under equilibrium conditions, followed by nitrogen dioxide and the hydroxyl radical. The hydroxyl radical is

considered the most reactive and damaging reactive oxygen species produced, capable of causing damage to molecules such as lipids, proteins, carbohydrates, amino acids, and nucleic acids, similar to superoxide. What makes the hydroxyl radical the most damaging is the lack of an enzymatic reaction with which to eliminate it. Superoxide dismutase works to detoxify superoxide to make it harmless, while the hydroxyl radical will continue to cause damage over its lifetime of 10^{-9} seconds [7, 8, 9]. **Figure 1.1** shows various pathways associated with oxidative stress in the brain.

Because nitric oxide and peroxynitrite have short half-lives of less than 5 seconds, they are difficult to detect directly [10, 11]. Sensors to detect these compounds have been developed, however it is difficult to measure these compounds and other biomarkers in the same location simultaneously [12, 13]. This limitation makes multiple biochemical pathway mapping under oxidative stress conditions infeasible. The need for the development of a method which is amenable to detecting nitric oxide production and reactive nitrogen species in the presence of other biomarkers, as an added tool for evaluating multiple mechanisms of function and damage, is necessary. Peroxynitrite itself is unstable, but will rapidly degrade to form the more stable products nitrite and nitrate, which may be monitored off-animal with minimal likelihood of analyte degradation [**14, 15**]. An advantage of

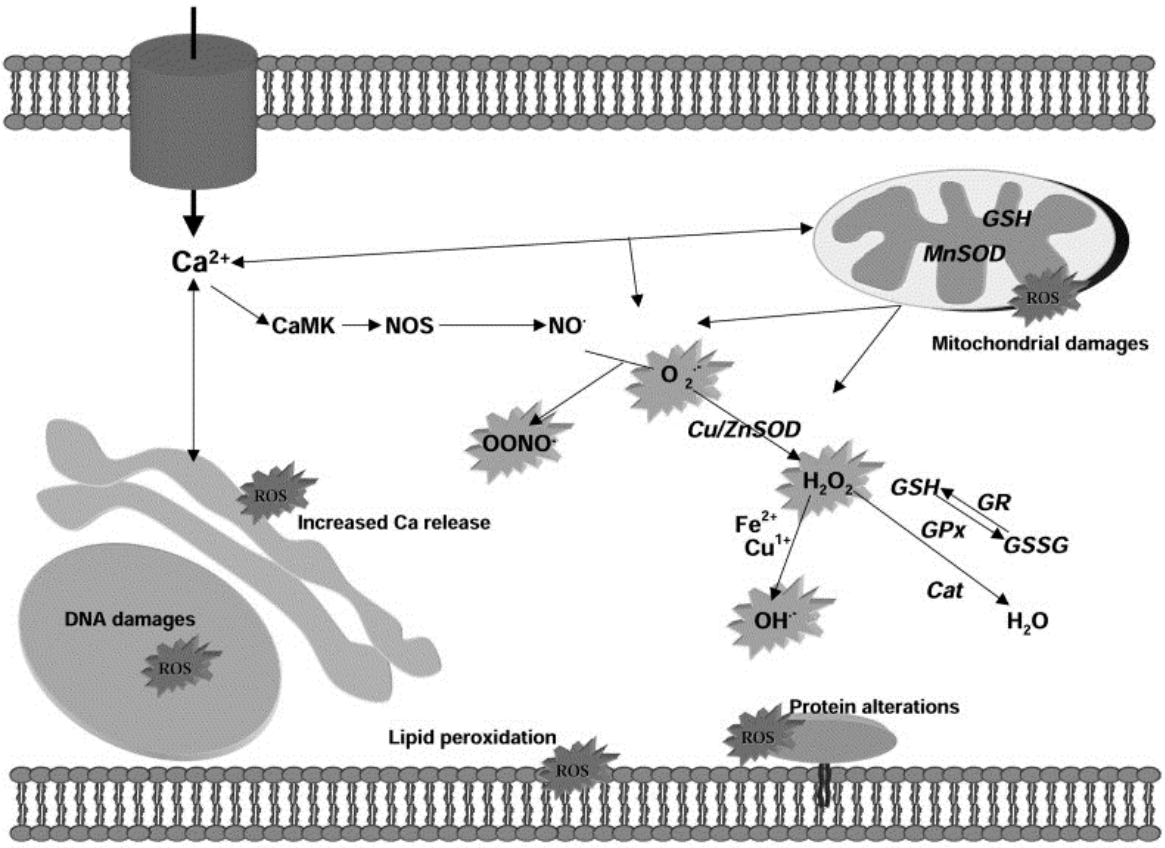

Figure 1.1: Illustration of events leading up to and as a result of oxidative stress in the brain. Influx of Ca^{2+} as a result of upregulation of ion channels leads to the activation of calmodulin and nitric oxide synthase (NOS). Oxidative stress results from the reaction of superoxide with NO to form peroxynitrite (ONOO-), resulting in protein, lipid, and DNA damage to the cell and leading to cell death. Figure reproduced with permission from Milhavet, et al. [7].

simultaneously monitoring multiple biomarkers in addition to just nitric oxide and/or peroxynitrite is that it provides a map of multiple processes ongoing in the brain during oxidative stress. The described methods in this thesis apply minimally invasive techniques which make multiple biomarker evaluation possible with high throughput.

Microdialysis sampling as an analyte collection method is popular for the analysis of small molecules and has been used extensively in our research group. The advantage of this sampling technique is the ability to monitor multiple analytes simultaneously, using off line analysis with multiple established methods. In this thesis, development and characterization of methods for the detection of nitrite and nitrate from *in vivo* studies were the central focus. A rat 3-mercaptopropionic acid (MPA) model, in which 3-MPA was administered to chemically induce seizures, was implemented as the first target of application of these methods [**16**]. The delivery of 3-MPA has been extensively studied by our group. The effect of 3-MPA administration on GABA and glutamate levels has been studied as well. In addition, its role in the formation of lipid peroxidates from lipids in neuronal cells by reactive oxygen species (ROS) has been studied in this research group. It was possible that ROS were not the only culprits in the formation of lipid peroxides as indicators of damage occurring in cells. Up until this point, reactive nitrogen species (RNS) formation and contribution to oxidative stress had not been evaluated, and it was suggested that concentrations of these biomarkers should be evaluated as molecules indicative of other pathways under

3-MPA administered conditions. The overall goal of this research was to use the developed LC EC method to monitor RNS production in multiple systems and animals, with the initial focus on chemically-induced seizure.

1.1.2 Seizure Models

Seizure is predominantly a physical manifestation of the disease epilepsy and has a frequency of 1% in the United States (US). According to 2011 US statistics, approximately 3 million of the United States population suffer from epilepsy [**17].** About 200,000 cases of epilepsy are diagnosed every year, with 20,000-50,000 deaths as a result of seizures and related causes. These seizures may be caused by fever, low blood sugar from abnormal levels of glucose or sodium in the blood, brain damage resulting from stroke, heart disease, head injury, aneurysm, or a tumor, as well as infection such as meningitis, or congenital in origin. In addition, withdrawal from certain drugs may exacerbate these events. Seizures and related causes result in a per year expenditure of over $15 billion a year in treatment costs.

A seizure can be thought of as an “electrical storm” in specific regions of the brain, resulting from hyperneuronal excitation. This results in rapid neuronal firing. There are many types of seizures, with the most common being associated with a “convulsion like” state. Some seizures display minor to no visible physical symptoms. Symptoms associated with a seizure are dependent upon the brain region(s) affected. Generalized tonic clonic seizures, more commonly known as

the “grand mal” type, are dictated by symptoms occurring over the entire body. Muscle rigidity, contraction, and loss of consciousness and incontinence are typical features of this type of seizure. Focal seizures are isolated to a single region of the brain, and as a result, generate symptoms dictated by the affected region. Muscle contraction, staring and blackout spells, repetitive movements, and abnormal sensations are just some of the features of this type of seizure. A seizure can occur due to epilepsy, or be idiopathic (i.e. unknown in origin). Treatments are available for many sufferers of epilepsy and other causally induced seizures. It is known, however, that approximately 30% of epileptically induced seizures are resistant to current treatments. In addition, neuro-cognitive deficits have been reported by those suffering from this condition. It has been found that patients who have several seizures over time can develop some brain damage, and those rapidly experiencing many seizures may experience a rapid progression of damage [18]. From a clinical perspective, hippocampal and thalamic atrophy, as well as neuronal loss and a reduced ability to function, have been reported [19]. The goal of this research is to have a greater understanding of what occurs biochemically in the brain under these conditions so that it may be possible for more effective treatments for epileptically induced seizures and/or the damage they cause.

1.1.3 Seizure and reactive nitrogen species

Nitric oxide (NO) serves as a molecule involved in cellular signaling and as a vasodilator in the central nervous system under normal conditions [20]. NO is

formed from the reaction of the amino acid L-arginine with the electron carrier NADPH and molecular oxygen. During normal conditions, endothelial and neuronal nitric oxide synthase (eNOS/nNOS) derived NO production is limited by the amounts present of the NO precursor molecule arginine as well as intracellular Ca^{2+}. eNOS and nNOS activation is Ca^{2+} dependent, and with a minimal influx of this ion, NO production is limited as well. Ca^{2+} is necessary for the activation of calmodulin, a messenger protein which binds and activates two types of NOS, neuronal and endothelial [McMurry 2011, 21]. It has been found that excessive levels of NO contribute to the formation of RNS such as peroxynitrite by reaction with superoxide [5]. It is these RNS which are believed to contribute to oxidative stress. Peroxynitrite undergoes protonation to form peroxynitrous acid and has been found to oxidize protein components such as thiols, amino groups, and methionine [5]. In addition, peroxynitrite can form the highly reactive hydroxide radical. It is this radical which is considered the most destructive of all reactive species [20, 22, 23]. Furthermore, ATP depletion results, followed by necrosis, leading to the rupture and death of the cell as shown in **Figure 1.1** [7, 24,25]. As a result of cellular necrosis, an inflammatory response is generated, resulting in the activation of leukocytes and inflammatory molecules that cause membrane blebbing (i.e. irregular bulging due to cytoskeleton decoupling) in the surrounding cells and an increase in NO, leading to further RNS production [26, 27, 28, 29].

1.2 Methods

1.2.1 High Performance Liquid Chromatography

High performance liquid chromatography (LC) is a popular analytical technique implemented in the 1960's for the separation of a wide variety of compounds [30]. Recently, LC has been applied toward solving a plethora of biochemical/clinical, forensic, environmental, food, and pharmaceutical related problems [31]. Columns consisting of dimensions of internal diameters (i.d.) of 1-2 mm and lengths ranging from 50-150 mm make it possible to use sample injection volumes as small as several microliters, making current LC amenable to analyzing small sample volumes [32]. These low injection volumes make it possible to perform multiple separate LC analyses of microdialysis samples. LC has several advantages over other separation methods such as capillary electrophoresis (CE). Lifetimes of liquid chromatography columns are much higher than capillaries used in CE. In addition, variability in retention time with LC is also significantly lower in comparison to CE methods. Furthermore, LC is more compatible with high ionic strength samples.

A common LC system consists of a high pressure pumping system, of which is connected to an injection valve, followed by a chromatographic column responsible for analyte separation, and a detection system (UV-VIS, EC, mass spectrometer) as shown in **Figure 1.2** [33]. The first step in LC is the pumping of mobile phase responsible for analyte transport from a reservoir to the injection valve and into the chromatographic column. Sample is introduced into the system at the injection valve, resulting in the transport of the sample plug onto the chromatographic column. This process is followed by a separation process on

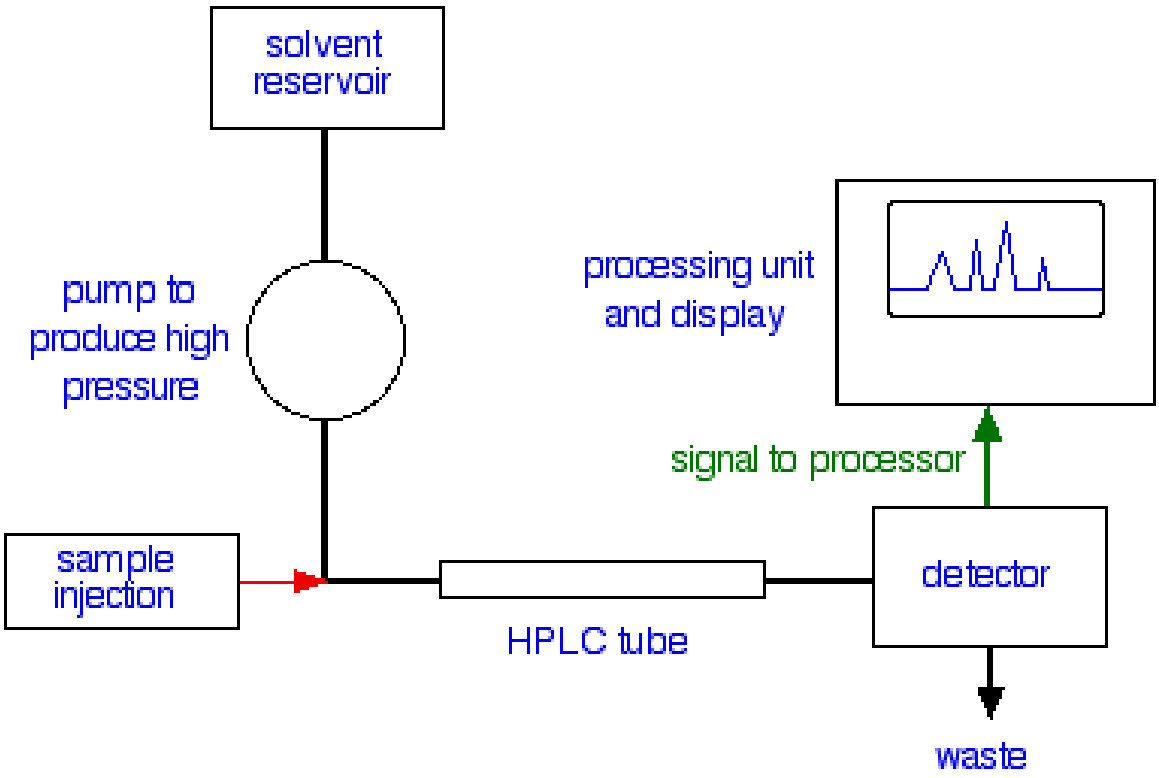

Figure 1.2: LC and detection schematic [33]

the chromatographic column where analytes are separated based upon their degree of interactions with the stationary phase. Chromatographic separation, in general, depends upon a variety of factors. Flow rates, mobile phase, and stationary phase conditions all play a role in compound separation.

In theory, chromatography works based upon distribution of analytes between phases. A theoretical plate model helps to explain ongoing processes in a column during chromatographic separation. In addition, it is used as a method to measure column efficiency in practice. The number of theoretical plates (N) is the most commonly reported value of column efficiency, with a higher efficiency associated with a larger N value: $N = \frac{5.55 t_R^2}{w_{1/2}^2}$, where t_R is the retention time of the peak of interest and $w_{1/2}$ is the width at half-height of this peak [34]. The number of plates for a column is dependent upon the width of the peak of an analyte in a separation. A narrower analyte peak allows for not only maximization of resolution between it and other peaks present, but for equivalent peak areas, maximization of peak height, with the greater the peak height for an analyte at any given concentration, the lower the potential limits of detection for that analyte.

Resolution is the degree of separation between two peaks in a chromatogram and is defined as: $R_s = \frac{2(t_{r_2} - t_{r_1})}{w_1 + w_2}$, where tr1 and tr2 represent the difference in retention times of the two peaks and w1+w2 represent the addition of the peak widths of the two peaks at the base. A resolution of >1.5 is desired for complete baseline resolution [35].

1.2.2 Reverse Phase (Partition) Chromatography

In this development of chromatography, the column contents consist of a solid support covered by a covalently attached stationary phase (bonded phase). Analyte equilibrates between this phase and the mobile phase moving through the column. It is due to this equilibrium state that different analytes are separated. All analytes are traveling at the same speed through the mobile phase; however, the greater the affinity of the analyte for the stationary phase, the more time it will spend in the stationary phase in comparison with analytes of lesser affinity [36]. The ability of analytes to be separated based upon stationary and mobile phase conditions can be stated as a result of differences in partition coefficients. This coefficient is a mathematical ratio of the concentrations of an analyte present in two phases of a mixture consisting of two solvents which are immiscible with one another, all at equilibrium [37].

In the case of partition chromatography, one phase is the bonded stationary phase, and the other phase is the mobile phase. The stationary phase for reversed phase chromatography is considered hydrophobic/lipophilic, and the

mobile phase is considered hydrophilic/lipophobic [38]. Due to the relationship of "like dissolves like", the partition coefficient can be viewed to be a measure of the affinity of analyte for a hydrophobic phase over that for a hydrophilic phase, or the hydophobicity of an analyte [39]. For partition chromatography involving a hydrophobic stationary phase and hydrophilic mobile phase, the partition coefficient of a particular analyte would be its concentration in the stationary phase over that in the mobile phase.

Reversed phase chromatography can apply a wide variety of hydrophobic stationary phases to separate analytes. The general form of these hydrophobic phases is the presence of alkyl chains bonded to a resin support containing silanol groups. The most common alkyl group used for reversed phase chromatography is the octadecyl (C-18) group [40]. Less common alkyl groups used are octyl (C-8) and phenyl based groups. In addition, any exposed silanol group may have various organic groups added to increase selectivity of the stationary phase. The more hydrophobic an analyte is, the more strongly it will bind to these groups of the stationary phase, separating it from the more hydrophilic compounds eluted first from the column. **Figure 1.3** shows this process [40]. The composition of the mobile phase is important as well. Organics soluble in water are commonly used in mobile phases to elute analytes strongly bound to the hydrophobic stationary phase, and may be used in a constant concentration or added as a gradient [41].

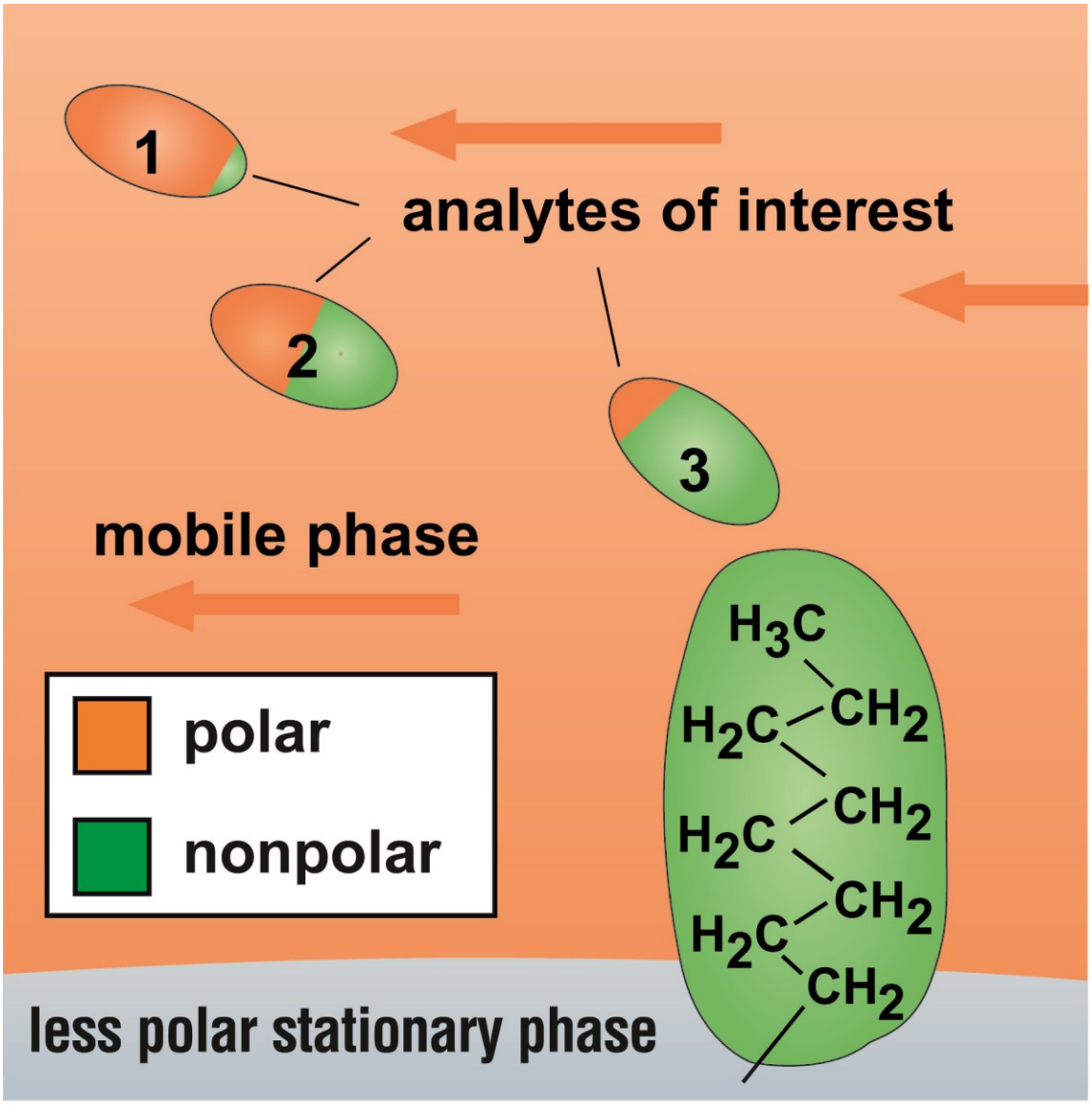

Figure 1.3: Reversed phase separation of various analytes based upon their hydrophobicity, as a result of the degree of their interactions with the hydrophobic stationary phase. Reproduced by permission of Restek Corporation.

1.2.3 Ion-Exchange Chromatography

In this type of chromatography, a negatively or positively charged ion is covalently attached to a solid stationary phase consisting of a resin. Analyte molecules of an opposite charge traveling in mobile phase are attracted electrostatically to the charged ions of the stationary phase, as shown in **Figure 1.4**. The degree of attraction of molecules for this ion exchanger is dependent upon the degree of electrostatic attraction due to the magnitude and location of opposite charges [42]. To bind an analyte to the stationary phase, it is typically introduced as a sample in mobile phase of low ionic strength. The molecules can then be eluted by increasing the concentration of similarly charged species in the mobile phase which compete with the analyte for the ion exchanger, or shield the analyte from the exchanger and allow it to elute. The use of a gradient of increasing ionic strength makes it possible to separate several analytes, with analytes possessing weaker ionic interactions with the ion exchanger being eluted earliest [42, 43].

In addition, pH may be altered to elute charged analytes attracted to the ion exchanger. In the case of cation-exchange chromatography, where the ion exchanger is negatively charged and the analyte is positively charged, an increase in pH will make the analyte neutral or negatively charged, reducing or eliminating its electrostatic attraction and allowing it to elute from the column. With anion-exchange chromatography, the opposite is the case. Negatively

charged analytes will be eluted from the positively charged ion exchanger by lowering mobile phase pH, protonating the negatively charged groups of the analyte and reducing or eliminating its electrostatic attraction for the exchanger and allowing it to elute from the column [44]. To retain the analyte on the ion exchanger, the pH of the mobile phase must be between the pKa of the analyte and that of the charge ion exchanger [45].

1.2.4 Ion-Pairing Chromatography

Ion-pair chromatography is a mobile phase modification that allows a reversed-phase column (typically C-18) to separate ionic analytes which would typically not be retained otherwise. Modification of the mobile phase occurs through the addition of an ion-pair reagent as a component. Common reagents include tetra-alkylammonium, alkyl sulfates, alkyl sulfonates, and trifluoroacetic acid. Tetrabutylammonium hydroxide, a tetra-alkylammonium, was used as the ion-pair reagent in this research and is shown in **Figure 1.5** [44]. Typically without such a compound present, negatively charged and positively charged analytes are retained the least and are too close to one another to distinguish them in a chromatogram, while neutral analytes are retained relatively longer [45, 46, 47, 48].

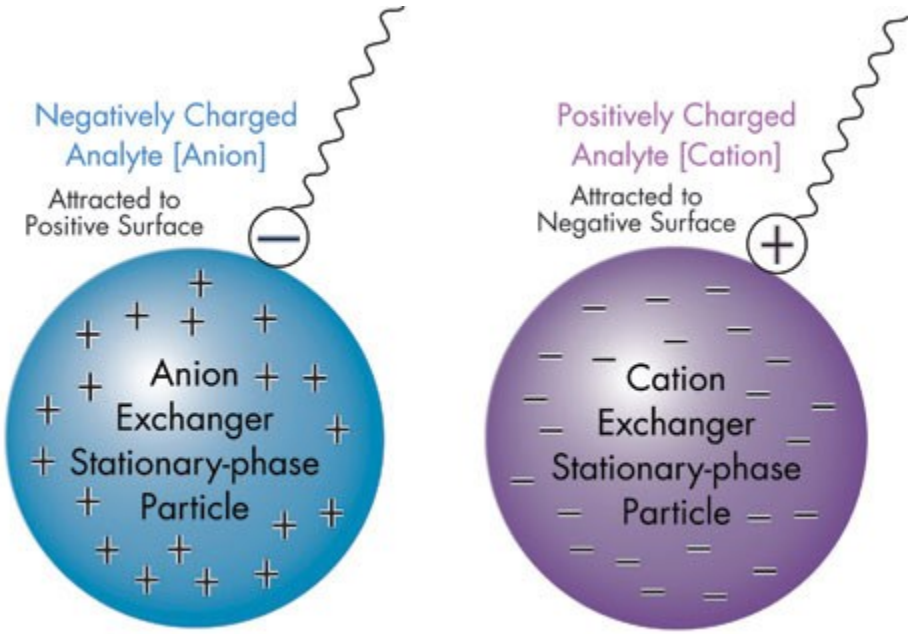

Figure 1.4: Ion exchange analyte separation based upon electrostatic attraction. Oppositely charged ions of analyte are attracted to the ion exchanger for retention. Reproduced by permission of Waters Corporation.

The type of the ion-pair reagent, such as its charge and hydrophobicity, dictate interactions. When an ion-pair agent is added to the column environment, the hydrophobic groups adsorb to the column stationary phase, leaving the charged head group free to interact with charged analytes transported through the column. In addition, the type of analyte influences the degree of interaction with the ion-pair head groups and hydrophobic stationary phase. Like charges repel like charges, meaning that analytes with the same charge as that of the ion-pair head group will interact the least and will be repelled from those groups on the stationary phase. As a result, these analytes will be retained the least on the column. Neutral charged molecules do not interact with the charged head groups of the ion-pair reagents; however, because they are not repelled as like charges are, they have the opportunity to interact with the hydrophobic regions of the stationary phase, making them retained longer on the column than like charged analytes. Molecules with charges of opposite polarity of the ion-pair head group will be retained the longest on the column as a result of two factors: the opposite charge of the analyte will cause it to electrostatically interact with the ion-pair head group, and hydrophobic regions of the analyte will interact with the hydrophobic region of the stationary phase [45, 46, 47, 48].

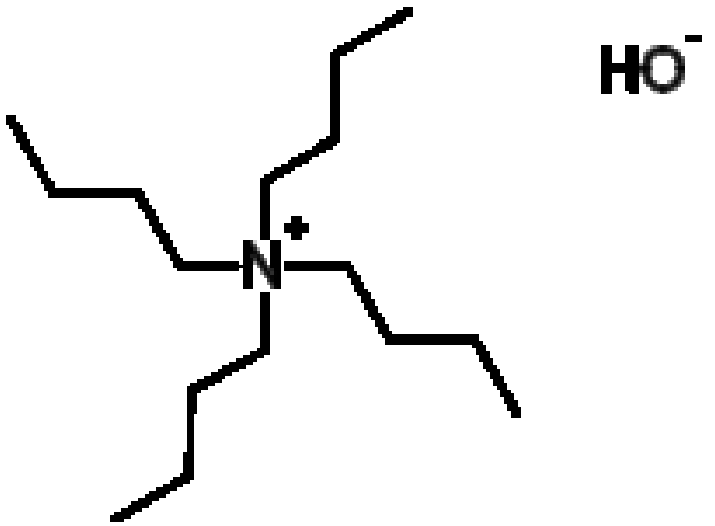

Figure 1.5: Ion-pairing reagent tetrabutylammonium hydroxide [44].

The interactions of counter ions with those of the ion pairing reagent on the stationary phase surface follow the electrical double layer model, shown in **Figure 1.6** [49]. Ions are not distributed linearly next to the surface of these agents with the remainder distributed randomly, but are ordered such that the counter ions are distributed to generate the least amount of energy in an equilibrium state. An electrostatic potential is generated due to the difference in charge polarity. This potential is dependent upon the concentration of ion pairing reagent on the surface [50]. The Gouy-Chapman theory assumes the surface potential is a function of the charge density of the surface as well as the ionic strength of the analyte of interest. This means that the greater the charge density of the ion pairing reagent head groups and the higher the analyte ionic strength, the higher the surface potential. In this case, the ion pairing agent interaction with the stationary phase assumes a charged, planar surface.

In addition to its charge state, the concentration of ion-pairing reagent has an effect upon the retention of analytes. A critical concentration of the reagent is necessary such that the analyte is retained long enough for separation, however not so much that analyte retention is reduced. Once the ion-pair reagent adsorbs a maximum number of hydrophobic stationary phase locations, excess of this reagent flows through the column and is eluted. If too high of a concentration of ion-pair reagent is present in the mobile phase, analyte will interact more with this reagent that is flowing through and less with that adsorbed to the column stationary phase.

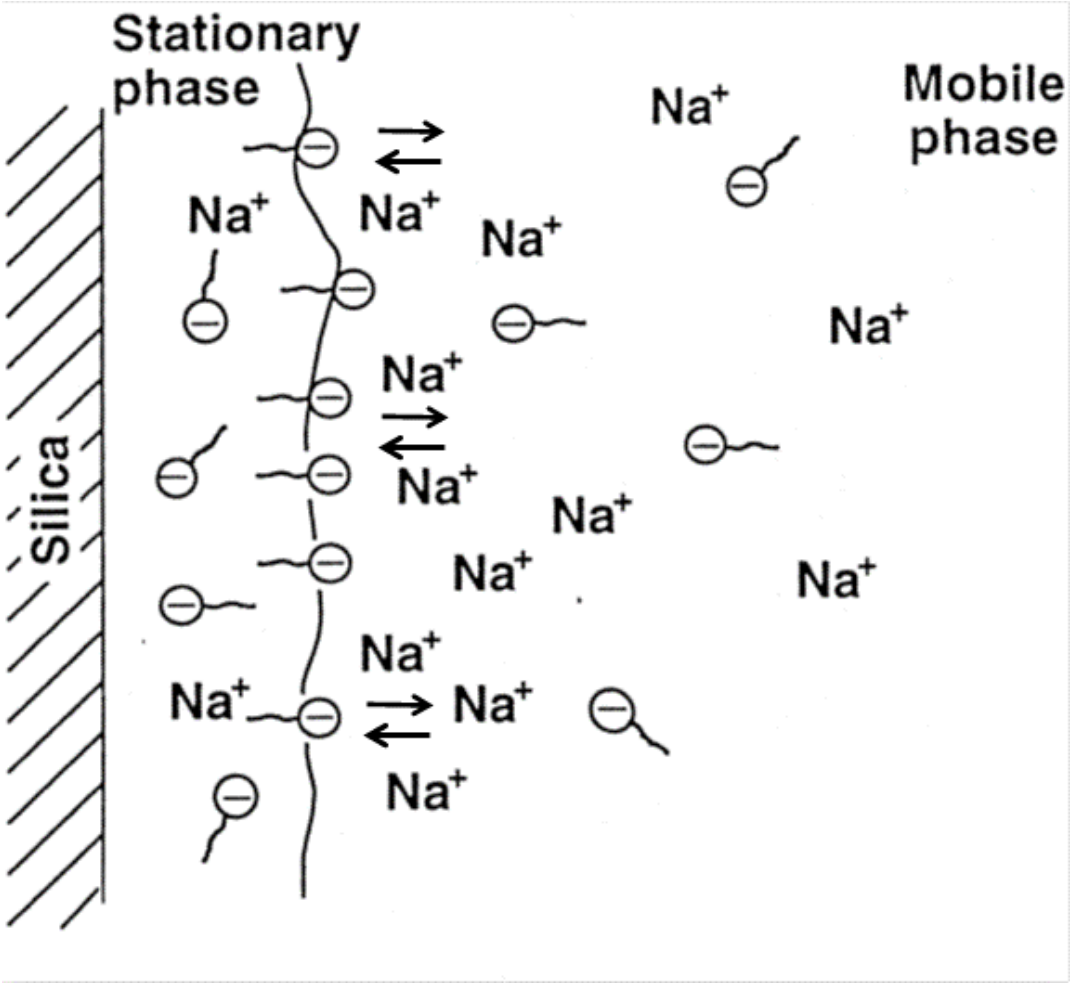

Figure 1.6: Electrical double layer model for ion pair reagent chromatography. In this picture, the ion pair reagent is depicted as negatively charged head groups with hydrophobic tails. The analyte of interest in this case is Na^+. The reversed phase portion of the stationary phase is shown as the layer between the silica substrate and the negatively charged head groups of the ion pairing reagent at the reversed phase outermost surface [49]

A result is a reduction of retention time for the analyte of interest, which may negatively affect the separation.

The presence of an organic modifier as well as its concentration in the mobile phase affects the performance of ion-pair reagents [51]. Modifiers such as methanol or acetonitrile tend to interact with the hydrophobic regions of the reagent as well as the stationary phase, resulting in the reduction of ion pair reagent adsorption to the column stationary phase and retention of analytes of interest. Modifiers such as carboxylic acids above their pKa values will be negatively charged and interact electrostatically with the positively charged ion-pair head groups; in addition their hydrophobic regions interact with the stationary phase and ion-pair reagent hydrophobic groups. A result is a reduction in the number of sites available for analyte electrostatic and hydrophobic interactions, leading to a reduction in retention time of the analytes of interest.

Ionic strength and the type of ions in the mobile phase additionally has an effect upon ion-pair separation [51, 54]. Competition with the analyte for the ion-pair head group can reduce analyte retention, affecting the separation. This may be beneficial or not for the analysis. Retention of analytes on the column for too short a period of time may result in co-elution with other compounds. On the other hand, retention of analytes for too long can result in significant peak broadening leading to co-elution with other compounds.

1.2.5 Electrochemical detection

Electrochemical (EC) detection relies upon the induction of a chemical reaction by an applied voltage and the measurement of electron transfer as a result of this reaction. This detection method was developed originally for the detection of the catecholamines, which are aromatic compounds present in the central nervous system and are partially responsible for its function [54, 55]. Advantages of EC detection are low limits of detection, high sensitivity, and high selectivity. This method functions based upon the detection of easily oxidized or reduced analytes. Amperometry or fixed potential EC detection is the most common form of this type of detection method, allowing for the identification and quantitation of electrochemically active analytes.

An EC system is typically composed of a potentiostat that acts as a voltage delivery source, and a flow-through EC cell where the oxidation or reduction process occurs for the analyte identification and quantitation as the mobile phase is delivered from a LC system. The EC cell is made up of 3 electrodes, a working electrode, counter electrode, and reference electrode. The working electrode serves as the site where the analyte of interest is oxidized or reduced. The counter electrode serves as a site to which a potential difference from the working electrode is applied and will serve as a cathode during oxidation reactions and as an anode during reduction reactions [54, 55, 56]. The reference electrode contains a well-known, stable potential. This quality allows it to be used to account for measuring the potential drop between the working electrode surface and the solution. A commonly used reference electrode is the silver chloride

(Ag/AgCl) type, with a standard potential of +0.210V at 3.0 mol/kg KCl [57, 58, 59]. Shown in **Figure 1.7** is a response versus applied potential plot (hydrodynamic voltammogram) for a glassy carbon working electrode versus Ag/AgCl detection of nitrite using an electrochemical flow cell.

1.2.6 Ultraviolet-Visible (UV-Vis) Spectroscopy

UV-Vis spectroscopy is reliant upon absorption, which is proportional to the path length of the solution containing the absorbing molecule and the concentration of the molecule. Linking absorbance as a detection method to LC requires the use of a spectrophotometer composed of a flow cell, a light source(s), a diffraction grating which selects for a specific wavelength(s) to enter the flow cell, a half mirror responsible for directing some incident light to get an initial intensity reading by a detector, and a second detector behind the flow cell receiving transmitted light. From the collection of the intensities of the incoming and transmitted light by the two detectors, the UV-Vis detection system can determine an absorbance value. **Figure 1.8** shows a UV-Vis spectrum of absorbance intensity versus wavelength, with maximum absorbance intensity at 200nm and minimum absorbance intensity at 235nm.

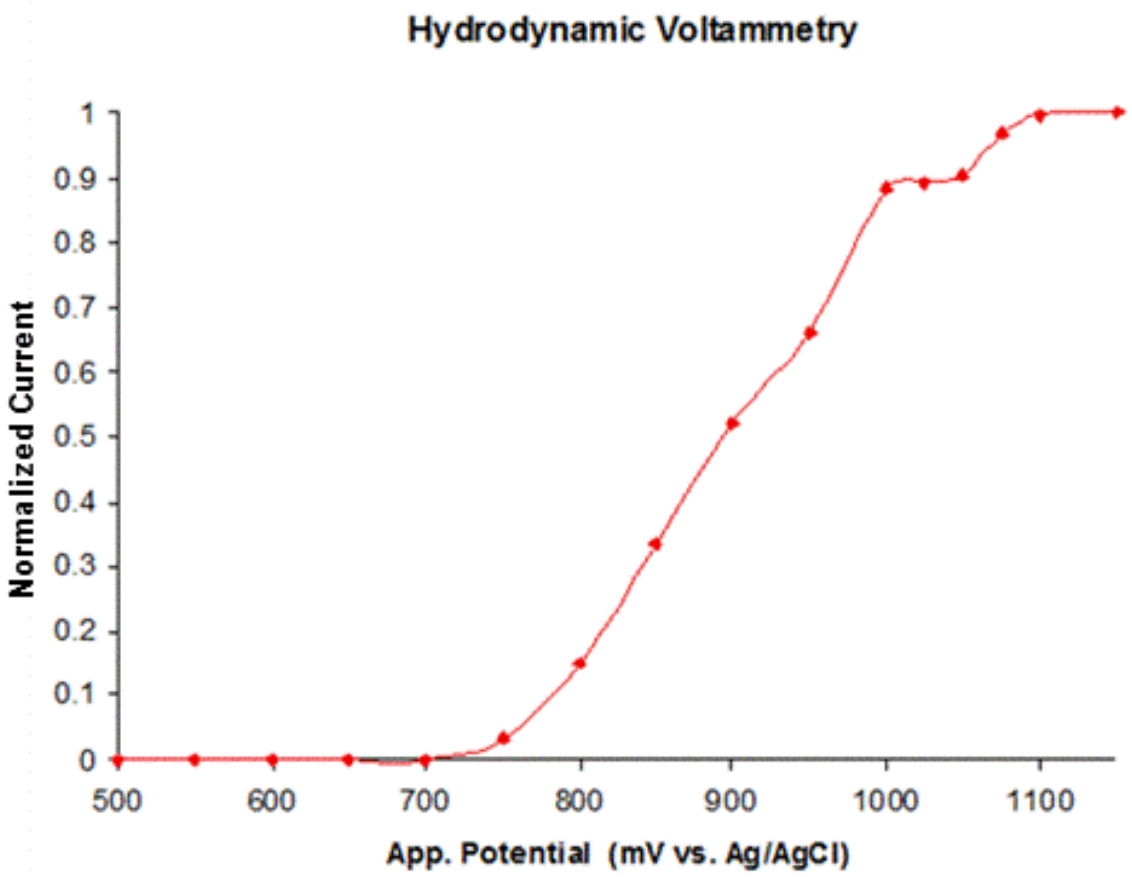

Figure 1.7: Hydrodynamic voltammogram of nitrite, showing an increase in response from 700mV up to 1100mV.

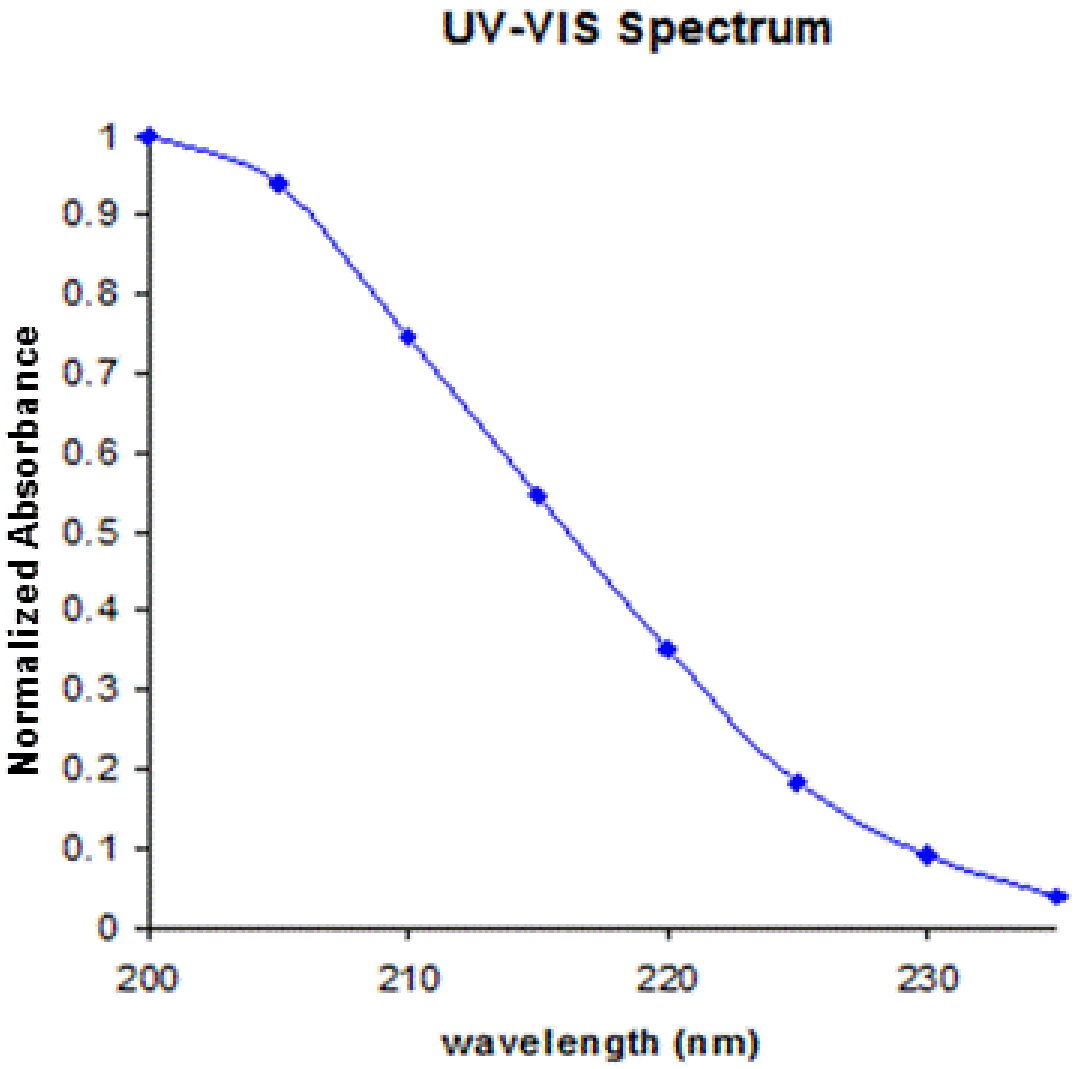

Figure 1.8: UV-VIS-vis spectrum of nitrate showing a decrease in response from 200nm to 235nm.

1.2.7 Microdialysis collection

Microdialysis is a method of sampling which allows for continuous and direct collection of compounds around the implanted probe. It is advantageous for *in vivo* studies due to its ability to monitor multiple analytes simultaneously in animals under anesthesia or that are awake and mobile. Samples collected lack proteins, increasing sample stability and reducing or eliminating sample cleanup prior to analysis. In addition, probes used for sample collection may be also used for delivery of compounds that are pharmacologically relevant to the study, eliminating additional implantation procedures. Probes are composed of a dialysis membrane sandwiched between an inner and outer tube comprising the cannula. The membrane itself can vary in length as well as composition, with its construction material dictating the molecular weight cutoff of sampled analytes, ranging from 20-100 kDa. Probes are perfused with solutions that match the tonic characteristics of the sampling environment as closely as possible. For brain studies, probes used consist of a cylindrical tube, with a tip at which a variable length dialysis membrane is attached. The recovery of the analyte of interest is dependent upon analyte molecular weight, with a rapid reduction in recovery if molecular weight exceeds ¼ of the cutoff of the microdialysis membrane. In addition, the solubility of the analyte dictates diffusion ability across this membrane. Water-soluble compounds such as glucose cross freely, while lipophilic compounds such as oleate present in fats have a reduced capability of membrane crossing [60, 61, 62]. Artificial cerebral spinal fluid or Ringer's solution is perfused through the probe to the microdialysis membrane where it picks up

analytes which have diffused into the probe from the surrounding environment, as shown in **Figure 1.9** [63].

Microdialysis is a two direction process. Sampling using microdialysis is not an equilibrium based process, and as result, analytes collected are representative of the concentrations sampled in the tissues. These representations are fractions of the concentrations present in the probe sampling environment, and can be expressed as efficiencies. Extraction efficiency (EE) is the most common method used to describe probe performance and is defined as the analyte exchange rate across the microdialysis membrane. In other words, EE represents the difference between the loss and gain of an analyte (C_p-C_d) over the difference in concentration of the perfusate and that of the sampling site (C_p-C_s), or $EE = \frac{C_p - C_d}{C_p - C_s}$. EE is independent of the analyte concentration at steady-state, as concentrations collected may be variable with constant flow rates, or the use of a single concentration at variable flow rates results in EE's of the same value. The ratio of (C_p-C_d) and (C_p-C_s) remains the same [62].

Compounds possessing higher concentrations of the analyte of interest in the perfusate pumped into the probe will display a net movement out of the probe unit area per unit time, or delivery. In contrast, compounds that have a higher concentration in the site surrounding the probe display a net movement into the probe unit area per unit time, defined as recovery. These processes occur with no net loss of fluid from the sampling site [64, 65]. Relative recovery is dependent

upon a number of factors, such as analyte composition, probe membrane composition and length or diameter, as well as perfusate flow rate [58, 59]. The relative recovery for an analyte is determined by sampling it from an *in vitro* environment using microdialysis and a perfusate of composition as similar to the tonic quality of the unadulterated sampling environment as possible. The equation needed to determine probe recovery is determined using extraction efficiency in recovery mode: $E_R = \frac{C_{d.}}{C_s} x100\%$. In this equation, C_d is the concentration of analyte recovered in the dialysate and C_s is the concentration of analyte in the sampling environment. The relationship between flow rate and analyte relative recovery is an inverse one. Analyte recovery is greatest at sub 1μL/min sampling rates, however temporal resolution suffers at such low values. On the other hand, high rates of perfusion, approaching 5μL/min, result in substantial reduction in relative recovery. Flow rates are selected to maximize analyte recovery, at the same time allowing for sufficient sample sizes and temporal resolution for analysis. Common sampling rates vary from 0.1 to 5.0 μL/min [66, 67].

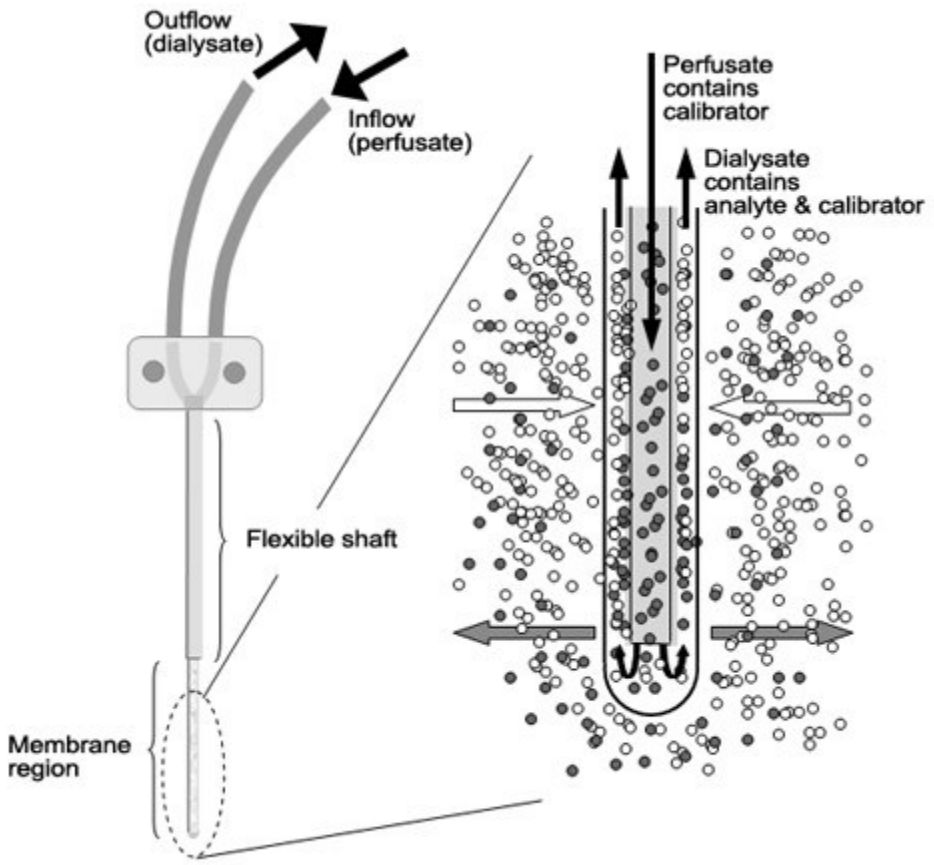

Figure 1.9: Microdialysis probe used for sampling from the rat brain. Note that diffusion occurs across the membrane due to an analyte gradient with no net fluid loss. Reproduced by permission of Chaurasia, et al. [63].

1.3 Objectives

The primary objective of this research was to develop chromatographic separations and UV-Vis-EC detection methods to identify and quantify the compounds nitrite and nitrate, with a goal of using microdialysis sampling to measure compounds in brain and subcutaneous tissue. Separation optimization experiments were carried out using nitrite and nitrate standards dissolved in mobile phase, followed by a solution of identical composition as basal perfusate expected to be used under *in vivo* conditions. Basal dialysate samples from *in vivo* experiments were then spiked with nitrite and nitrate standards to optimize their separation from other endogenous compounds present under *in vivo* conditions.

Microdialysis was used to monitor the formation and concentration of stable end products indicative of RNS generation under conditions of oxidative stress. Epileptic seizures induce the formation of lipid peroxidates as a result of cellular damage under conditions of oxidative stress. However, the role of RNS has not been specifically studied under these conditions as presented by the 3-MPA model. In further studies, chromatographic conditions were optimized for the presence of 3-MPA and its artifacts. In addition, NOS upregulation and RNS formation were studied in subcutaneous regions of sheep in response to administration of histamine injection, nitroglycerin cream, and nitroglycerin perfusion. A LC-UV method was also modified to detect and quantify

nitroglycerin, to support microdialysis delivery studies. Discussion of these experiments will occur in greater detail in the following chapters.

1.3 References

[1] Hou, YC, Janczuk, A (1999). "Current trends in the development of nitric oxide donors". *Curr. Pharm. Des.* **5** (6): 417-441.

[2] Lennon, SV, Martin, SJ (1991). "Dose-dependent induction of apoptosis in human tumour cell lines by widely diverging stimuli". *Cell Prolif.* **24** (2): 203-214.

[3] Ramond A, Godin-Ribuot D, Ribuot C, Totoson P, Koritchneva I, Cachot S, Levy P, Joyeux-Faure M. (December 2011). "Oxidative stress mediates cardiac infarction aggravation induced by intermittent hypoxia.". *Fundam. Clin. Pharmacol*. DOI:10.1111/j.1472-8206.2011.01015.x. PMID 22145601.

[4] Pacher, P, Beckman, JS (2007) "Nitric oxide and peroxynitrite in health and disease". *Physiol. Rev.* **87** (1): 315-424.

[5] Szabo, C, Ischiropoulous, H (2007). "Peroxynitrite: biochemistry, pathophysiology, and development of therapeutics". *Nat. Rev. Drug Discov*. **6**: 662-680.

[6] Vinten-Johansen, J (2000). "Physiological effects of peroxynitrite: potential products of the environment". *Circ. Res.* **91**: 173-179.

[7] Milhavet, O, Lehmann, S (2002). "Oxidative stress and the prion protein in transmissable spongiform encephalopathies." *Brain Res. Rev.* **3**: 328-339.

[8] Reiter, RJ, Melchiorri, L (1995) "A review of the evidence supporting melatonin's role as an antioxidant". *J. Pineal Res.* **18** (1): 1-11.

[9] Reiter, RJ, Carneiro, RC (1997) "Melatonin in relation to cellular antioxidative defense mechanisms". *Horm. Metab. Res.* **29** (8): 363-72.

[10] Bates, JN (1992). "The study of biological nitric oxide". *Neuroprotocols.* **1**: 99-107.

[11] Beckman, JS (1990). "Apparent hydroxyl radical production by peroxynitrite: Implications for endothelial injury from nitric oxide and superoxide". *Proc. Natl. Acad. Sci.* **87**: 1620-1624.

[12] Amatore, C, Arbault, S (2006). "Nitric Oxide Release during Evoked Neuronal Activity in Cerebellum Slices: Detection with Platinized Carbon-Fiber Microelectrodes". *Chem Phys Chem.* **7** (1): 181-187.

[13] Kubant, R, Malinski, C (2005). "Peroxynitrite/Nitrite Balance in Ischemia/Reperfusion Injury-Nanomedical Approach". *Electroanalysis* **18** (4): 410-425.

[14] Radi, R, Peluffro, G (2000). "Unravelling peroxynitrite formation in biological systems". *Free Rad. Biol. & Med.* **30** (5): 463-488.

[15] Pfeiffer, S, Gorren, ACF (1997). "Metabolic Fate of Peroxynitrite in Aqueous Solution". *J. Biol. Chem.* **272** (6): 3465-3470.

[16] Crick, EW, Osorio, I (2007). "An investigation into the pharmacokinetics of 3-mercaptopropionic acid and development of a steady-state chemical seizure model using in vivo microdialysis and electrophysiological monitoring". *Epilepsy Res.* **74** (2-3): 116-125.

[17] Hirtz, D, Thurman, DJ (2007). "How common are the "common" neurologic Disorders?" *Neurology.* **68** (5): 326-337.

[18] Meador, KJ (2005) "Cognitive Effects of Epilepsy and Its Treatment." *Clin. Interview.* **5** (6C): 589-593.

[19] Elger, CE, Helmstaedter, C (2004) "Chronic Epilepsy and Cognition." *Lancet Neurol.* **3**: 663-672.

[20] Hou, YC; Janczuk, A; Wang, PG (1999). "Current trends in the development of nitric oxide donors". *Curr. Pharm. Des.* **5** (6): 417–41.

[21] McMurry, JL, Chrestensen, CA (2011). "Rate, affinity and calcium dependence of nitric oxide synthase isoform binding to the primary physiological regulator calmodulin". *FEBS J.* **278** (24): 4943-4954.

[22] Sies, H. (1985). "Oxidative stress: introductory remarks". In H. Sies, (Ed.). *Ox. Stress*. London: Academic Press. pp. 1–7.

[23] Docampo, R. (1995). "Antioxidant mechanisms". In J. Marr and M. Müller, (Eds.). *Biochemistry and Molecular Biology of Parasites*. London: Academic Press. pp. 147–160.

[24] Rice-Evans CA, Gopinathan V (1995). "Oxygen toxicity, free radicals and antioxidants in human disease: biochemical implications in atherosclerosis and the problems of premature neonates". *Essays Biochem.* **29**: 39–63.

[25] Lelli JL, Becks LL, Dabrowska MI, Hinshaw DB (1998). "ATP converts necrosis to apoptosis in oxidant-injured endothelial cells". *Free Radic. Biol. Med.* **25** (6): 694–702.

[26] Lee YJ, Shacter E (1999). "Oxidative stress inhibits apoptosis in human lymphoma cells". *J. Biol. Chem.* **274** (28): 19792–8.

[27] Fackler, OT, Grosse, R (2008). "Cell motility through plasma membrane blebbing". *J Cell Biol.* **181** (6): 879-884.

[28] Rathore, N, John, S (1998) "Lipid Peroxidation and Antioxidant Enzymes in Isoproterenol Induced Oxidative Stress in Rat Tissues." *Pharmacological Research.* **38** (4): 297-303.

[29] Patel, M (2004) "Mitochrondrial Dysfunction and Oxidative Stress: Cause and Consequence of Epileptic Seizures." *Free Radic. Biol. Med*. **37** (12): 1951-1962.

[30] Horvath, C, Preiss, BA (1967) "Fast Liquid Chromatography: An Investigation of Operating Parameters and the Separation of Nucleotides on Pellicular Ion Exchangers". *Anal. Chem.* 36: 1178-1186.

[31] Swadesh, J (1997). "HPLC—Practical and Industrial Applications". CRC Press Inc. pp. 1-2.

[32] Meyer, VR (2006). "*Practical High-Performance Liquid Chromatography. 4th Ed.*" Wiley&Sons, Ltd. (Online Ed.). http://onlinelibrary.wiley.com/doi/10.1002/0470032677.fmatter/pdf.

[33] Clark, J. (2007) chemguide.co.uk/analysis/chromatography/hplc.html

[34] Nic, M, Jirat, J (2006). "plate number, N". *IUPAC Compendium of Chemical Terminology.* (Online Ed.). http://goldbook.iupac.org/

[35] Dorsey, JG, Cooper, WT (1994). "Retention Mechanisms of Bonded Phase Liquid Chromatography". *Anal Chem* **66** (17): 857-867.

[36] Leo, A, Hansch, C (1971). "Partition coefficients and their uses". *Chem Rev.* **71** (6): 525-616.

[37] Nic, M, Jirat, (2006) "Reversed-phase chromatography". *IUPAC Compendium of Chemical Terminology.* (Online Ed.) http://goldbook.iupac.org/

[38] Sangster, J (1997). "Octanol-Water Partition Coefficients: Fundamentals and Physical Chemistry." *European J Med Chem.* **32** (11): 842-842.

[39] Chromatographic Reagents Used in USP-NF and Pharmacopeial Forum (2007).

[40] Restek Corporation (2002). “Ultra Aqueous C18 HPLC Columns: Achieve Stable Rentention in 100% Aqueous Mobile Phase”.

[41] Snyder, LR, Dolan, JW (2006). “*High-Performance Gradient Elution: The Practical Application of the Linear-Solvent-Strength Model*”. Wiley Interscience.

[42] Jackson, P, Haddad, PR (1990). “*Ion chromatography: principles and applications*”. Amsterdam: Elsevier. 13-39.

[43] Smith, R (1951). *Ion Chromatography Applications*. Boca Raton: CRC Press. pp. 29-36.

[44] Bos, ME (2004). “Encyclopedia of Reagents for Organic Synthesis”. Ed: Paquette, L. J. Wiley&Sons, New York. (Online Ed.). http://onlinelibrary.wiley.com/book/10.1002/047084289X

[45] Malmquist, G, Lundell, N (1992). “Characterization of the influence of displacing salts on retention in gradient elution ion-exchange chromatography of proteins and peptides”. *J. Chrom.* (627): 107-124.

[46] Kopaciewicz, W, Rounds, MA (1983). “Retention Model for High-Performance Ion-Exchange Chromatography”. *J. Chrom.* (266): 3-21.

[47] Waters Corporation (2012). “Separations based on Charge: Ion-Exchange Chromatography”. HPLC Separation Modes.

[48] Bos, ME (2004). “Encyclopedia of Reagents for Organic Synthesis”. Ed: Paquette, L. J. Wiley&Sons, New York. (Online Ed.). http://onlinelibrary.wiley.com/book/10.1002/047084289X

[49] Bartha, A, Stahlberg, J (1994). “Electrostatic Retention Model of Reversed-Phase Ion-Pair Chromatography”. *J Chrom A.* **668** (2): 255-284.

[50] Stahlberg, J (1999). “Retention models for ions in chromatography”. *J Chrom A.* **855** (1): 3-55.

[51] Chen, J (1993). “Electrical double-layer models of ion-modified (ion-pair) reversed-phase liquid chromatography”. *J Chrom A.* **656** (2): 549-576.

[52] Cecci, T (2010). *Ion Pair Chromatography and Related Technologies*. CRC Press, Boca Raton. 99-103.

[53] Horvath, C, Melander, W (1977). “Enhancement of Retention by Ion-Pair Formation in Liquid Chromatography with Nonpolar Stationary Phases”. *Anal. Chem.* **49** (14): 2295-2305.

[54] Kissinger, PT, Refshaug, C (1973). "Electrochemical Detector for Liquid Chromatography With Picogram Sensitivity". *Anal. Lett.* **6** (5): 465-477.

[55] Refshaug, C, Kissinger, PT (1974). "New High-Performance Liquid-Chromatographic Analysis of Brain Catecholamines". *Life Sci.* **15** (7): 1335-1342.

[56] Kissinger, P, Heineman, W (1996). *Laboratory Techniques in Electroanalytical Chemistry*. 2nd Edition. Boca Raton: CRC Press.

[57] Bard, AJ, Faulkner, LR (2000). *Electrochemical Methods: Fundamentals and Applications*. 2nd Edition. John Wiley & Sons.

[58] Zoski, CG (2007). *Handbook of Electrochemistry*. Elsevier Science.

[59] Sawyer, DT, Sobkowiak, A (1995) *Electrochemistry for Chemists*. 2nd Ed. J. Wiley & Sons.

[60] Stahl, M, Bouw, R. (2002) "Human Microdialysis". *Curr. Pharm. Biotechnol.* **3** (2): 165-78.

[61] Jorgensen, A, Groth, L (1997). "In vitro microdialysis of hydrophilic and lipophilic compounds". *Analytica Chemica Acta.* **355** (1): 75-83.

[62] Carneheim, C, Stahle, L (1991). "Microdialysis of lipophilic compounds: a methodological study". *Pharmacol. Toxicol.* **69** (5): 378-380.

[63] Chaurasia, CS, Muller, M (2007). "AAPS-FDA Workshop White Paper: Microdialysis Principles, Application and Regulatory Perspectives". *Pharm Res.* **24** (5): 1014-1025.

[64] Bird, BR, Stewart, WE (1960) *A Transport Phenomena*. Wiley.

[65] Chaurasia, CR, Muller, M (2005) AAPS-FDA Workshop White Paper: Microdialysis Principles, Application, and Regulatory Perspectives Report From the Joint AAPS-FDA Workshop, Nashville, TN.

[66] Davies, MI, Cooper, JD (2000) "Analytical considerations for microdialysis sampling." *Adv Drug Deliv Rev.* **45** (1-2): 169-188.

[67] DeLange, ECM, De Bock, AH (1998) "BBB transport and P-glycoprotein functionality using MDR1A(-/-) and wild-type mice: total brain versus microdialysis concentration profiles of rhodamine-123" *Pharmacol. Res.* **15**: 1657-1665.

2. Methods

2.1 Introduction

Nitrite and nitrate have been separated using capillary electrophoresis and detected with UV-absorbance or fluorescence following derivatization [1]. However, using these methods to detect both nitrite and nitrate is problematic. UV-absorbance detection is not an amenable method for nitrite quantitation *in vivo* as the compound is present in sub-micromolar concentrations. Furthermore, derivatization of these analytes to produce a fluorescent compound requires larger sample volumes as well as steps needed to reduce nitrate to nitrite. Nitrite and nitrate have been separated by LC and detected by UV-absorbance and EC methods [2, 3]. **Figure 2.1** shows the instrumental setup for analysis of these compounds. The advantage of using these methods of separation and detection is the elimination of sample preparation steps, allowing for a high throughput analysis. In this thesis, LC-EC-UV was used to separate, identify, and quantify these analytes. In addition, *in vitro* studies were conducted with a nitric oxide donor used by the S. Lunte research group.

2.2 Objectives

The purpose of this research was to develop an LC-EC-UV method capable of separating and detecting secondary products of RNS in microdialysis samples. Optimizations of nitrite and nitrate detector parameters were accomplished to allow for the lowest detection limits possible. Nitrite and nitrate

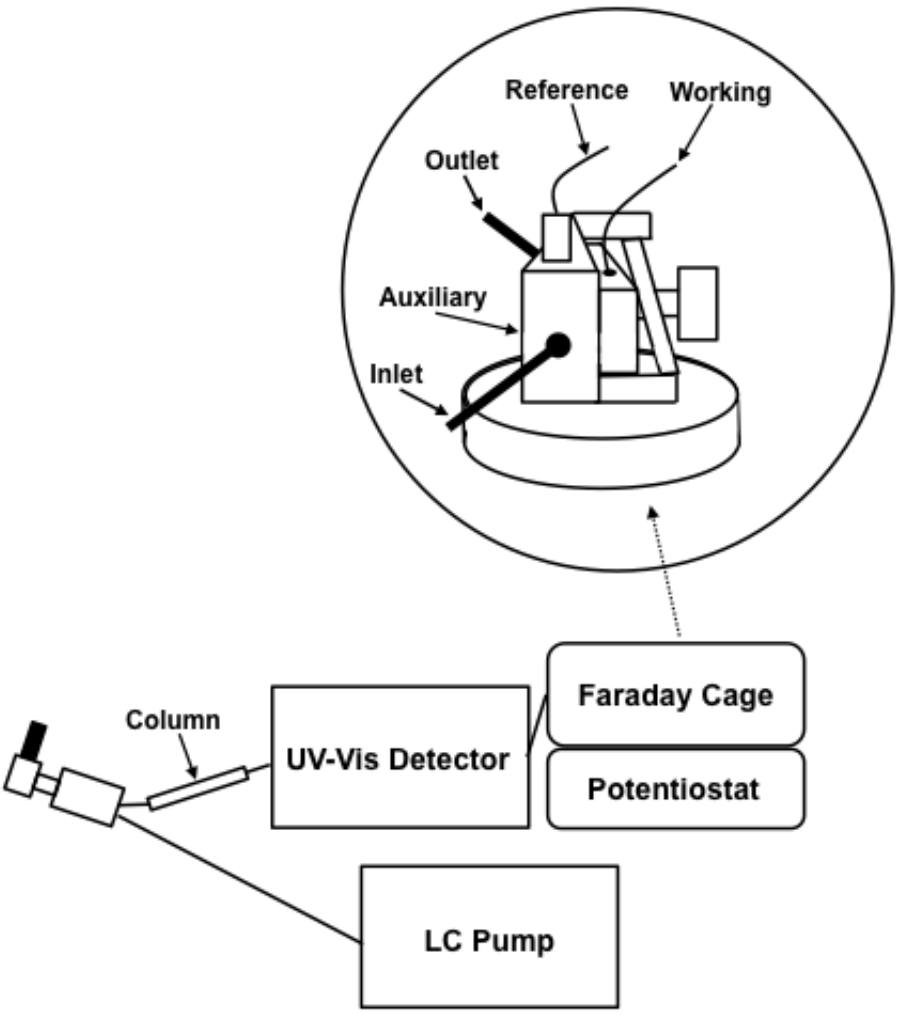

Figure 2.1: Schematic of LC-EC-UV instrument setup.

standard separation and retention times were optimized to allow for identification and quantitation in microdialysis samples. In addition, microdialysis probe calibration was conducted to determine more realistic *in vivo* concentrations of nitrite and nitrate. Finally, an *in vitro* investigation of NO release from a donor evaluated the ability of the method to indirectly detect RNS formation by analysis of stable secondary products was performed.

2.3 Nitric oxide product standard separation and detection, and separation of basal microdialysis samples

2.3.1 Optimization of nitric oxide primary and secondary product standard separation

Studies were first conducted using nitrite and nitrate standards in mobile phase using LC-UV (SPD-10A, Shimadzu Corp., Kyoto, Japan) to determine their retention times as well as peak efficiencies and resolution. The column used was a Phenomenex ® Synergi 4 µm Hydro-RP 80 Å (Phenomenex, Torrance, CA) with dimensions of 2 mm x 250 mm. The mobile phase was 1 mM tetrabutylammonium hydroxide (TBAOH) and 10 mM sodium acetate at a pH of 5.0. Mixtures of nitrite and nitrate in mobile phase were injected for the analysis using a Rheodyne ® 7725i injector (IDEX Health & Sci., Rohnert Park, CA). The use of an ion-pair reagent allowed for sufficient retention of polar, hydrophilic nitrite and nitrate beyond the void volume, allowing for separation, identification, and quantitation of these compounds. The purpose behind using acetic acid was to influence the degree of interaction of nitrite/nitrate and the charged head groups of the ion-pair reagent, and to serve as an electrolyte for the

electrochemical system next in line for development. The pH of the mobile phase was increased beyond that of the pKa of acetic acid (4.74), allowing for a majority (66%) of this compound to be present as the conjugate base needed for conduction in the electrochemical system. Separation of nitrite and nitrate was achieved. Because the eventual goal was to work in a biological matrix with many other compounds, it was desired to optimize mobile phase conditions further. The goals of additional optimization were to reduce the time required for a chromatographic run and allow for the sharpest peak shape and highest resolution possible. It became necessary to reduce the concentration of TBAOH (0.5 mM) and increase the concentration of acetate (50 mM) to ensure that adequately separated nitrite and nitrate peaks were eluting in under 10 minutes. **Figure 2.2** shows these separations.

Acetate appeared to have the greatest influence on the retention times of nitrite and nitrate. It was finally decided to increase the acetate concentration to 100mM to accomplish the separation accomplished in about 5 minutes. The presence of this organic acid acted to reduce the extent of interaction of nitrite and nitrate with the ion-pair modified stationary phase. As a result of molecular structure, charge distribution, and size differences, nitrate had a longer retention time than nitrite. At pH 5.0, acetate was sufficiently deprotonated, leaving it free to compete with nitrite and nitrate for the positively charged ion-pair modified stationary phase and reducing the retention times of these analytes as a result.

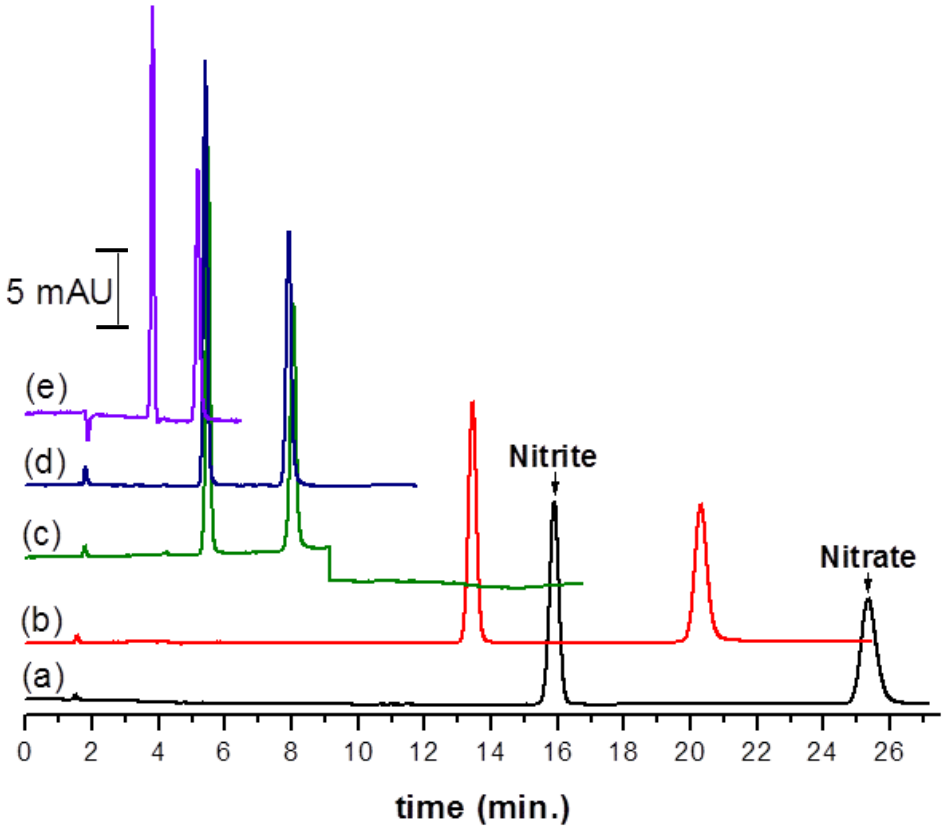

Figure 2.2: Chromatograms of nitrite and nitrate standards injected. The graph is an overlay of the UV chromatograms showing a reduction of retention times for nitrite and nitrate standards as well as reductions in peak widths of each analyte. Standards are in mobile phase at a flow rate of 0.4 mL/min. and are detected at a wavelength of 220 nm. Traces are: (a) 1 mM TBAOH, 10 mM acetate, pH 5.0; (b) 0.5 mM TBAOH, 10 mM acetate, pH 5.0; (c) 0.5 mM TBAOH, 50 mM acetate, pH 5.0; (d) 0.5 mM TBAOH, 50 mM acetate, pH 6.0; (e) 0.5 mM TBAOH, 100 mM acetate, pH 6.0.

Overlays of nitrite and nitrate as a result of mobile phase optimization are shown in **Figure 2.2**.

2.3.2 Optimization of nitric oxide secondary product detection and separation in mobile phase and Ringer's solutions

The EC system consisting of an electrochemical cell, CC-5 faradaic cage, and LC-4C amperometric detector (Bioanalytical Systems Inc., West Lafayette, IN) was set up initially with an applied potential of +0.750 V as an initial proof of concept. After running additional hydrodynamic voltammograms, it was decided to increase the applied potential of the EC system to +1.0V and the pH of the mobile phase to 6.0. The specific reason this change was made was to give a greater response in the electrochemical system. Increasing the pH of the mobile phase deprotonated more of the acetic acid, increasing the concentration of the electrolyte acetate form. Retention times were insignificantly affected, most likely due to a lack of significant equilibrium conditions disruption with ion-pair reagent adsorbed to the stationary phase. In addition, increasing the applied potential of the amperometric detector allowed for greater oxidation of nitrite. Maximizing detector response for an analyte is desired, to allow for the lowest detection limits possible. **Figure 2.3** shows a comparison of the effects of pH and applied potential changes upon detector response for a nitrite standard. Both an increase in pH and applied potential increased the oxidation of nitrite. The ultimate goal of mobile phase modifications was to separate nitrite and nitrate and detect the lowest concentrations possible of nitrite in Ringer's solution or artificial cerebral

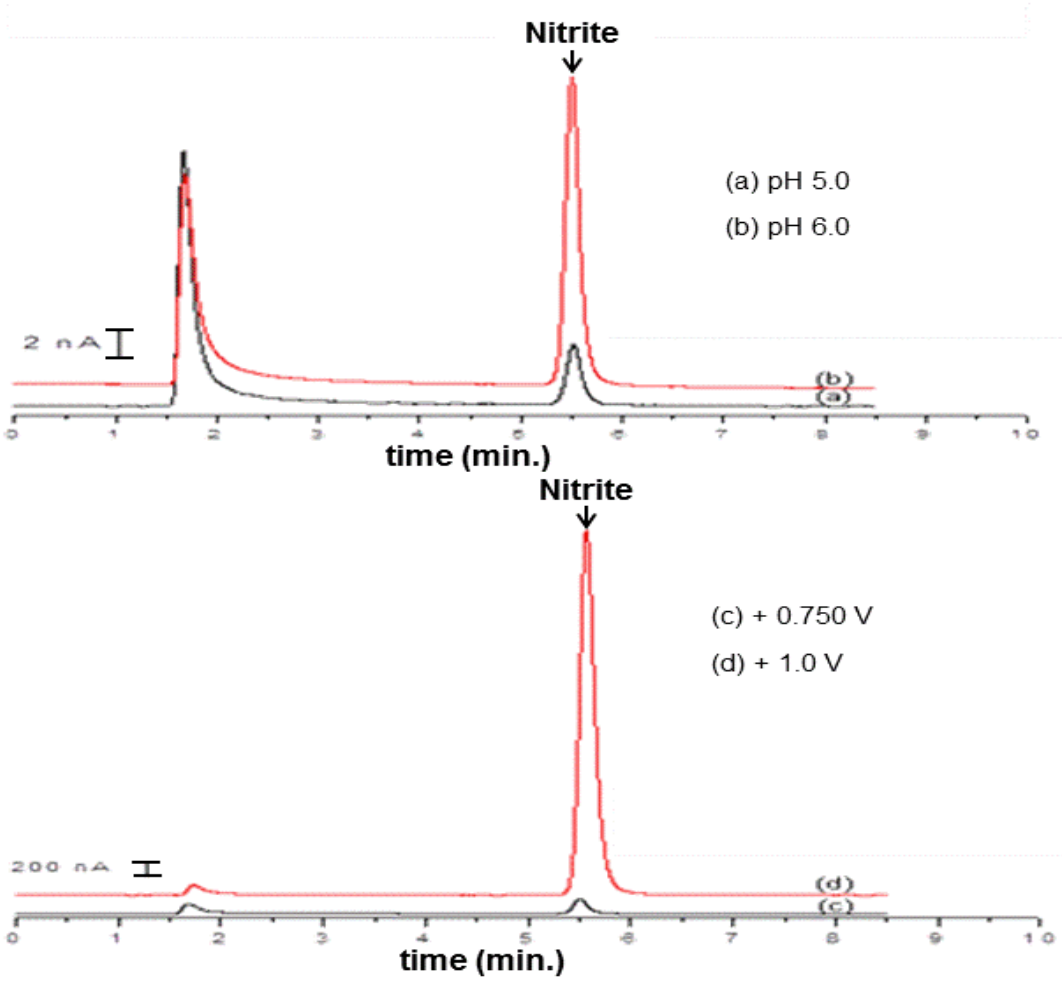

Figure 2.3: Overlays of chromatograms comparing changes in amperometric detector response as a result of increasing mobile phase pH and applied potential at a flow rate of 0.4 mL/min. In the top overlay, trace (a) consists of nitrite standard dissolved in and injected using mobile phase composed of 50 mM acetate and 0.5 mM TBAOH at a pH of 5.0. Trace (b) consists of nitrite standard dissolved in and injected using mobile phase composed of 50 mM Acetate, 0.5 mM TBAOH at a pH of 6.0. In the bottom overlay, trace (c) is an applied potential of + 0.750 V, and trace (d) is an applied potential of + 1.0 V for amperometric detection of nitrite.

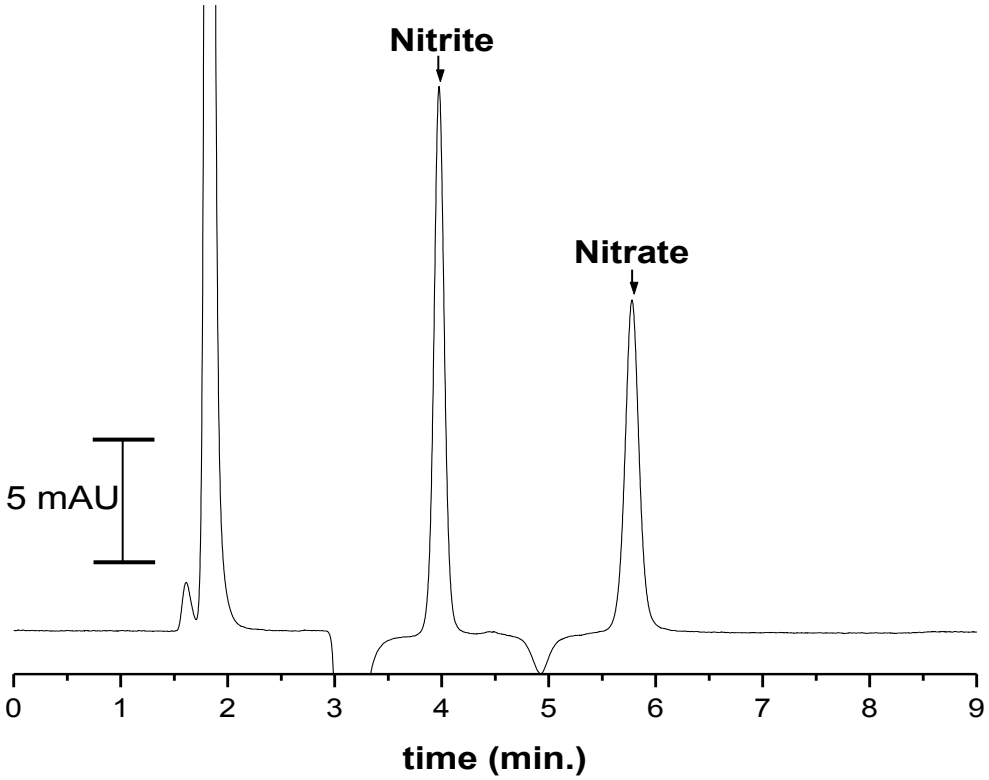

Figure 2.4: UV chromatogram of nitrite and nitrate standards in Ringer's solution. Standards (50 uM) are dissolved in Ringer's Solution and injected using mobile phase of 100 mM acetate and 0.5 mM TBAOH at a pH of 6.0 with a flow rate of 0.4 mL/min. Standards were detected at 220 nm.

spinal fluid (aCSF) in preparation for microdialysis sampling *in-vivo*. **Figure 2.4** shows this separation using UV detection, allowing for visualization of both nitrite and nitrate separation on the same chromatogram.

2.3.3 Separation and detection optimization of nitrite and nitrate in basal microdialysis samples

Dialysate samples from various sources were examined. First, basal rat plasma dialysate samples were analyzed. Nitrite and nitrate were identified by retention times in comparison to standards. At this stage, the analysis of plasma dialysate samples was to test the method as a proof of concept to determine if analytes in dialysate could be detected. The initial goal was to use this method to examine the presence of nitrite and nitrate in the brain, however microdialysis samples from a variety of tissues were available and worth examining.

Prefrontal cortex, liver, and plasma dialysis samples were analyzed. Studying rat dialysate samples from the pre-frontal cortex of the brain and the plasma, as well as liver, as modifications of the method progressed brought up an interesting problem: the co-elution of an electrochemically active compound with nitrite. These chromatograms are shown in **Figure 2.5**. The concentration of acetate was reduced to 75mM in order to retain the analytes longer on the column to increase separation between the interferent and nitrite. In addition, the pH of the mobile phase was reduced to 4.0 to allow for complete resolution of the interferent from nitrite. Under these new mobile phase conditions, dialysate from

the lumen of the large intestine and from the liver of a rat was analyzed. Separation between nitrate and the interferent was achieved; however, detection of nitrate in lumen dialysate proved difficult, as shown in **Figure 2.6**.

UV detector wavelength changes were evaluated as well as that of the detector filter. Closer to 205 nm, analyte signal response was high, but elevation in noise was significant. On the other hand, noise was significantly lower closer to 230 nm, but with a reduction in analyte signal. The best signal to noise (S/N) was achieved at 220 nm. Filter settings can be adjusted to remove high frequency noise by altering the time constant, improving S/N. Setting the response to a lower value of less than 5 (1.5 sec) increases the response with a minimal increase in noise. In addition, setting the response to a value of 6 or higher (3.0 sec) reduces the response, but also substantially reduces noise [4]. Adjustments of filter settings were attempted, with selection of one providing the best S/N. The optimal S/N setting was achieved by increasing the time constant of the filter from 0.5 sec to 3.0 sec, achieved by changing the response from 3 to 6, respectively.

The pursuit of animal studies demonstrated the need for a method capable of sub-μM limits of detection utilizing sample injection sizes below 5uL. To minimize the sample size needed for analysis as well as reduce mobile phase required for analysis, the original 2x250 mm column was replaced with one of a smaller inner diameter and length with identical stationary phase (Phenomenex Synergi 4 μm Hydro-RP 80 Å, 1 mm x 150 mm). A decrease in column diameter

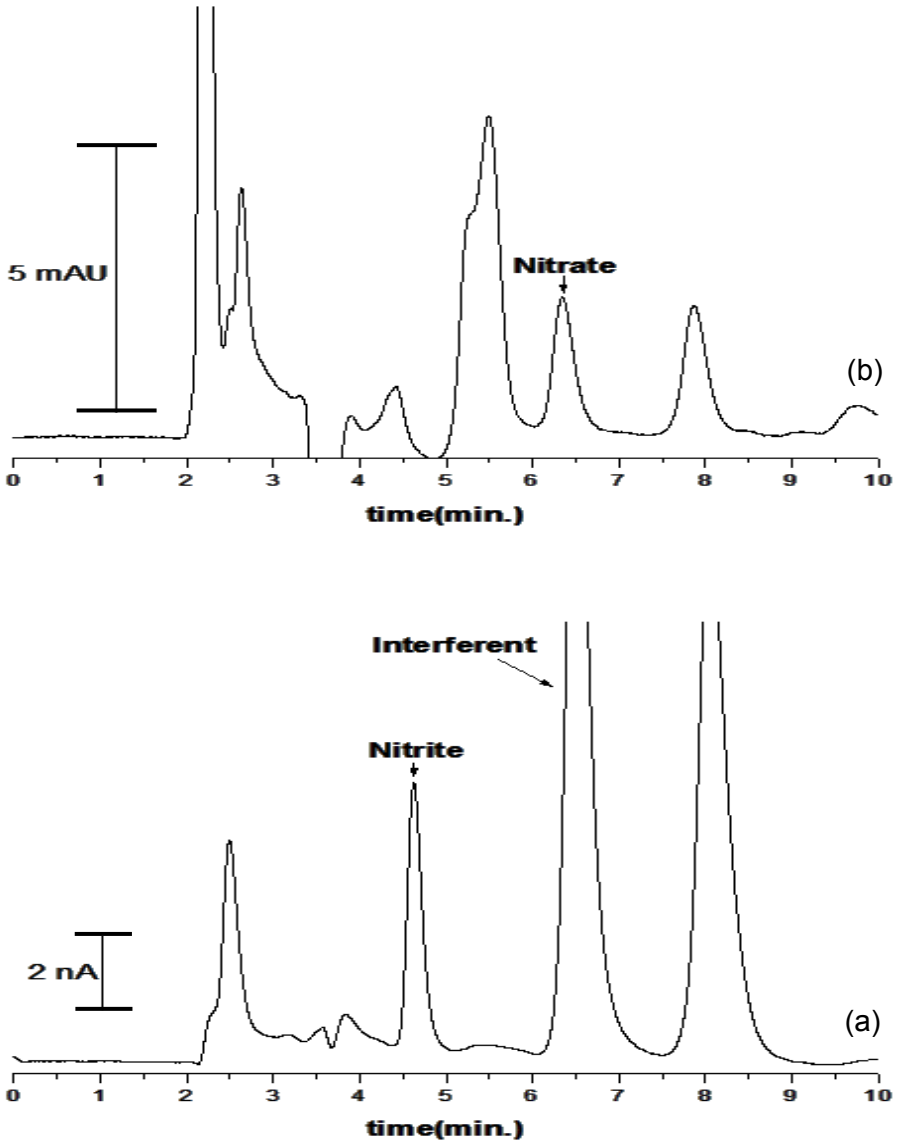

Figure 2.5: Chromatograms of rat plasma dialysate. Mobile phase conditions are the same as shown in the previous figure. Nitrite and nitrate are detected using +1.0 V as an applied potential (a) and 220 nm as a detection wavelength (b), respectively. Note the presence of an electrochemically active interferent co-eluting with nitrate.

increased mobile phase back pressure and required a decrease in flow rate from 0.4 mL/min. to 0.1 mL/min. Furthermore, the injection loop and corresponding injection volumes were reduced from 5 µL and 3 µL to that of 2 µL and 1 µL, respectively. Upon running standards through the new column under previous chromatographic conditions, inadequate separation of nitrite from an interferent, as well as the presence of significant background noise on nitrate chromatograms, was problematic. A reduction in acetate concentration to 50 mM and an increase in the ion-pair reagent to 2.5 mM improved both separation and reduced noise. From a reduction in column dimensions, it was possible to obtain an increase in nitrite and nitrate peak response by a factor of 4. A reduction in injection volume by a factor of 3 resulted in a decrease in response by a factor of close to 3. What this means is that taking into consideration both the change to the smaller column (increased response by 4) as well as a reduction in injection volume (decreasing the initial gain in response that resulted from switching to a small column by a factor of 3), that the change in peak response resulting from these modifications is approximately 1.5 times greater than that achieved with the larger column and injection loop. A table showing these modifications as well as changes in peak response for nitrite is shown in **Figure 2.7**.

The decision was made to change from an organic acid to an inorganic one. The premise behind using another type of acid was to minimize background noise. Acetate absorbs strongly in the UV region at less than 230 nm where analysis occurs. Sulfuric acid was chosen as it does not absorb in the UV region

of analysis and after several concentration optimization experiments, was added at a concentration of 15 mM. Subsequently, tetrabutylammonium hydroxide (TBAOH) was increased to 12 mM and the final pH set to 4.0. A further increase in pH would increase the oxidation of nitrite, however resulted in reduced resolution between the analyte and other compounds. Furthermore, due to a combination of a review of past hydrodynamic voltammograms and the change in mobile phase conditions, it was also decided to increase the applied potential from +1.0 V to +1.025 V. The reasoning behind this increase is that it puts nitrite response in the middle of a plateau, such that any minor potential fluctuation will not affect response. The final conditions were 12 mM TBAOH, 15 mM H_2SO_4, at pH: 4.0, with detection conditions at 220 nm for absorbance and an applied potential of +1.025 V vs. Ag/AgCl for amperometric detection.

2.4 Method Validation

All validation parameters were evaluated according to established good laboratory procedures [5]. These parameters were determined for nitrite and nitrate standards in Ringer's Solution and saline solution.

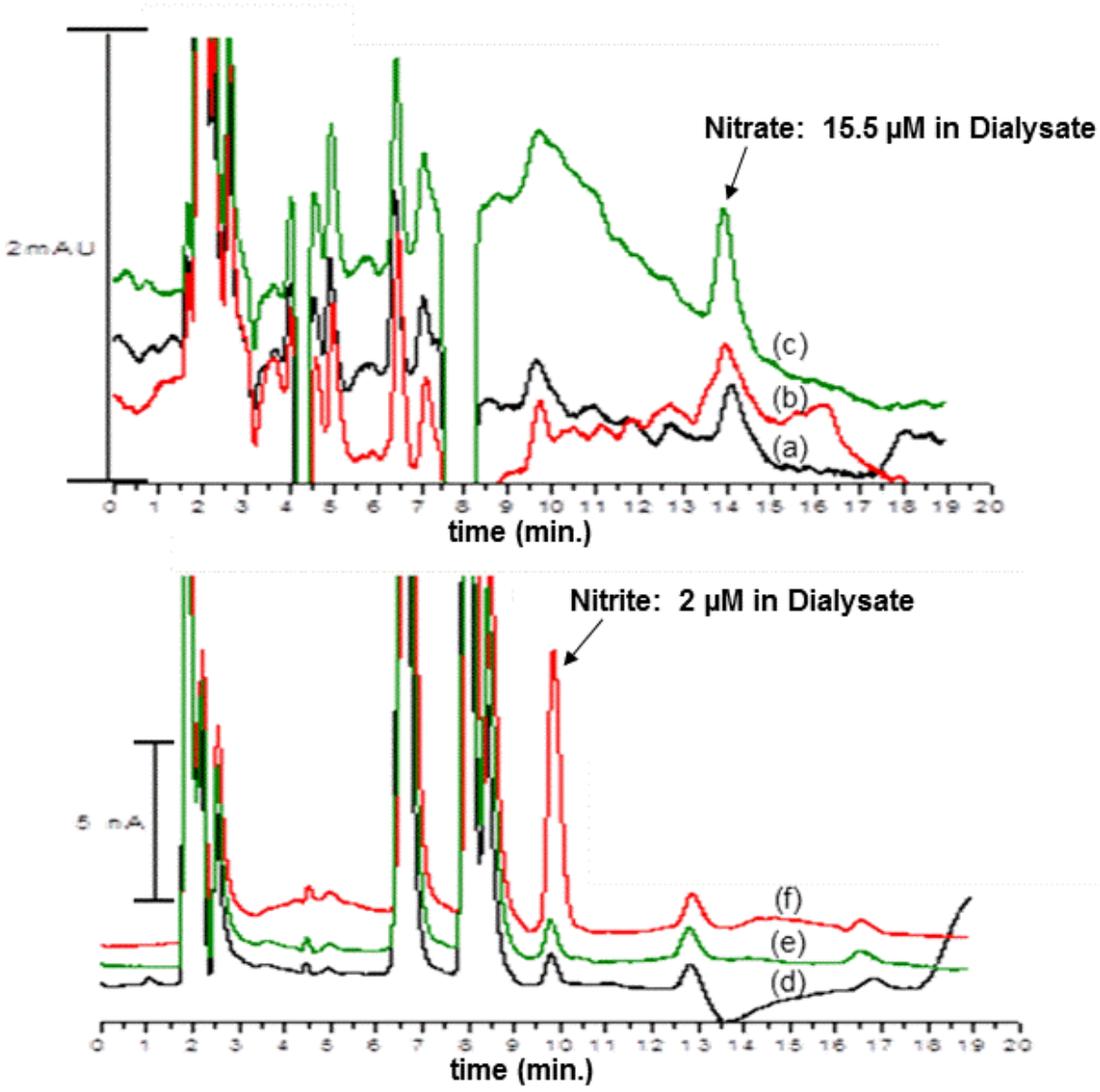
Nitrate: 15.5 µM in Dialysate
2mAU
(c)
(b)
(a)
0 1 2 3 4 5 6 7 8 9 10 11 12 13 14 15 16 17 18 19 20
time (min.)
Nitrite: 2 µM in Dialysate
5 nA
(f)
(e)
(d)
0 1 2 3 4 5 6 7 8 9 10 11 12 13 14 15 16 17 18 19 20
time (min.)

Figure 2.6: Chromatograms of spiked rat large intestine lumen (probe implanted 5 cm superior of rectum) dialysate. Note that on the UV chromatogram, quantitation of nitrate is problematic. Trace (a) is 5 cm lumen dialysate, trace (b) is 5 cm lumen dialysate with 2 μM nitrite spiked in, and trace (c) is 5 cm lumen dialysate spiked with 13 μM nitrite for the top UV overlay. For the bottom EC overlay, trace (d) is 5 cm lumen dialysate, trace (e) 13 μM nitrate spiked in, and trace (f) is 2 μM nitrite spiked in. Nitrite and nitrate were detected using the same applied potential and wavelength as in the previous figure. Mobile phase conditions were comprised of 75 mM acetate, 0.5 mM TBAOH at a pH of 4.0. Detection conditions were 220 nm for UV-absorbance and an applied potential of +1.025 V vs. Ag/AgCl for amperometric detection

Column, Injection Loop, and Mobile Phase Modifications		
Column	Phenomenex Synergi ® Hydro RP 2x250mm 4µm 80Å	Phenomenex Synergi ® Hydro RP 1x150mm 4µm 80Å
Mobile Phase	0.5 mM TBAOH, 75 mM acetate, pH: 4.0	2.5 mM TBAOH, 50 mM acetate, pH: 4.0
Flow Rate	0.4 mL/min.	0.1 mL/min.
Injection Loop Volume	5 µL	2 µL
Injection Volume	3 µL	1 µL
Average Nitrite Response	6.97 nA	11.6 nA

Figure 2.7: Table comparing changes made in column, injection loop, and mobile phase and their influence on response of a 1µM nitrite standard injected.

2.4.1 Variability in Retention Times and Peak Areas

The retention times of these compounds were examined through repetitive injections. Intraday RSD values for nitrite and nitrate standards were calculated as 1.25% and 0.239% respectively, well below 5%. Multiple injections of nitrite and nitrate standards were evalutated for peak areas. RSD values for peak areas of nitrite and nitrate were 2.66% and 1.74%, respectively.

2.4.2 Limits of Detection (LOD) and Quantitation (LOQ)

The limits of detection for these compounds were established through the successive dilution and injection of nitrite and nitrate standards in aCSF, Ringer's solution, and saline solution in those solutions, respectively. For the analytes of nitrite and nitrate the limits of detection (S/N = 3) were 96 nM and 700 nM, respectively. For the analytes nitrite and nitrate the lower limits of quantitation (S/N = 10) were 320 nM and 2.7 μM, respectively. LOD and LOQ values were independent of the solution standards were dissolved in.

2.4.3 Linear Range of Nitrite and Nitrate

The linear ranges for nitrite and nitrate were established through the injection, separation, detection, and quantitation of nitrite standards present in aCSF, Ringer's solution, and saline solution in concentrations from 320 nM to 1000 μM. Plots of response versus concentration were made for each analyte, with determined R^2 values of 0.999. Nitrite was determined to have a linear range of 320 nM-1000 μM. The value of 320 mM is at the limit of quantitation for this

	Standards	
Parameter	**Nitrite**	**Nitrate**
Intra-day Retention RSD	1.25%	0.239%
Intra-day Peak Area RSD	2.66%	1.74%
Limit of Detection (S/N)=3	96nM	710nM
Limit of Quantitation (S/N)=10	320nM	2.4μM
Linear Range	320nM-1000μM	3-1000μM

Figure 2.8: Method validation parameters. Nitrite was evaulated using amperometric detection at an applied potential of + 1.025 V. Nitrate was evaluated using an absorbance wavelength of 220 nm. Note the lower detection and quantitation limits allowed by amperometric detection of nitrite.

micromolar levels than that of nitrite in basal dialysate, making UV-vis amenable for nitrate concentration change studies. **Figure 2.8** shows a table of the validation of these parameters.

analyte using the developed EC cell-based amperometric detection method. Nitrate was determined to have a linear range of 2.7-1000 μM. The value of 2.7 μM is at the limit of quantitation established by the development of the UV-Vis detection method. The higher limit of quantitation of nitrate was due to higher limits of detection for this compound, a limitation of the UV-Vis detection system. However, nitrate was found to be present in higher concentrations of low micromolar levels than that of nitrite in basal dialysate, making UV-vis amenable for nitrate concentration change studies. **Figure 2.8** shows a table of the validation of these parameters.

2.5 *In vitro* studies

2.5.1 Introduction of Diethylamine (DEA) NONOate

DEA NONOate is a member of the NONOate class of compounds. What makes these compounds similar is that they are all composed of the general chemical formula $R^1R^2N\text{-}(NO^-)\text{-}N{=}O$. In this formula, R^1 and R^2 are alkyl groups and are the only differences in structure between the various NONOates. These compounds act as NO donors when dissolved in aqueous solution, with a wide variety of literature supporting their study [6, 7, 8, 9]. The structure of diethylamine NONOate consists of two ethyl groups attached to a nitrogen attached to a NO- group and terminal nitrosyl group. It is these adjacent NO containing groups which form two NO molecules upon decomposition [10].

The stability of these NO donors is pH dependent. Below pH 8.0, DEA NONOate decomposes in a first-order process. At pH 7.4 and temperature of

37°C, this compound has a half-life of 2 minutes. In addition, one mole DEA NONOate releases 2 moles of NO upon decomposition [11].

2.5.2 *In vitro* collection of NO from DEA NONOate sampling

To evaluate the relative generation of NO and nitrate from DEA NONOate, an *in vitro* cell was used in which various concentrations of DEA NONOate was added. The DEA NONOate (Cayman Chemical, Ann Arbor, MI) was made up in a vial in a 1mL volume at a concentration of 10mg/mL using Ringer's solution containing 0.1M NaOH (Sigma, St. Louis, MO). This stock solution was then diluted five-fold to 2 mg/mL or 1 mM using Ringer's solution. The probe was immersed in the cell containing the DEA NONOate standard made up in Ringer's solution, stirred at a temperature of 37ºC, to mimic *in vivo* conditions as closely as possible. A 1mL syringe containing aCSF was used to perfuse the probe at a flow rate of 1µL/min. Dialysate was collected in microcentrifuge tubes at 10 minute intervals. Collected samples were then analyzed using the LC-UV-EC system to determine the overall change in response reflective of concentration. Upon completion of the 1 mM *in vitro* study, addition studies were conducted with 100µM and 1 µM concentrations. An overlay of two chromatograms of nitrite standard and a sampling from 100 minutes after the start of the 1 mM DEA NONOate introduction to the *in vitro* cell are shown in **Figure 2.9**. It is clear that the peak resulting from the DEA NONOate sampling experiment is nitrite.

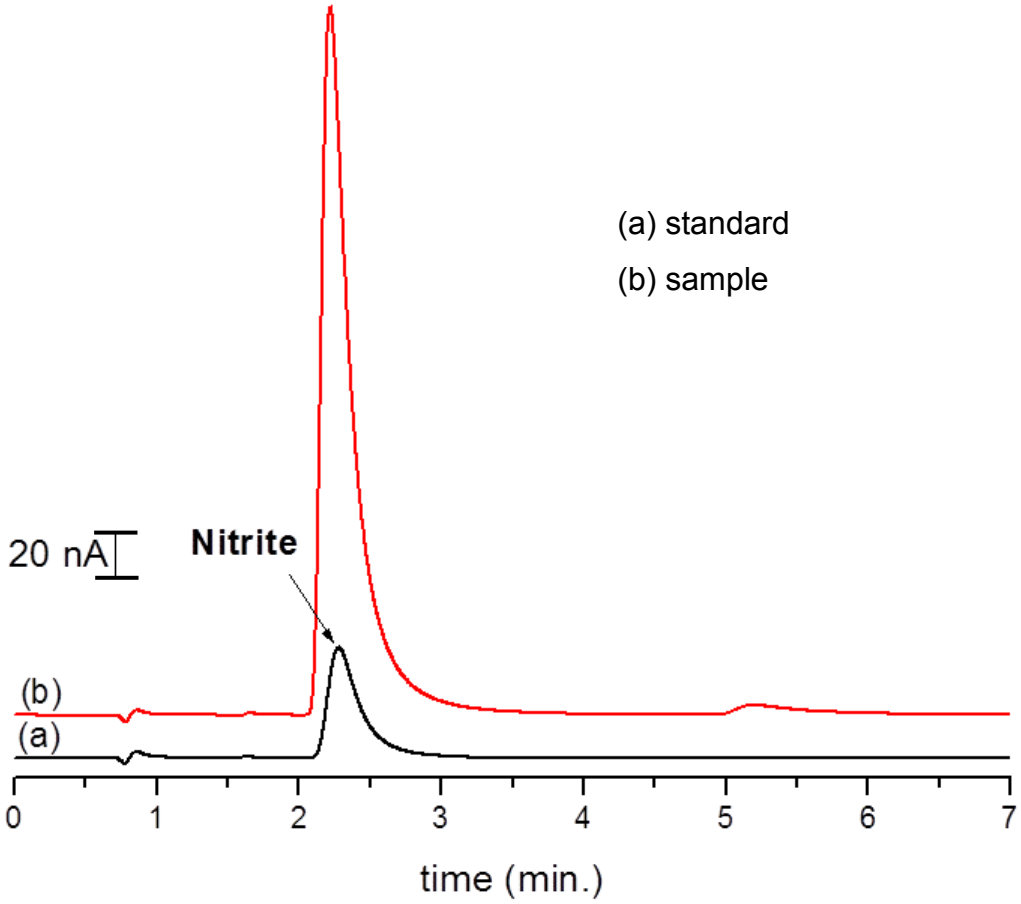

Figure 2.9: Overlay of chromatograms from 1 mM DEA NONOate sample and 100 µM nitrite Standard. The peak from DEA NONOate administration is nitrite. Trace (a) is a 100 µM nitrite standard and trace (b) is nitrite produced from a 1 mM DEA NONOate sample. Mobile phase conditions are comprised of 12 mM TBAOH, 15 mM H_2SO_4, pH 4.0 at a flow rate of 0.1 mL/min. Nitrite was detected using an applied potential of +1.025 V.

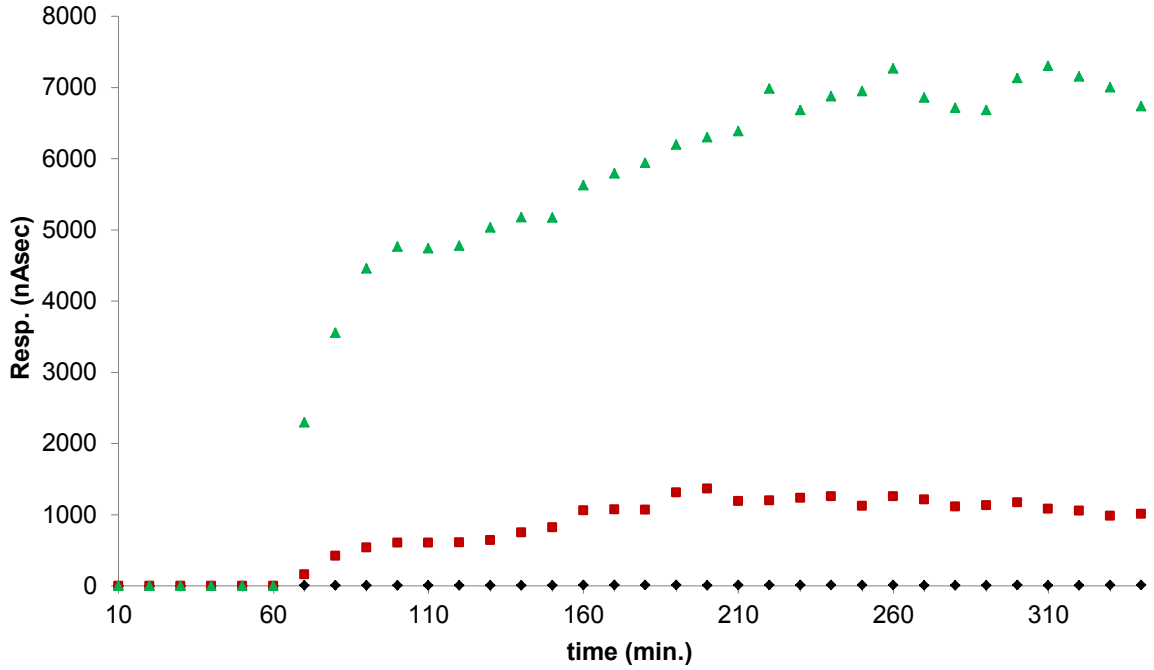
8000
7000
6000
5000
4000
3000
2000
1000
0
Resp. (nAsec)
10
60
110
160
210
260
310
time (min.)

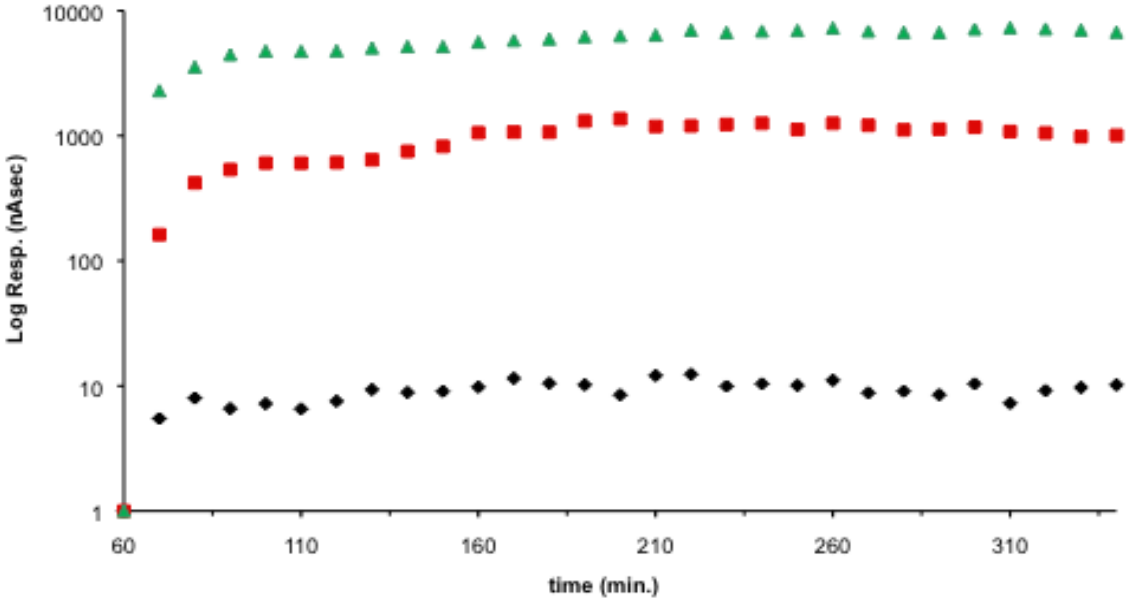
10000
1000
100
10
1
Log Resp. (nAsec)
60
110
160
210
260
310
time (min.)

Figure 2.10: Comparison of response and log response due to nitrite obtained from 3 DEA NONOate concentrations in *in vitro* studies during time course experiments after 60 minutes of basal collection. DEA NONOate concentrations of 1μM, 100uM, and 1mM were used in these experiments. The bottom diamond plot is 1 μM DEA NONOate, the middle square plot is 100 μM DEA NONOate, and the top triangle plot is 1 mM DEA NONOate. Mobile phase conditions are the same as in the previous figure. Nitrite detection parameters are the same as previously established.

Additionally, experimental graphs of response for nitrite versus time for the 3 concentrations used in the experiments are shown in **Figure 2.10**. Similar DEA NONOate studies have been conducted by the S. Lunte research group and showed similar results [6].

2.6 Microdialysis probe calibration

To evaluate the relative recovery of nitrite and nitrate based upon probe type and flow rate used for experiments, an *in vitro* microdialysis cell was used in which nitrite and nitrate standards were added. A 1mL syringe containing aCSF was used to perfuse the probe at a flow rate of 1μL/min. Dialysate was collected in microcentrifuge tubes at 10 minute intervals. Collected samples were then analyzed using the LC-UV-EC system to determine their concentrations. This experiment served to monitor recovery of these analytes to compensate for resistance to analyte diffusion from the sampling environment to the internal portion of the probe as dialysate.

The process of recovery is composed of several steps where compound of interest first moves through the tissue present in the proximal environment. When the compound encounters the microdialysis membrane, it then diffuses due to the presence of an osmotic gradient. In other words, the concentration of the analyte in the surrounding medium is greater than that in the perfusate, so the analyte will cross the membrane to establish an equal concentration on both sides. Finally, once present in the dialysate the analyte freely diffuses.

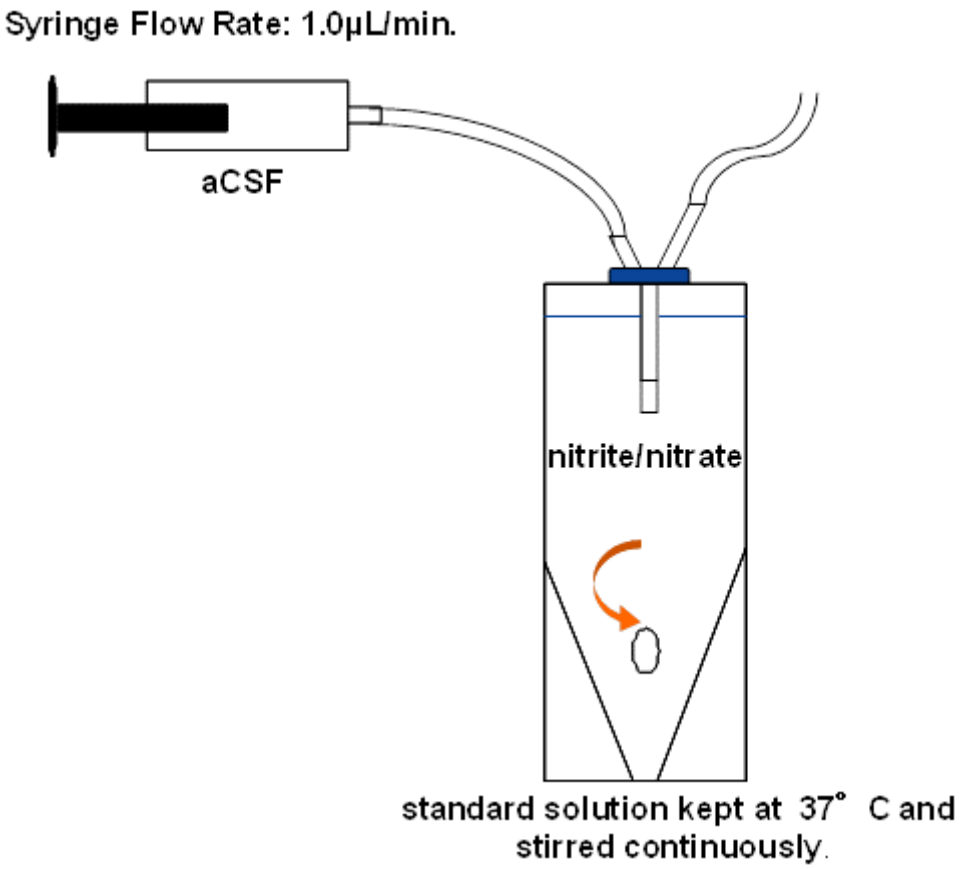

Figure 2.11: *In vitro* cell setup with analyte stirred and maintained at physiological temperature. Artificial cerebrospinal fluid (aSCF) is perfused through the probe and analyte is collected as dialysate.

Achievement of a steady-state concentration prior to a decline in concentration in the sampling vessel was used to determine analyte recovery. A simplified equation shown in the first chapter ($R = \frac{C_{dial.}}{C_{sample}} x100\%$) was used as a good determinant of analyte recovery. The steady-state concentration found was divided by the known concentration in the cell and multiplied by 100 to give the relative recovery of each analyte. The relative recoveries for nitrite and nitrate were found to be $49.3 \pm 0.6\%$ and $37 \pm 1\%$, respectively. **Figure 2.11** shows the *in vitro* cell setup.

2.7 Analysis of microdialysis samples

Upon development of ideal separation conditions for nitrite and nitrate standards, microdialysis samples collected under basal conditions in rats were analyzed. Two regions were examined in the final stage of method development. Dialysate collected from the mucosal region of the large intestine and that of the hippocampus region of the brain were studied. To identify peaks, all samples were spiked with nitrite and nitrate standards. All samples were injected into the chromatographic system and analyzed by UV and EC detection. Resulting chromatograms are shown in **Figures 2.12** and **2.13**.

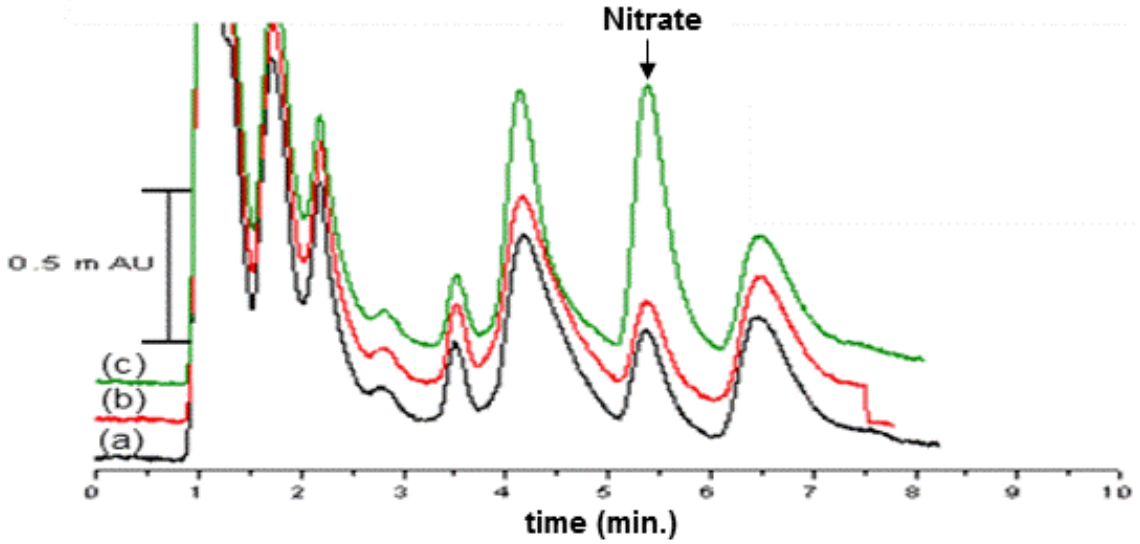
Nitrate
0.5 m AU
(c)
(b)
(a)
0
1
2
3
4
5
6
7
8
9
10
time (min.)

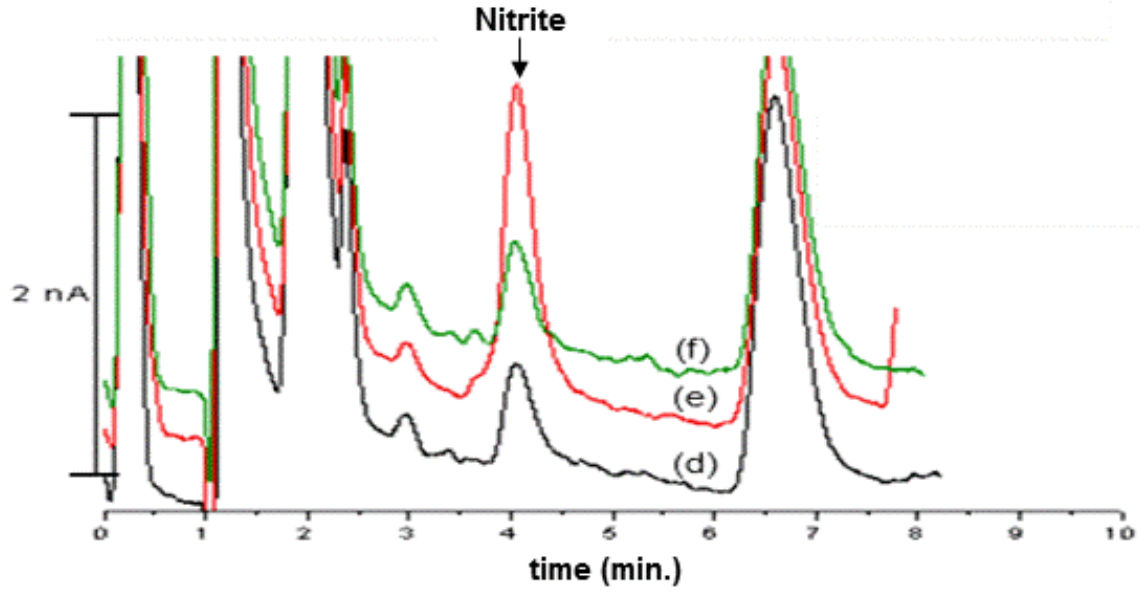
Nitrite
2 nA
(f)
(e)
(d)
0
1
2
3
4
5
6
7
8
9
10
time (min.)

Figure 2.12: Rat intestine 5 cm submucosa (probe 5 cm superior to the rectum) dialysate samples spiked with nitrite and nitrate standards. In the top overlay, trace (a) is 5 cm submucosa, trace (b) is 5 cm submucosa spiked with 1 μM nitrite, and trace (c) showing an increased response for nitrite is 5 cm submucosa with 13 μM nitrite spiked in for the top UV overlay. The bottom overlay, trace (d) is 5 cm submucosa, trace (e) is 5 cm submucosa spiked with 1μM nitrite, and trace (f) is 5 cm submucosa with 13 μM nitrite spiked in. Mobile phase conditions consist of 12 mM TBAOH and 15 mM H_2SO_4 at a pH of 4.0. Mobile phase flow rate was 0.1 mL/min. Nitrite and nitrate are detected using the same parameters as previously established.

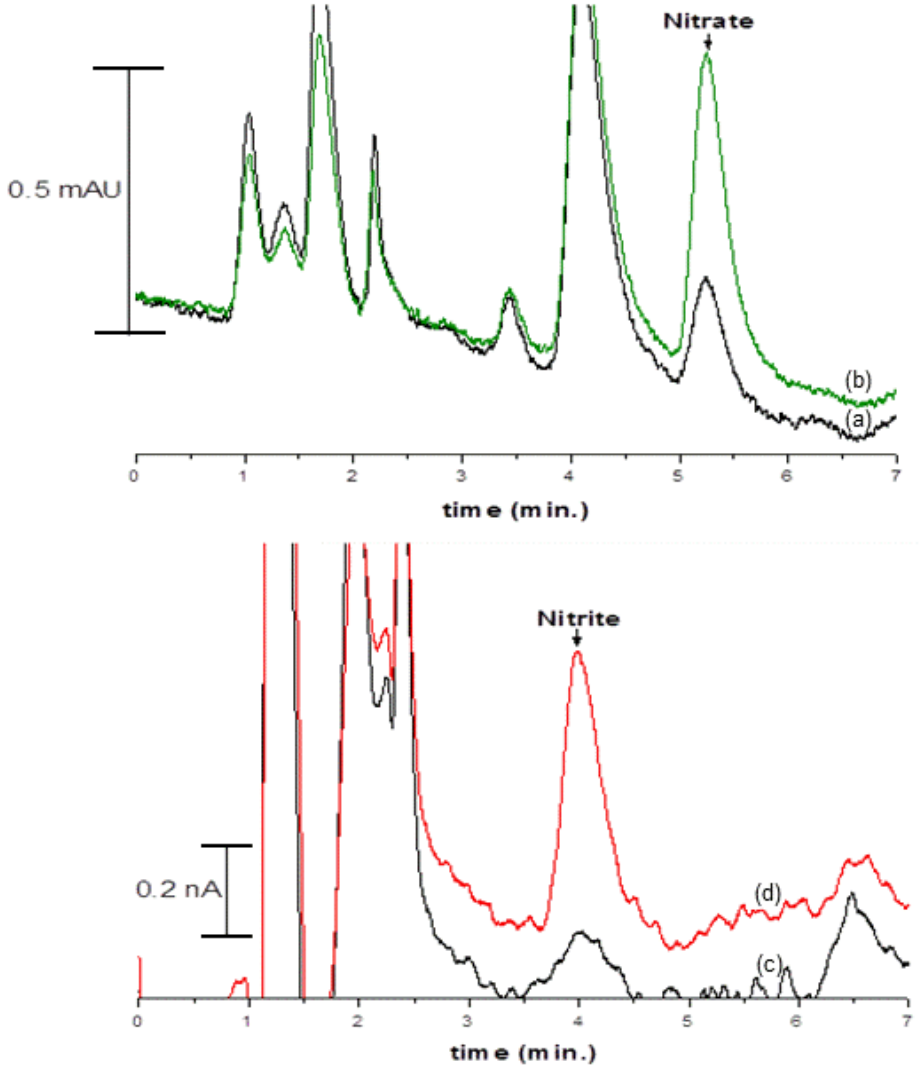

Figure 2.13: Basal rat brain hippocampus dialysate samples spiked with nitrite and nitrate standards. Trace (a) is basal dialysate and trace (b) is basal dialysate spiked with 10 μM nitrate for the top UV overlay. Trace (a) trace is basal dialysate and trace (b) is basal dialysate spiked with 1 μM nitrite for the bottom EC overlay. Mobile phase and detection conditions are the same as described in the previous figure.

2.8 Summary

An LC-based UV-EC system was developed through the optimization of multiple parameters. Examining changes in applied potential and absorbance wavelength and their effects upon analyte response and background noise made it possible to select detection parameters to make analyte identification at concentrations seen in basal dialysate samples possible. Chromatographic separative conditions were optimized to separate nitrite and nitrate. In addition, this method was validated for variability in retention times and peak areas, limits of detection and quantitation, and linear ranges of the analytes studied. Also, *in vitro* studies were pursued to demonstrate that this method was capable of detecting and quantifying stable secondary products resulting from RNS formation. Upon completion of these studies, nitrite and nitrate were separated from other compounds present in basal dialysate samples.

Microdialysis probes were calibrated through nitrite and nitrate recovery studies under *in vitro* conditions designed to mimic the rat brain environment as closely as possible. Through the determination of recoveries of these compounds, it is possible to then compensate and calculate for the true analyte concentrations as they would be in the rat brain environment. Upon completion of these experiments, it was possible to move on to the final stages of chromatographic as well as UV-Vis and EC method development. Upon completion of development of this method, it was possible to move on to animal studies.

2.9 References

[1] Moorcroft, MJ, Davis, J (2001). "Detection and determination of nitrate and nitrite: a review". *Talanta* **54**: 785-803.

[2] Jedlickova, V, Paluch, Z (2002). "Determination of nitrate and nitrite by high-performance liquid chromatography in human plasma". *J Chrom B* **780** (1): 193-197.

[3] Rizzo, V, Montalbetti, L. (1998) "Nitrite/nitrate balance during photoinduced cerebral ischemia in the rat determined by high-performance liquid chromatography with UV and electrochemical detection". *J Chrom A* **798** (1-2): 103-108.

[4] Shimadzu Co. (1991) Ultraviolet-Visible Spectrophotometric Detector, SPD-10AV Module for Shimadzu High Performance Liquid Chromatography. Chromatographic Instruments Division Internal Marketing Div. Tokyo 101, Japan.

[5] FDA (2001). "Guidance for Industry. Bioanalytical Method Validation". http://www.fda.gov/downloads/Drugs/.../Guidances/ucm070107.pdf

[6] Gunasekara, DB, Hulvey, M (2012). "Microchip electrophoresis with amperometric detection for the study of the generation of nitric oxide by NONOate salts". *Anal Bioanal Chem* **403** (8): 2377-2384.

[7] Griveau S, Dumezy, C (2007). "*In vivo* electrochemical detection of nitric oxide in tumor-bearing mice". *Anal Chem* 79 (3): 1030-1033.

[8] Wegener, JW, Godecke, A (2002). "Effects of nitric oxide donors on cardiac contractility in wild-type and myoglobin-deficient mice". *B J Pharm* **135**: 415-420.

[9] Wiley, K, Davenport, A (2007). :Novel nitrite oxide donors reverse endothelin-1-mediated constriction in human blood vessels". *J Cardiovasc Pharm* **36**: 151-152.

[10] Dutton, AS, Fukuta, JM (2005). "Quantum mechanical determinations of reaction mechanisms, acid base, and redox properties of nitrogen oxides and their donors". *Meth in Enzymol* **396**: 26-44.

[11] Keefer, LK, Nims, RW (1996). "NONOates" (1-substituted diazen-1-ium-1,2-diolates) as nitric oxide donors: Convenient nitric oxide dosage forms *Meth in Enzymol* **268**: 281-293.

3 Animal methods and 3-MPA rat microdialysis studies

3.1 Introduction

The 3-MPA rat model was previously developed in this research group to monitor changes in the levels of the neurotransmitters glutamate and GABA, with the goal of facilitating a greater understanding of cellular biochemical changes caused by induced seizures [1]. Previous studies using this model have shown that under 3-MPA-induced oxidative stress conditions, biomarkers such as the neurotransmitters glutamate and GABA (Mayer thesis) and lipid peroxidate malondialdehyde (Cooley thesis) are produced at elevated concentrations. However, nitric oxide production under these oxidative stress conditions has not been evaluated. Nitric oxide is biomolecule of interest for this thesis; however, it is very labile and must be measured though the analysis of stable secondary products [2, 3].

3.2 Objectives

Formation of RNS and their contribution to oxdative stress had not been evaluated in the 3-MPA rat model. The primary goal of these studies was to use the methods discussed in the previous chapter to study RNS generation in the rat brain as a result of 3-MPA infusion. Data gathered from these experiments would complement previous studies monitoring changes in glutamate and GABA levels, as well as lipid peroxide formation. A multiple biomarker evaluation will offer greater insight into the biochemical pathways involved, and from that, a greater understanding of oxidative stress. Brain surgeries were conducted in rats to

create pharmacologic induction of oxidative stress and to measure changes in nitrite, the biomarker of nitric oxide production. From monitoring of nitrite levels, it was possible to determine if RNS generation was one factor contributing to oxidative stress and the associated cellular damage.

3.3 Animal Methods

3.3.1 Surgical procedure for microdialysis sampling

All animal experiments were conducted in accordance with Institutional Animal Care and Use Committee (IACUC) animal use procedures. Male Wistar rats in the body mass range of 200-225g were used for all surgeries. Rats were placed under anesthesia via induction with isoflurane inhalation followed by subcutaneous injection of a mixture containing acepromazine (0.67mg/kg), ketamine (67.5mg/kg) and xylazine (3.4mg/kg). Body temperature was regulated using a rectal temperature probe interfaced with a temperature controlled heating pad. To prepare the animal for surgical incision, the cranial area from the upper region of the neck to the front of the eyes was clipped of hair. In addition, the eyes were covered with Surgilube®, a protective bacteriostatic lubricant to prevent drying (Fougera Pharmaceuticals, Melville, NY).

The animal was placed into a stereotaxic frame, and the skull was pinned just prior to the auricular canal. An example is shown and coordinate system of the stereotax used in these surgeries is described in **Figure 3.1**.

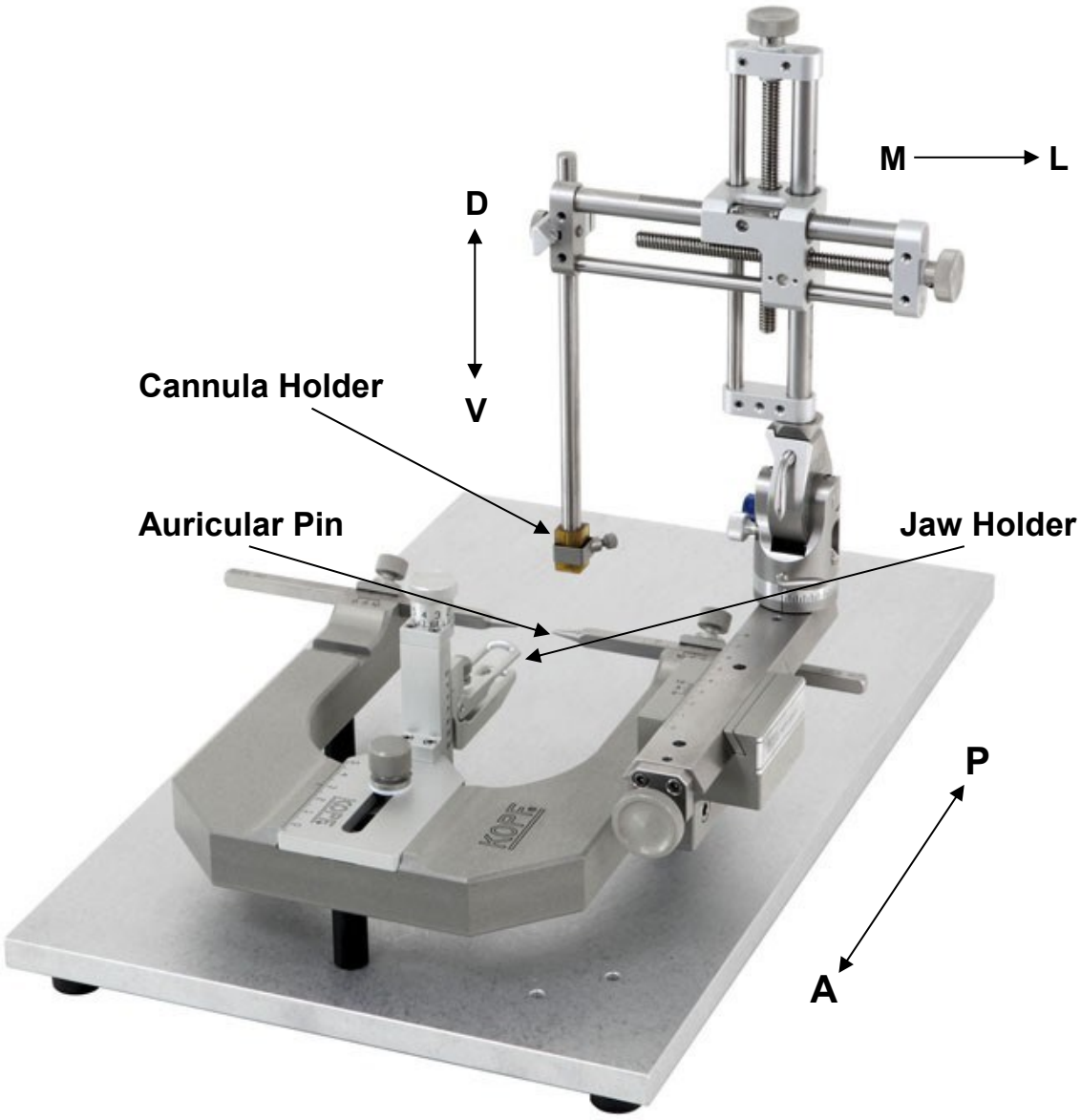

Figure 3.1: Stereotax showing A/P, M/L, and D/V coordinates for accurate and precise marking and skull penetration for brain surgeries. In addition, note locations of auricular pins and jaw holder for cranial immobilization and holder for cannula implantation. Reproduced with permission from Bilaney Consultants.

Upon positioning of the skull, the site of incision was scrubbed with iodine and isopropyl alcohol alternatingly and allowed to dry. An incision was made using a #10 blade in the medial position, running in the anterior position from the brow posteriorly to the occipital process. Four bulldog clips were used to retract the skin and underlying tissue from the incision site, revealing the skull. A cotton-tipped applicator was dipped in syringe filter sterilized saline and used to brush away the adventitial membrane covering the skull at the site. A cannula was placed into the stereotaxic armature and lowered into position at the intersection of the frontal and parietal bones, known as the bregma. This intersection served as a zero point and was marked with a surgical pen. Stereotaxic coordinates of -3.3 (A/P), +1.7 (M/L), and -2.7 (D/V) were used to mark the position for cannula and probe insertion.

To facilitate stable cannulation, one small mark was made several millimeters medial to the probe implantation site. Holes were drilled at the probe implantation site and medial site using a hand powered drill bit holder, using 1 and 2 millimeter bits. A guide cannula and bone screw was implanted at the stereotaxic coordinate and medial holes, respectively. The purpose of the bone screw was to serve as an anchor point for the dental acrylic necessary for cannula fixation. The dental acrylic was applied on the skull around the cannula and bone screw, with special care to ensure the cement covered the external portion of the cannula.

Upon incision closure around the probe, a microdialysis probe (CMA 20, Solna, Sweden) was inserted into the guide cannula and seated. The microdialysis probe inlet and outlet were composed of FEP tubing. The probe inlet was then connected to a 1mL syringe (Hamilton, Reno, NV) containing aCSF and perfused at a flow rate of 1uL/min. The aCSF was comprised of calcium chloride (1.2 mM), magnesium chloride (1.0 mM), potassium chloride (2.7 mM), sodium chloride (145 mM), sodium phosphate monobasic (0.45 mM), and sodium phosphate dibasic (2.33 mM). The probe was initially allowed to perfuse for an hour, or about the time required for surgical cannula implantation. Upon completion of the probe implantation and before basal collection, the probe was allowed to perfuse for an hour to flush for recovery. Samples were collected into microcentrifuge tubes for a duration of 10 minutes each.

3.3.2 Microdialysis Sample Collection

All microdialysis probes were perfused with Ringers solution for initial DEA NONOate studies. For rat hippocampus studies, aCSF was perfused at a flow rate of 1μL/min for the duration of the implantation procedure. Upon insertion of the probe into the sampling site, flushing was allowed to occur for 1 hour at 1μL/min into a microcentrifuge tube inserted into a vacant location of a vial holder. The flushed solution as one large volume was collected for analysis over this period. After the hour-long waiting period, a new microcentrifuge tube was inserted into the vial holder and dialysate was collected for 10 minutes. Following this period, the vial was switched with an empty one and the 10 minute collection

time was repeated. This process was repeated for approximately one hour as basal collection. The syringe containing Ringers or saline was then switched with that containing a known concentration of the pharmacological agent of study. Dialysate was then collected at 10 minute intervals for the remainder of time dictated for the agent perfusion. After the administration period, the syringe containing the pharmacological agent (3-MPA) was switched with that of Ringers or saline and that perfusate was delivered for the remainder of the experiment. All microcentrifuge tubes collected were immediately frozen at -20ºC before being transferred to a -80ºC freezer if they were not to be analyzed at the time of the animal experiment. Analyte concentrations were stable for several months upon storage in the -80ºC freezer.

3.3.3 Microdialysis Sample Injection

Following sample thawing, all samples were vortexed (Barnstead International, Dubuque, IA). Samples were divided in two, with one half going toward analysis using the methods described in this thesis, and the other going toward another group member's research. A Shimadzu LC-20AD pump was used to pump mobile phase (60: 40, acetonitrile: H_2O) to the Rheodyne ® 7725i injector. Standards were pulled up into the barrel of an injection syringe (Hamilton, Reno, NV) at the 1µL mark and the syringe needle was inserted into the injector port. The contents of the syringe barrel were then pushed into the 2µL injection loop and the injection valve was turned to inject the sample. Injected samples were separated chromatographically using a Phenomenex ®

Synergi Hydro-RP 4μ 80Å and detected using Shimadzu SPD-10AV ultraviolet and Bioanalytical Systems LC-4C amperometric detection systems in series as described in chapter 2.

3.4 Initial Rat Studies Results

3.4.1 3-MPA study

3-MPA is a chemical whose use has been extensively investigated in this research group. The compound has been specifically used to induce neuronal damage resulting from oxidative stress. 3-MPA accomplishes this via the inhibition of glutamate decarboxylase (GAD) [4]. The enzyme is responsible for the conversion of the excitatory amino acid glutamate into an inhibitory amino acid γ-aminobutyric acid (GABA), keeping neuronal firing in balance. As a result of inhibition of this enzyme, an increase in glutamate occurs, with a reduction in GABA, leading to neuronal hyper-excitation [5, 6]. Furthermore, glutamate acts upon several ionotropic and metabotropic neuronal cell membrane receptors responsible for calcium influx.

Upregulation of N-methyl-D-aspartate (NMDA), kainate, and α-amino-3-hydroxy-5-methyl-4-isoxazolepropionic acid (AMPA) receptors leads to a cellular influx of Ca^{2+}. In addition, glutamate activates the metabotropic glutamate receptors (mGluRs), which in turn activate additional ionotropic receptors. An intracellular influx of Ca^{2+} results in nicotinamide adenine dinucleotide phosphate (NADPH) oxidase and cyclooxygenase (COX) activation and the generation of superoxide anion. Previous studies investigated the change in concentrations of

the glutamate and GABA, as well as the formation of lipid peroxides (Crick thesis, Mayer thesis, Cooley thesis).

Research conducted in this group has found that both glutamate and GABA increase in a dose dependent manner after direct 3-MPA administration (Meyer thesis). One explanation of the increase in GABA is that it is a result of an inhibitory surround, a self-preservation mechanism where surrounding neurons secrete GABA in an attempt to get affected cell hyperexcitation under control and minimize damage [7]. It has also been shown that free lipids such as arachidonic acid are attacked by superoxide and converted to bicyclic endoperoxides 8]. These compounds are further degraded to 4-hydroxynonenal, acrolein, and malondialdehyde (MDA). A method has been developed in our group to detect and quantify MDA. Increases in the production of MDA in a dose-related manner have been observed (Cooley thesis). This finding most likely suggests that superoxide is generated at levels proportional to NADPH oxidase and COX upregulation as a result of administered 3-MPA concentrations [9, 10].

Studies of RNS formation as a result of 3-MPA administration were conducted as part of this thesis. Results of these studies have been rather surprising, as no increase in nitrite formation from RNS production as a result of 3-MPA administration was found. This finding could be due to several reasons. The first is that RNS production is dependent upon a large Ca^{2+} influx necessary for eNOS and nNOS activation. It is very possible that the increased production

of glutamate from 3-MPA administration has a limited effect on ionotropic glutamate receptors. This shortcoming could also be due to the use of ketamine as an anesthesia of choice.

Ketamine is known to antagonize the ionotropic glutamate receptors NMDA and AMPA. From reduced NMDA and AMPA activity, a reduction in Ca^{2+} intracellular influx may occur, reducing the amount of Ca^{2+} available for eNOS and nNOS activation. In an alternate hypothesis, multiple steps required for NOS activation and NO formation from 3-MPA administration to eNOS/nNOS upregulation and the limited efficiency of each step may reduce the concentration of Ca^{2+} available for eNOS/nNOS upregulation, resulting in little production of NO.

It was originally postulated that NO was generated at elevated levels, but remained peroxynitrite for an extended period of time such that conversion to nitrite was minimal. However, *in vitro* experiments with the NO donor DEA NONOate showed that under conditions similar to those encountered physiologically, NO was rapidly converted to nitrite. Nitrate was not seen under *in vitro* conditions.

3.4.2 Initial Study of 3-MPA Standards

Prior to the pursuit of 3-MPA microdialysis studies in rats, a 3-MPA standard was injected to confirm that no peaks interfered with nitrite. The delivery of 3-MPA was previously determined in this research group (Crick thesis) to be

about 90%, independent of analyte concentration. From experiments of 10 mM 3-MPA infusion, it was assumed that about 90% of the 3-MPA was delivered by the microdialysis probe.

As the result of a 1 mM 3-MPA injection, no peak close to the limit of quantitation of nitrite was visible. However, with the injection of 10 mM 3-MPA standards, a peak co-eluted at a response significantly above that of a 10 μM nitrite standard. Furthermore, in another experiment 3-MPA was spiked with nitrite. Retention times of peaks present in the chromatograms from this experiment were compared with those of peaks of individual 3-MPA and nitrite standards. The retention times essentially matched for nitrite in nitrite standards and a peak present in 3-MPA standards, with times of 5.6 and 5.9 min, respectively. This interference was not 3-MPA itself, which eluted at 17 min., but an unknown contaminant in the 3-MPA solution. Chromatograms comparing the retention times of these various peaks are shown in **Figures 3.2 and 3.3**. It became necessary to modify the mobile phase conditions to resolve the interferent in 3-MPA from nitrite and allow 3-MPA rat studies to commence. Mistaking an interferent of the pharmacological agent being dosed for nitrite would be disastrous if animal studies were conducted and would undermine the project.

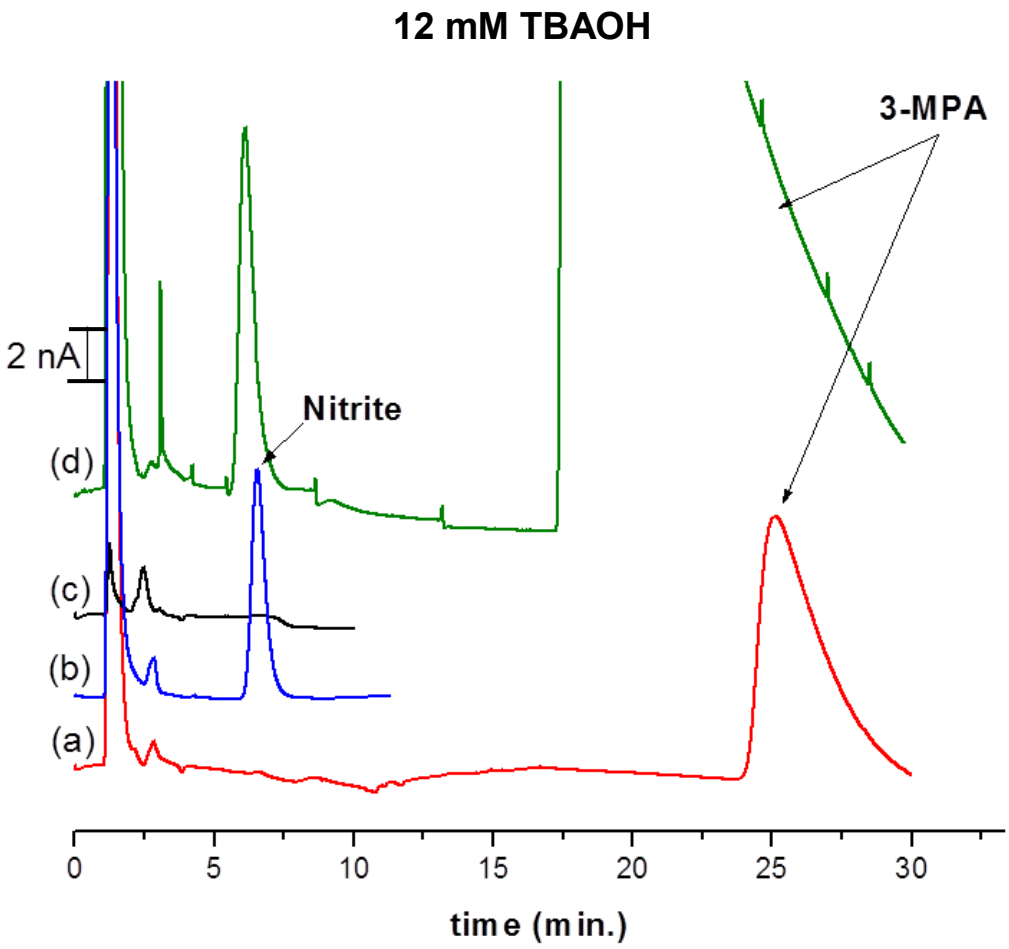

Figure 3.2: Overlay of various EC chromatograms evaluating the contribution of 3-MPA as an interferent with nitrite. Injection of 10 mM 3-MPA solution is significant in that an interferent with nitrite is present in levels giving a response greater than the limit of quantitation for nitrite. In addition, the response is significantly above nitrite generated under basal conditions in the rat hippocampus. At a 1mM concentration, 3-MPA solution doesn't contribute a significant interferent. Trace (a) is 1 mM 3-MPA, trace (b) is 10 µM nitrite, trace (c) is under basal conditions, and trace (d) is 10 mM 3-MPA. Mobile phase and detection conditions were identical to the last figure in the previous chapter.

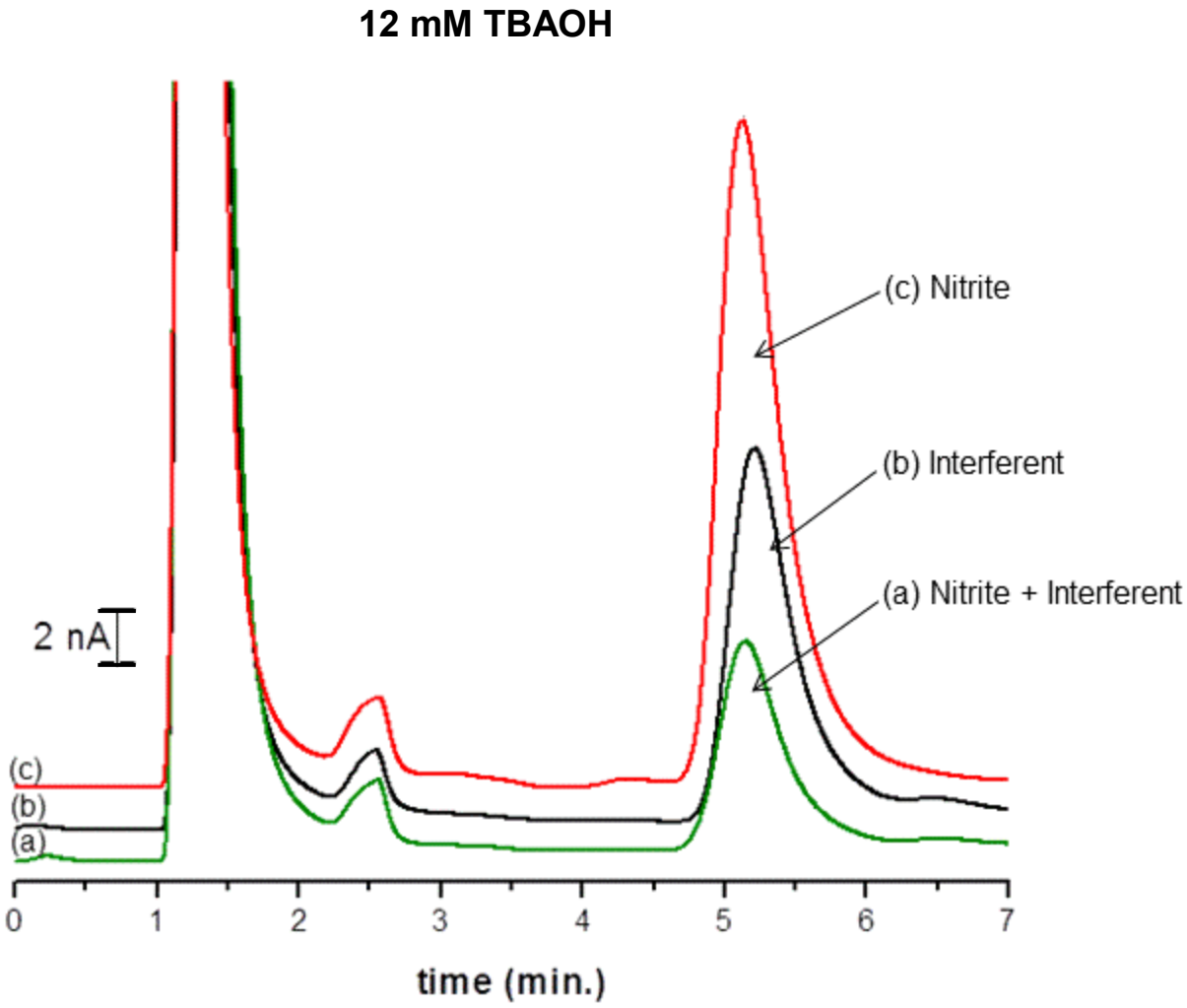

Figure 3.3: Comparison of EC chromatograms of a 3-MPA solution, a 3-MPA and nitrite mixture, and a nitrite standard. Note complete co-elution of the interferent and nitrite in the mixture, problematic for identification and quantitation of nitrite in dialysate. Trace (a) is 12 µM nitrite + interferent present in 5 µM 3-MPA, trace (b) is interferent present in 10 mM 3-MPA, and trace (c) is 25 µM nitrite. Detection and mobile phase conditions are the same as that of earlier figures in this chapter.

3.4.3 Mobile Phase Condition Modification for Interferent-Nitrite Resolution

Upon detection of this interferent, it was deemed necessary to modify mobile phase conditions in order to separate the previously identified interferent from nitrite and minimize the likelihood of problems in the future when using 3-MPA solutions. Alterations in pH and sulfuric acid concentrations would be problematic, as they would affect the detection characteristics of nitrite as well as the separation. Altering pH would affect retention times of nitrite and the interferent. Altering the concentration of the ion-pairing agent TBAOH seemed like the most logical approach to increasing the resolution between nitrite and the interferent. After making any change in the ion-pairing agent concentration, the mobile phase was run through the column for a 24 hour period to allow for equilibration, ensuring constant retention times for analytes.

The concentration of TBAOH was reduced from 12mM to 4 mM. This change resulted in the merging of nitrite and the 3-MPA artifact such that they were indistinguishable from one another (not shown). Reducing from 12 mM to 4 mM did not significantly improve the separation stems from the likelihood that excess ion-pairing reagent was present in amounts far greater than needed to saturate the stationary phase surface octadecyl groups. Any increase in ion-pairing agent beyond this saturation point does not increase analyte retention time.

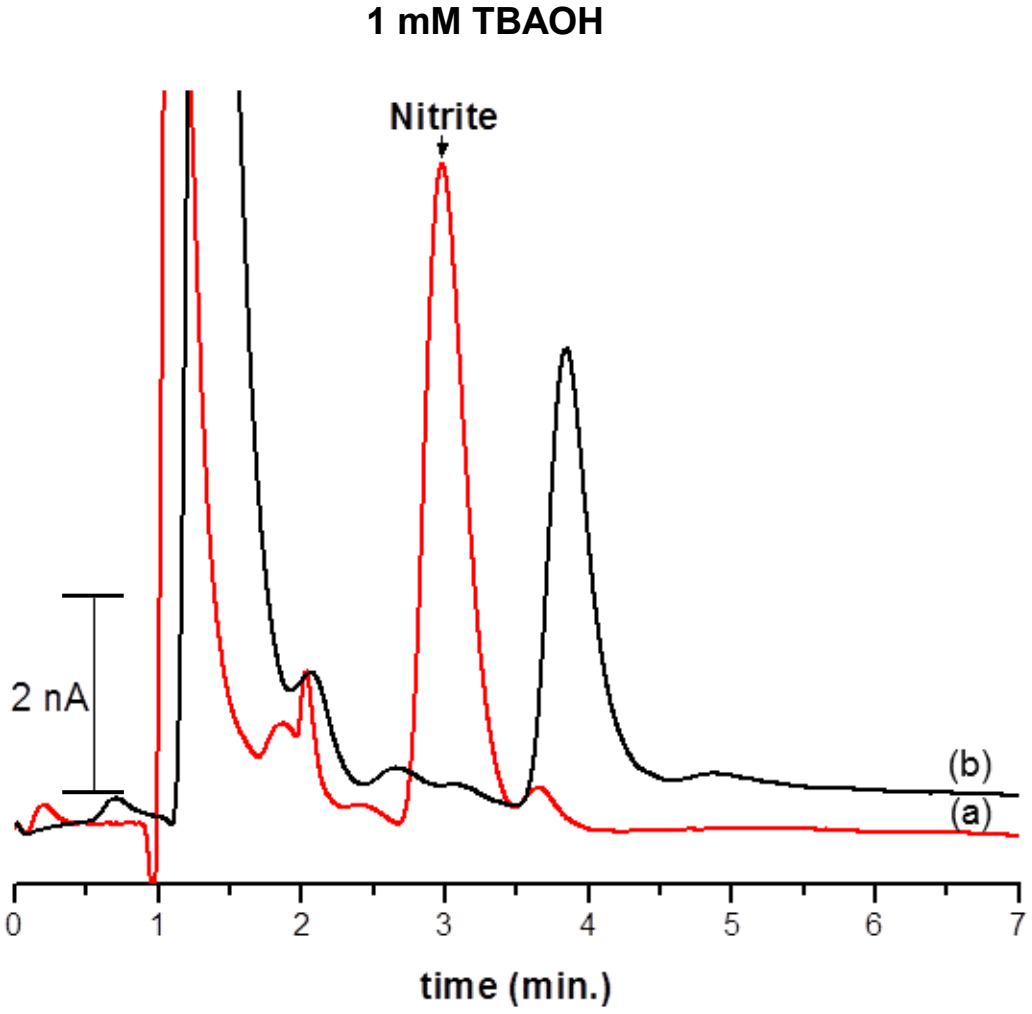

Figure 3.4: Comparison of nitrite standard with a rat hippocampus microdialysis sample at the height of 3-MPA administration. Note that the peak which corresponds with nitrite in the microdialysis sample is nonexistent, while that of the artifact at 4 minutes is prominent, a feature previously mistakenly identified as nitrite. Trace (a) is 5 μM nitrite and trace (b) is 50 minutes after 10 mM 3-MPA dosing. Detection conditions are unchanged. Mobile phase conditions are 1 mM TBAOH and 15 mM H_2SO_4 at pH 4.0.

Upon this finding, TBAOH was further reduced to 1 mM and showed an improvement in the resolution between the interferent and nitrite. The separation was improved because the stationary phase was likely at a saturated or under-saturated point. At a saturated point, maximum interaction of the analyte with the charged head groups of the ion-pair reagent occurs. Furthermore, at an under-saturated point, ion-pair charged head groups are able to interact with analyte whilst adsorbed to the stationary phase, in addition to the greater likelihood of the hydrophobic octadecyl groups of the stationary phase interacting with analyte as well.

To potentially improve the separation further from its current state, it was decided to decrease TBAOH to 0.5 mM to determine if any positive change in resolution could be achieved. The resolution was decreased as a result of this reduction to 0.5 mM; therefore, the TBAOH concentration was increased to 1 mM as the final modification. In addition, dead volume associated with the chromatographic system was reduced. Chromatographic tubing was cut to minimize the distance from the column outlet to the electrochemical cell of the detection system. This reduction in dead-volume made it possible to minimize band-broadening and increase resolution between nitrite and 3-MPA interferent peaks. Complete resolution between nitrite and the interferent was realized, as shown in **Figure 3.4**. This was confirmed by spiking as well with nitrite, shown in **Figure 3.5**. From these experiments, the final mobile phase consisted of 1 mM tetrabutylammonium hydroxide and 15 mM H_2SO_4, at pH 4.0. Final equipment

and conditions for the method developed to detect and quantify nitrite are shown in **Figure 3.6**.

3.4.4 Evaluation of nitric oxide product formation

It was observed from early basal injections that nitrite was generated in rat brains implanted with microdialysis probes and perfused with Ringer's or aCSF. Slight tissue trauma from probe implantation is common and leads to nitric oxide production from calcium influx due to probe-adjacent cyto-membrane damage and subsequent upregulation of NOS by Ca^{2+} [11,12]. UV and EC detection chromatograms showed the presence of RNS products nitrite and nitrate in basal dialysate samples. Nitrite production as a result of this early nitric oxide formation is shown in **Figure 3.7**. In this figure, nitrite production decreases from concentrations of close to 4μM to those below the limit of quantitation. Upon dosing with 3-MPA, no increase of nitrite was found to have occurred. **Figure 3.8** shows chromatograms from a rat experiment in which basal nitrite was below limits of detection, in comparison with dosing of 10 mM 3-MPA in which no increase in nitrite is observed. A 10 μM nitrite standard is in the overlay to confirm that an increase in nitrite production is not occurring.

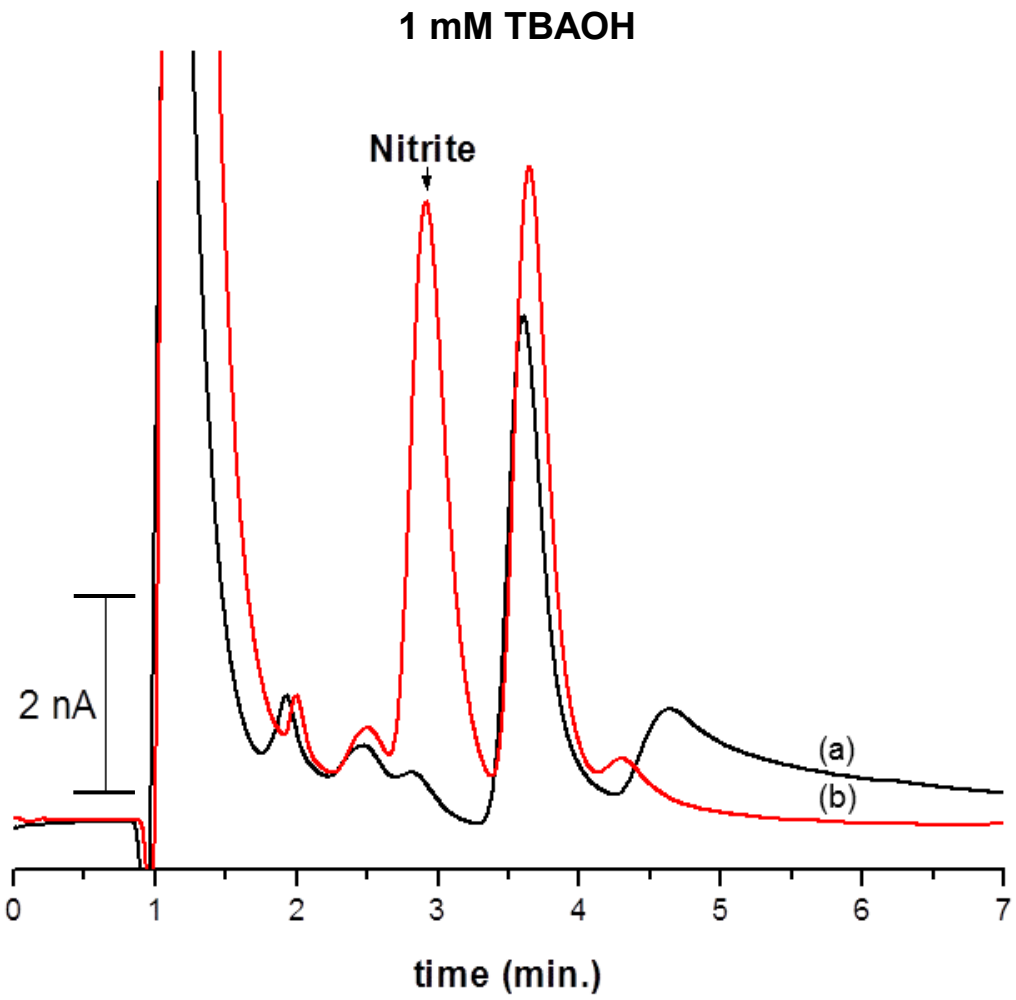

Figure 3.5: Spiking of a rat hippocampus microdialysis sample at the height of 3-MPA administration with nitrite standard. The growth of a peak at 3 minutes is confirmatory of the separation between nitrite and the 3-MPA artifact. Trace (a) is 50 minutes after dosing and trace (b) is 50 minutes after dosing + 2 μM nitrite spike. Detection and mobile phase conditions are the same as that of the previous figure.

EQUIPMENT: Shimadzu LC-20AD Pump	
Mobile Phase	1 mM TBAOH, 15 mM H_2SO_4, pH: 4.0
Flow Rate	0.1 mL/min.
Operating Pressure	2500 PSI
Analytical Column	Phenomenex Synergi ® Hydro RP 1x150mm 4µm 80A

EQUIPMENT: Bioanalytical Systems Inc. LC-4C Amperometric Detector	
Auxiliary Electrode	BAS MF-1092 Cross-flow with ref. port
Reference Electrode	BAS RE-6 Ag/AgCl
Working Electrode	BAS MF-1000 3 mm glassy carbon
Reference Electrode Storage Container	BAS MR-5275
O –Ring Seal for Reference Electrodes	BAS MR-2023
Electrochemical Cell Gasket	BAS MF-1044 13µm thick cross flow
Recording Device	Ampersand 24-bit AD converter
Recording Program	Ampersand ChromSpec ®
Applied Potential	+ 1.025 V
Output Range	0.5 µA

EQUIPMENT: Rheodyne ® 7725i Injector	
Injection Loop Volume	2 µL
Syringe Volume	10 µL
Loop Filling Method	8 µL Overfill
Number of Injections/Sample	3

Figure 3.6: Summarization of the final equipment used and conditions developed for the detection and quantitation of nitrite.

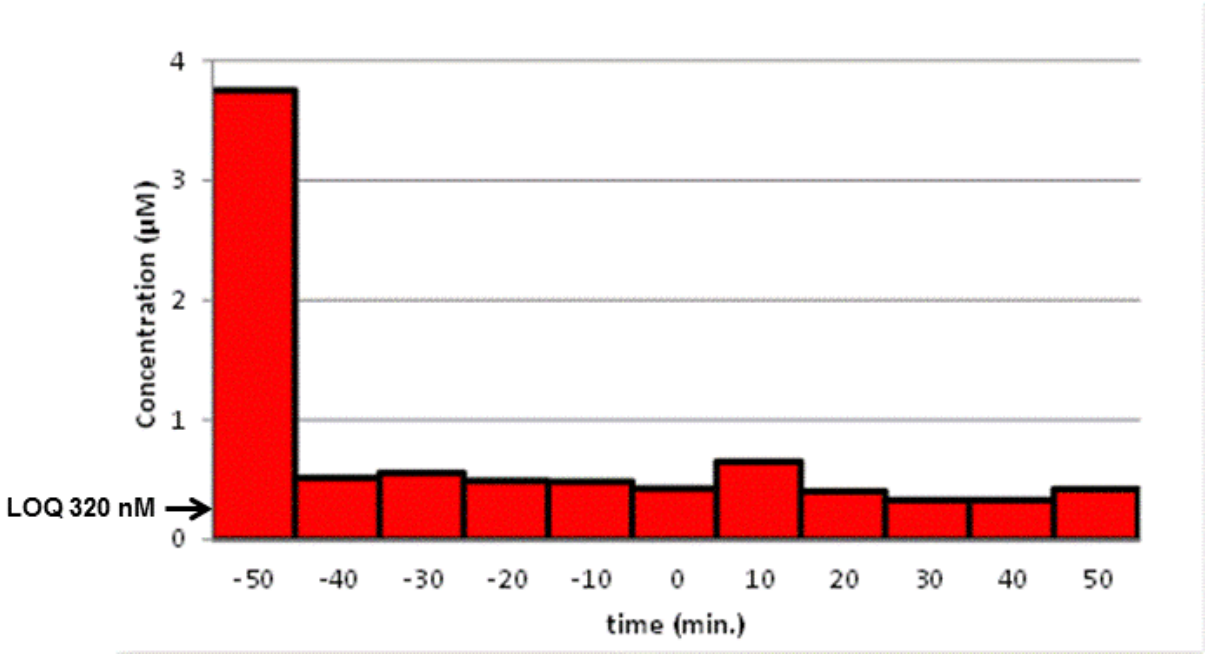

Figure 3.7: Time course nitrite graph of a rat experiment in which the initial 60 minute period is basal collection, followed by 50 minutes of 10 mM 3-MPA infusion. An initial concentration of nearly 4 µM is present due to initial trauma due to probe implantation. After 50 minutes of 10 mM 3-MPA dosing, nitrite concentration falls to below the limit of detection.

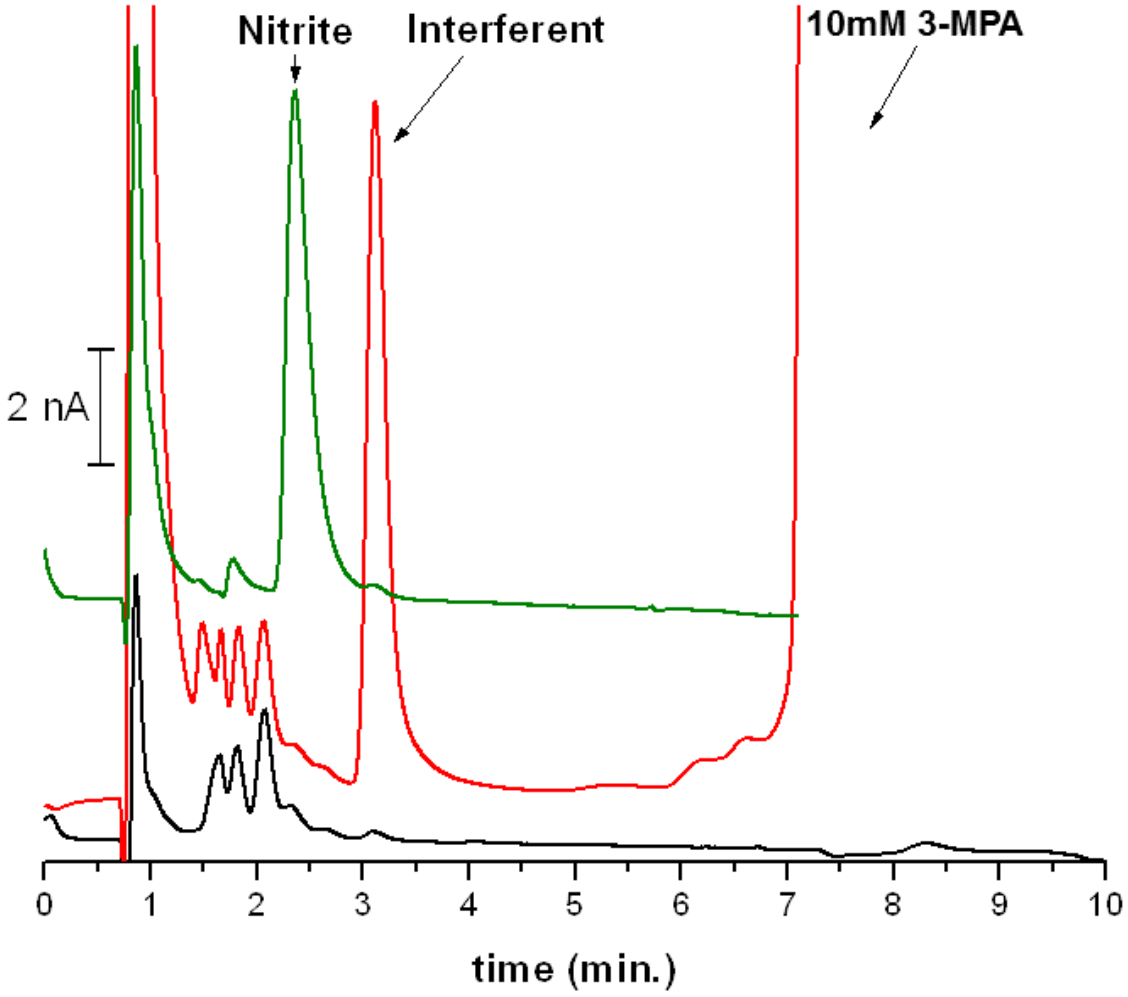

Figure 3.8: Overlay of basal and 3-MPA dosed rat hippocampus dialysate samples. In addition, a 10 µM nitrite standard is shown in the overlay to confirm that 3-MPA administration does not upregulate nitrite production. This means that an increase in RNS does not occur as a result of 3-MPA administration. Trace (a) is basal dialysate, trace (b) is 50 minutes after dosing, and trace (c) is 10 µM nitrite. Mobile phase and detection conditions are the same as that of the previous figure.

3.5 Summary

Surgeries were performed to implant probes for microdialysate collection in the brain of rats. From these procedures, it was possible to deliver pharmacologic agents into the brain as well as collect dialysate to monitor key endogenous compounds nitrite and nitrate in the future. The initial goal of these surgeries were to collect dialysate necessary to support the development of chromatographic separation as well as UV-Vis and EC detection methods Furthermore, these surgeries made it possible to continue further animal studies.

In this chapter, research was conducted to determine whether or not damage occurring in the brain of the rat as a result of 3-MPA administration was influenced by RNS formation and activity. In subsequent experiments, chromatographic conditions were further optimized to separate an artifact of 3-MPA co-eluting with nitrite. Maximization of resolution between these compounds was achieved with the promise of a return to animal experiments. Upon separation of these compounds, it was determined that 3-MPA does not significantly increase nitric oxide production, and therefore, does not increase other RNS formation. In conclusion, oxidative stress resulting from 3-MPA dosing is not influenced by RNS.

3.6 References

[1] Crick, EW, Osorio, I (2007). "An investigation into the pharmacokinetics of 3-mercaptopropionic acid and development of a steady-state chemical seizure model using in vivo microdialysis and electrophysiological monitoring". *Epilepsy Res.* **74** (2-3): 116-125.

[2] Dezfulian, C, Raat, N (2007). "Role of the anion nitrite in ischemia-reperfusion cytoprotection and therapeutics". *Cardiovasc Res* (75): 327-338.

[3] Butler, AR, Ridd, JH (2004). "The formation of nitric oxide from nitrous acid in ischemic tissue and skin". *Nitric Oxide* **10** (1): 20-24.

[4] Netopilova, M, Drsata, J (1997). "Inhibition of glutamate decarboxylase activity by 3-mercaptopopionic acid has different time course in the immature and adult rat brains". *Neurosci Lett*. **226** (1): 68-70

[5] Rodriguez de Lores Arnaiz, G, Alberici de Canal, M (2006). "The effect of the convulsant 3-mercaptopropionic acid on enzymes of the γ-amino-butyrate system in the rat cerebral cortex". *J Neurochem* **21** (3): 615-623.

[6] Horton, RW, Meldrum, BS (1973). "Seizures induced by allylglycine, 3-mercaptopropionic acid and 4-deoxypyridoxine in mice and photosensitive baboons, and different modes of inhibition of cerebral glutamate decarboxylase". *Br. J. Pharmaol.* (49): 52-63.

[7] Benali, A, Weiler, E (2008). "Excitation and Inhibition Jointly Regulate Cortical Reorganization in Adult Rats". *J Neurosci.* **28** (47): 12284-12293.

[8] Yin, H, Morrow, JD (2004). "Identification of a Novel Class of Endoperoxides from Arachidonate Autooxidation". *J Biol. Chem.* **(279)**: 8766-8776.

[9] Babior, BM, Lambeth, JD (2002). "The Neutrophil NADPH Oxidase". *Arch of Biochem and Phys.* **397** (2): 342-344.

[10] O'Banion, MK (1999). "Cyclooxygenase-2: molecular biology, pharmacology, and neurobiology. *Crit. Rev. Neurobiol.* **13**: 45-82.

[11] Minghetti,L, Levi, G (1998). "Microglia as effector cells in brain damage and repair: focus on prostanoids and nitric oxide". *Prog in Neurobiol*. **54**: 99-125.

[12] Zielasek, J, Muller, B (1995). "Inhibition of cytokine-inducible nitric oxide synthase in rat microglia and murine macrophages by methyl-2, 5-dihydroxycinnamate". *Neurochem. Int.* **29** (1): 83-87.

4. Sheep Studies

4.1 Introduction

The ultimate goal of these studies was to develop an on-animal sensor for nitric or NO production. Nitrite is the major product of NO metabolism. Collaboration with the S. Lunte research group evaluated the formation of nitrite from NO in sheep and rats administered various pharmacological agents including nitroglycerin and histamine. Until 1977, the mechanism of nitroglycerin contributing to vasodilatation was unknown [1]. In 2002, it was found that nitroglycerin releases NO through reduction by the mitochondrial enzyme aldehyde dehydrogenase [2, 3]. This method of bioactivation is of incredible interest due to wide application of nitroglycerin as a vasodilator and in the treatment of heart attacks [2, 3]. In addition, *in vivo* histamine production or administration has been linked to nitric oxide production, generating the vasodilatation observed in inflamed tissues [4]. In addition, the reactive nitrogen species, such as peroxynitrite, generated in these inflamed tissues through the reaction of NO and superoxide is of interest. The generation of nitrite as a biomarker of oxidative stress may help to explain cellular damage, which occurs upon these species' formation.

4.2 Objectives

The primary goal of this research was to use nitroglycerin and histamine to generate NO and hence nitrite in skin tissue to evaluate an on-animal separation based sensor. The formation of nitrite from administration of these compounds

meant vasodilatation was occurring in the tissue and that there was potential for RNS formation as well. In addition, working in collaboration with the S. Lunte research group studying this biomarker of nitric oxide production made it possible to evaluate the versatility of the developed analytical methods in this thesis for nitrite in multiple animal models. In particular, collaboration allowed for a direct comparison of the developed analytical method with microchip based methods for nitrite developed by the S. Lunte research group. This group has developed a microfluidic device capable of sampling, separation, and amperometric detection of nitrite in sheep, known as 'Lab on a Sheep', through collaboration with Pinnacle Technologies, a company responsible for the construction of the circuit board and supporting electronics necessary for the chip to operate. Through the comparison of the conventional and microchip methods, it was possible to use the method developed in this thesis to validate the 'LOS'-Pinnacle Board method in use by the S. Lunte research group. Furthermore, an LC-UV method was modified to identify and quantify nitroglycerin in solutions isoosmotic with respect to interstitial fluid encountered in sheep studies. This method was used to determine the delivery of nitroglycerin through a microdialysis probe in *in vitro* experiments.

4.3 Sheep nitroglycerin and histamine models

Sheep have long been established as models for research studies. Microdialysis sampling has been used in sheep to monitor the pharmacokinetics of drugs and the metabolism of various biomolecules [5]. The S. Lunte research

group previously used sheep subcutaneous microdialysis probe implantation to evaluate the production of nitrite from nitroglycerin dosing [6]. In addition, this same research group has described a goal to study nitrite production as a product of histamine administration using microdialysis.

4.4 LC-UV method modification for nitroglycerin detection

4.4.1 Introduction

A chromatographic method for nitroglycerin was developed to support *in vitro* studies was accomplished by injection, separation by a C-18 column using an acetonitrile and water mixture as mobile phase, and detection using a UV-Vis absorbance detector previously mentioned in this thesis at a wavelength of 210 nm. The separation and detection conditions were modified from those of Ahmad and colleagues [7], with the principle difference being the chromatographic column (Agilent ® Eclipse XDB 5µm 4.6x150 mm C-18), injection valve, and injection volume used by that group.

4.4.2 Separation equipment specifications and mobile phase conditions

The developed method used a Phenomenex ® Synergi Hydro-RP 4µm 80Å 2x150 mm C-18 column. In contrast to the smaller dimension column used in previous chapters for the separation of nitrite and nitrate, this column was sufficient for analysis of nitroglycerin as large volumes of concentrated nitroglycerin samples were to be used. The column used for nitroglycerin analysis in this thesis had polar endcapping on the stationary phase silanol groups. This

modification provides greater stationary phase stability when exposed to aqueous mobile phase and greater interaction of polar analytes with the C-18 groups. Furthermore, the smaller 4µm particle size allows for greater resolution of peaks, which is beneficial when analyzing *in vivo* microdialysis samples in future studies [8]. The pump used was a Shimadzu ® LC-20AD operating at a flow rate of 0.4 mL/min. and the mobile phase consisted of 60: 40 acetonitrile: water, which was ideal for separation of nitroglycerin from the void peak. Nitroglycerin is hydrophobic enough to have strong interactions with the stationary phase C-18 groups when present in aqueous mobile phase. The presence of acetonitrile as an organic modifier serves to reduce the interactions of nitroglycerin with the stationary phase to an extent that analyte is eluted in a sharp peak at about 3 minutes, which is ideal for obtaining the lowest possible limits of detection and quantitation. **Figure 4.1** shows the elution of nitroglycerin. The injection valve used was identical to that used in previous chapters of this thesis, a Rheodyne ® 7725i, with an injection loop volume of 2µL, using an 8µL overfill for injection. All nitroglycerin solutions used for these and animal studies were prepared from a 5 mg/mL stock solution containing ethanol (30%) and polyethylene glycol (30%) (American Regent, Inc., Shirley, NY).

4.4.3 Detection conditions optimization

Detection conditions were modified from those established by Ahmad and colleagues [7], to be amenable to nitroglycerin analysis using the Shimadzu SPD-10AV UV-Vis detector used in previous chapters of this thesis. The method used

an absorbance wavelength of 210 nm [7]. The linear range of the method was 1-1000 μM. Final equipment and conditions for the method used to detect and quantify nitroglycerin are shown in **Figure 4.2**.

4.5 Nitroglycerin *in vitro* delivery study

Nitroglycerin delivery through a microdialysis probe was evaluated to determine its delivery into tissue in animal studies. The experiment is set up in much the same way as that of DEA NONOate perfusion in chapter 2, except the solution was unstirred. Nitroglycerin (5mg/mL) dissolved in ethanol (30%) and polyethylene glycol (30%) was loaded into a syringe (CMA 106, CMA Microdialysis, Solna, Sweden). The syringe was loaded into a syringe pump (CMA 107, CMA Microdialysis, Solna, Sweden) and connected to tubing bonded to a 1 cm linear microdialysis probe with a polyacrylonitrile (30 kDa cutoff) membrane (MF-7049, Bionanalytical Systems Inc.). The membrane was inserted into an *in vitro* cell containing 500 μL of Ringer's solution and the connecting tubing was taped at the top of the cell to maintain probe position. The flow rate of the nitroglycerin containing perfusate was set at 1 μL/min.

Nitroglycerin was allowed to perfuse for approximately 8 hours to ensure adequate delivery of this compound into the vial. At the end of this period, a sample of the solution in the vial containing the microdialysis probe was collected, diluted, and analyzed.

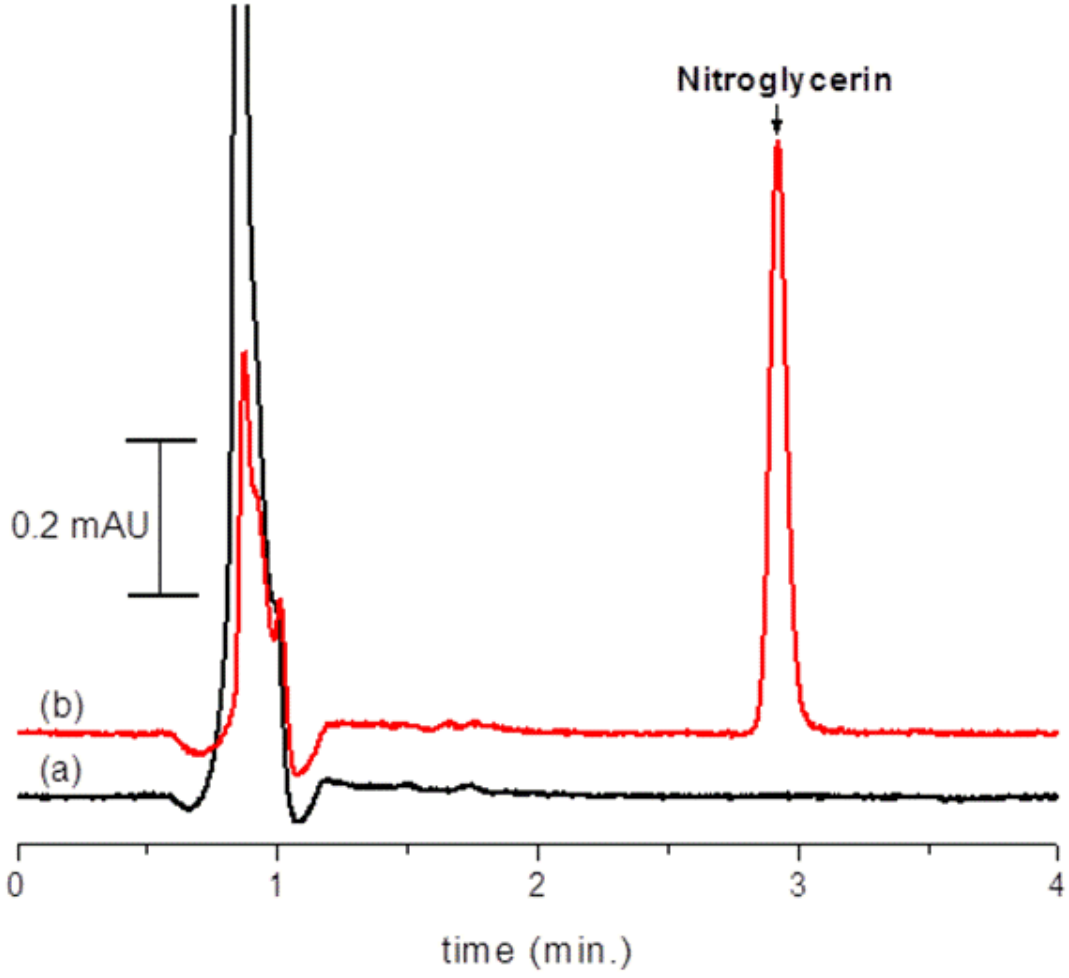

Figure 4.1: Overlay of UV chromatograms of 100 μM nitroglycerin (b) and saline solution (a). Mobile phase consists of acetonitrile: water, 60: 40. Absorbance detection is at 210 nm.

EQUIPMENT: Shimadzu LC-20AD Pump	
Mobile Phase	ACN: H_2O 60: 40
Flow Rate	0.3 mL/min.
Operating Pressure	1400 PSI
Analytical Column	Phenomenex Synergi ® Hydro RP 2x150mm 4µm 80A

EQUIPMENT: Shimadzu SPD-10A UV-Vis Detector	
Flow Cell	Shimadzu Semi-micro 2.5µL
Response Value	3 (0.5 sec)
Output Range	0.1000 AUFS
Lamp	Deuterium
Absorbance Wavelength	210 nm
Recording Device	Ampersand 24-bit AD converter
Recording Program	Ampersand ChromSpec ®

EQUIPMENT: Rheodyne ® 7725i Injector	
Injection Loop Volume	2 µL
Syringe Volume	10 µL
Loop Filling Method	8 µL Overfill
Number of Injections/Sample	3

Figure 4.2: Summarization of the final equipment used and conditions modified for the detection and quantitation of nitroglycerin.

After 3 injections for each sample, responses generated from each injection were compiled and averaged. The average response generated by the sample collected was converted to a concentration by the use of a nitroglycerin calibration curve (1-000 μM) compiled during the sample analysis period. Nitroglycerin obtained from the vial was diluted by a factor of 20 prior to analysis to ensure it was in the linear range of the calibration curve and analyzed. Nitroglycerin perfusate (5mg/mL) from the syringe was diluted by a factor of 40 to ensure that it was in the linear range of the calibration curve. To compensate for the dilution factor, the concentration determined by each sample was then multiplied by that factor. Analyte delivery was determined by the equation $R = \frac{C_{sample}}{C_{perfusate}} x100\%$.

Nitroglycerin relative delivery was calculated by dividing the steady-state concentration of this analyte in the sample measured from the vial at the end of 8 hours by the known concentration in the perfusate and multiplied by 100. The relative delivery for nitroglycerin was found to be $10.6 \pm 1.2\%$.

4.6 Initial study of histamine and nitroglycerin standards

Prior to the pursuit of sheep studies, histamine and nitroglycerin standards were injected into the LC-EC system to determine if there was any interference with nitrite. Histamine was injected at concentrations up to 1 mM without interferents. Injection of nitroglycerin above 2.5 mg/mL concentrations in saline resulted in a peak which co-eluted with nitrite. **Figure 4.3** shows an overlay of the

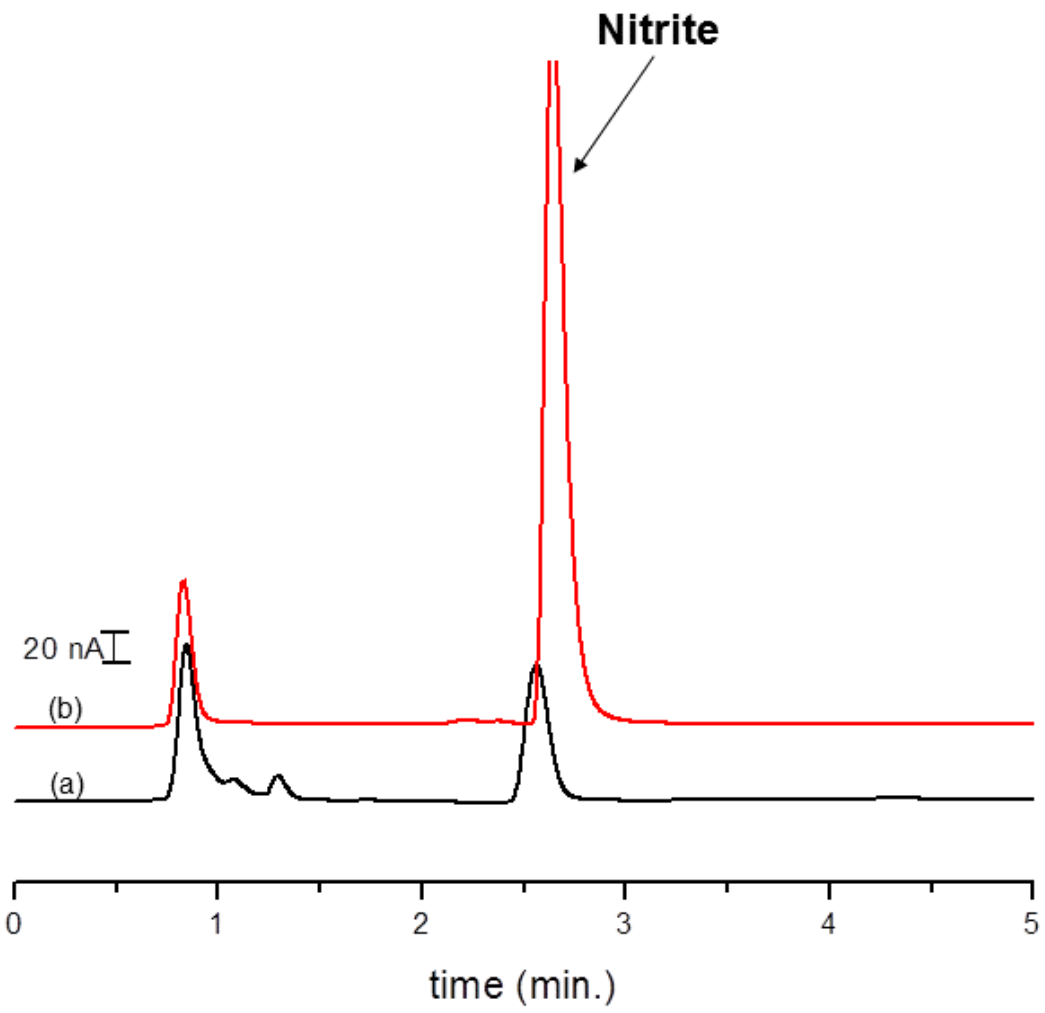

Figure 4.3: Overlay of co-elution of a compound present in nitroglycerin solution (2.5 mg/mL) (a) with a 5 µM nitrite standard (b). Presence of ethanol (15%) and propylene glycol (15%) in the nitroglycerin solution (a) has shifted the retention time of the co-eluent in. Detection was accomplished using an applied potential of +1.025 V. Mobile phase conditions are 1 mM TBAOH and 15 mM H_2SO_4 at pH 4.0.

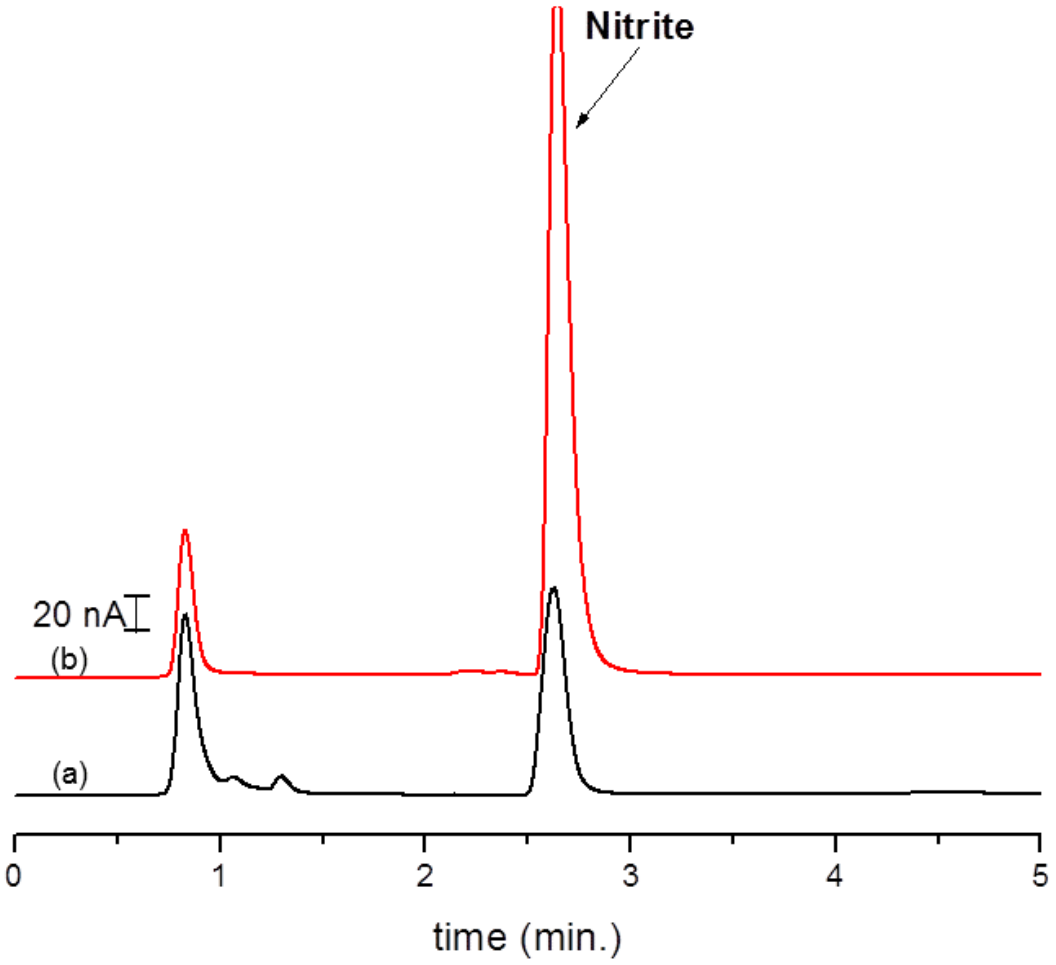

Figure 4.4: Overlay of 2 mg/mL nitroglycerin sample (a) (spiked with a 1 µM nitrite standard) with a 5 µM nitrite standard (b). Note the co-migration of the peaks from each. Mobile phase and detection conditions are the same as in the previous overlay.

co-eluent with a 5 μM nitrite standard in saline. It was believed that the interferent was nitrite as a nitroglycerin impurity present in small amounts. The shift in retention time of the nitrite present in the nitroglycerin sample from that of the 5 μL nitrite standards was likely due to the presence of ethanol (15%) and propylene glycol (15%) from the nitroglycerin concentrated solution (5 mg/mL). Spiking of the nitroglycerin sample with 1 μM nitrite shows a co-elution in **Figure 4.4**. Nitroglycerin itself is in an oxidized form, and was unlikely to be an interferent. Furthermore, ethanol and propylene glycol present from the concentrated nitroglycerin solution were unlikely to oxidize at a potential of +1.025 V. Stability of the nitroglycerin solution was tested by examining changes in nitrite produced over time at room temperature. Fresh 2.5 mg/mL nitroglycerin solution was injected into the LC-EC system, generating a response for nitrite equal to approximately 750 nM. This response would be equal to 1.5 μM nitrite in the nitroglycerin concentrated solution (5 mg/mL). The vial containing the solution (2.5 mg/mL nitroglycerin) was then left out for a 24 hour period. At the end of this period, the nitroglycerin solution was injected, generating a response for nitrite unchanged from that produced by the fresh solution, shown in **Figure 4.5**.

4.7 Analysis of sheep subcutaneous microdialysis samples

4.7.1 Sheep Experiment

Dialysate samples from ongoing sheep experiments at Purdue University (West Lafayette, IN) were examined. All sheep had 1 cm linear microdialysis probes with a polyacrylonitrile membrane possessing a 30 kDa molecular weight

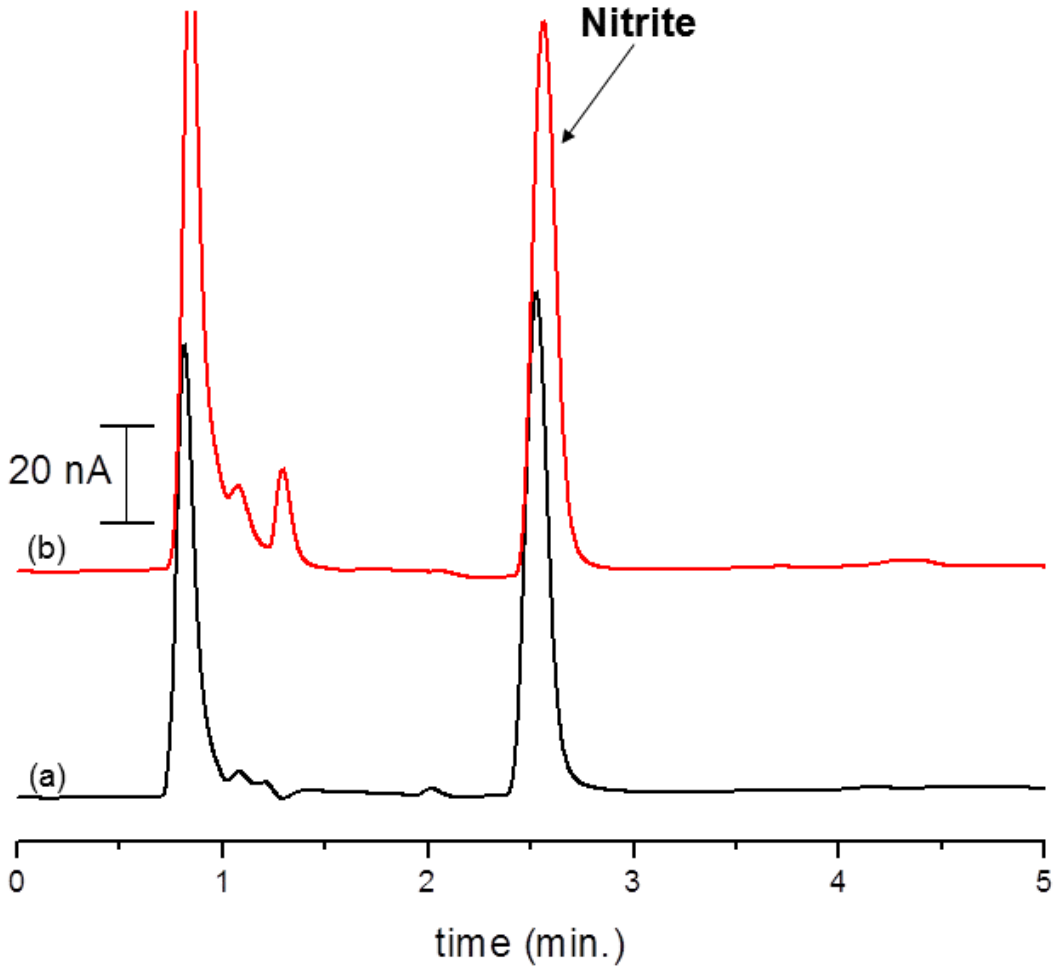

Figure 4.5: Overlay of two nitroglycerin samples injected from the nitroglycerin stability study. Trace (a) is a 2.5 mg/mL fresh nitroglycerin sample containing 750 nM nitrite. Trace (b) is a 2.5 mg/mL nitroglycerin sample after 24 hours. No significant change in nitrite is evident. Mobile phase and detection conditions are the same as in the previous overlay.

cutoff (BASinc, West Lafayette, IN) implanted subcutaneously. The probes were perfused with 0.9% w/w saline (NaCl) solution (Fisher Scientific) at a rate of 1 µL per minute. Dialysate samples were collected every 10 minutes. Basal dialysate was collected for 60 minutes, followed by administration of the pharmacological agent and collection for the remainder of the experiment of approximately 120 minutes.

4.7.2 Analysis of nitroglycerin perfused subcutaneous dialysate

After a basal collection period of 60 minutes, the syringe containing 0.9% saline solution was switched with that one containing 5mg/mL of nitroglycerin in saline. Nitrite concentrations were measured starting at the 10 minute mark, with an increase in nitrite levels with each subsequent time point thereafter to peak at 100 minutes. After a peak in nitrite levels, a slight decrease occurred for the remainder of the experiment. Confirmation of nitrite peak identity was determined by spiking the sample with a nitrite standard. An example chromatogram overlay comparing nitrite levels in basal samples to that during nitroglycerin administration is shown in **Figure 4.6**.

Concentration changes in nitrite during these experiments were evaluated using the developed LC-EC method. An increase in nitrite occurred from infusing nitroglycerin in these experiments as shown in the time-course plot in **Figure 4.7**. In these nitroglycerin infusion experiments, sheep nitrite concentration peaked at

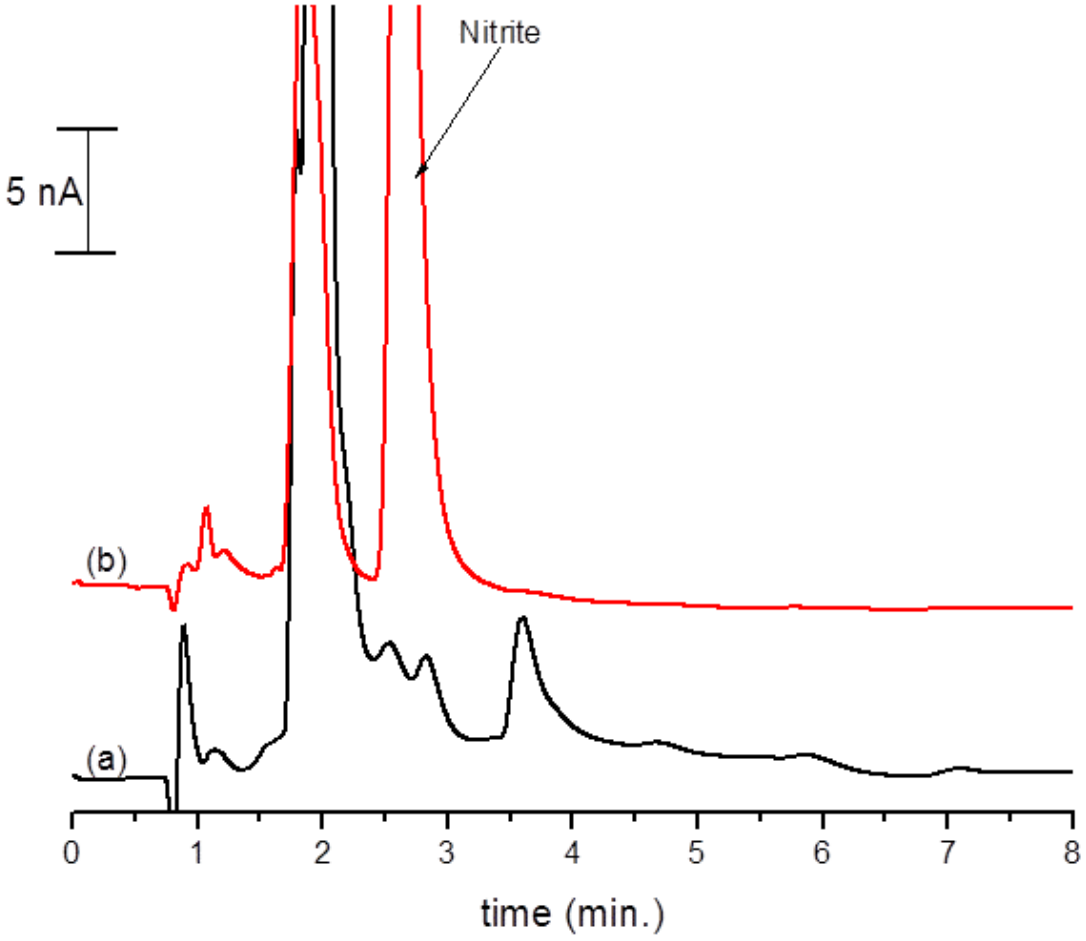

Figure 4.6: Overlay of chromatograms from the 0 time point of basal collection and 100 minutes after switching the syringe containing saline to that containing nitroglycerin (5mg/mL) in saline. Trace (a) is under basal conditions and trace (b) is during nitroglycerin infusion. Mobile phase conditions are 1 mM TBAOH and 15 mM H_2SO_4 at pH 4.0.

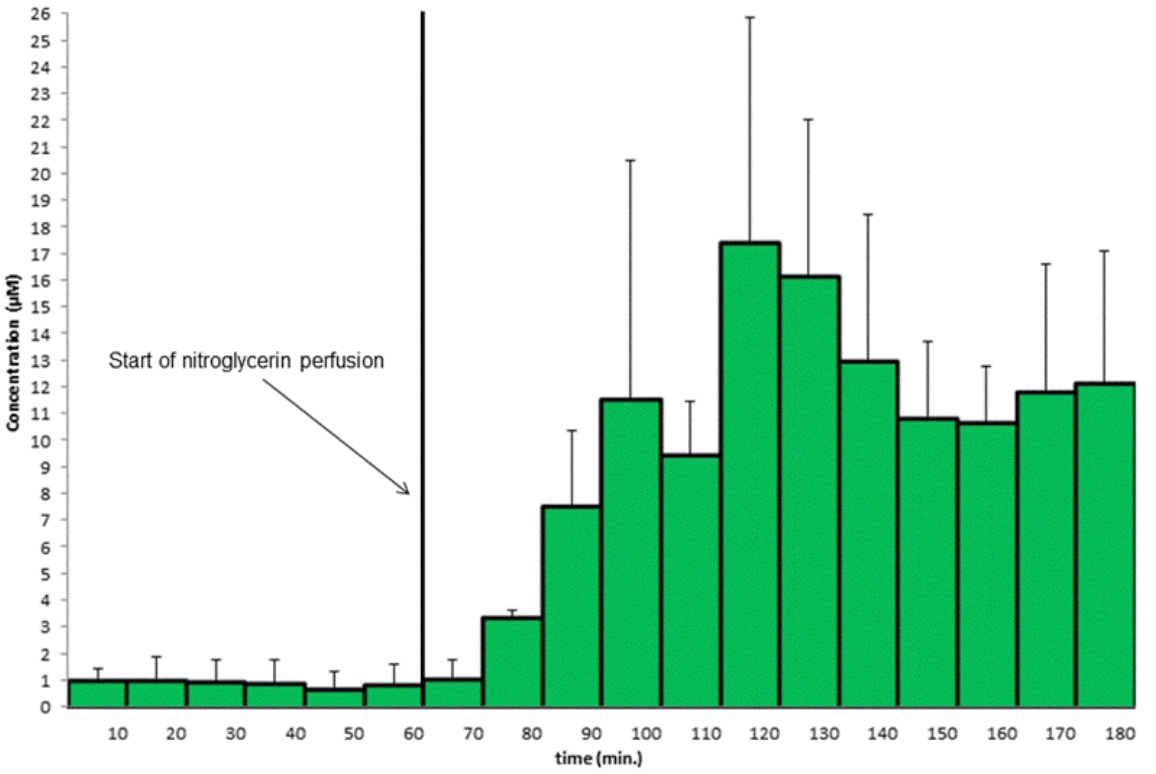

Figure 4.7: Time-course plot of change in nitrite concentration as a result of nitroglycerin infused subcutaneously in multiple sheep at the 60 minute mark. An n of 3 was collected for these experiments, with error bars representing standard deviation from average concentration. The average maximum nitrite production was approximately 17 μM, taking recovery into account.

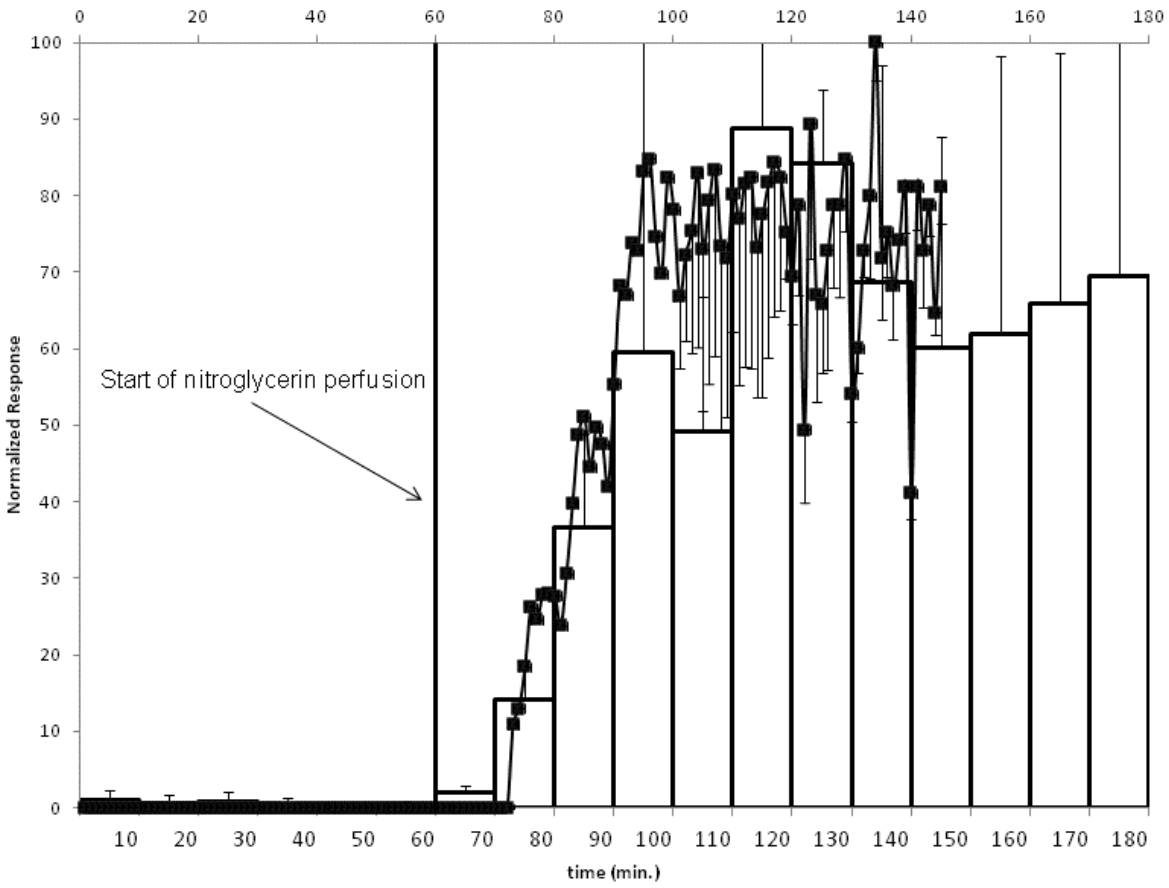

Figure 4.8: Time course graph of nitrite normalized response as a function of following nitroglycerin (5mg/mL) infusion through the microdialysis probe subcutaneously implanted in sheep. Normalization was accomplished by dividing each response by the maximum response in that experiment and multiplying the value to 100 to obtain a percentage. The lined scatter plot trace is response based upon the LOS collection, separation, and amperometric detection method, and is shifted to take in account lag time. The transparent bar graph is response using the developed LC-EC detection method.

an average of approximately 17 μM, taking recovery into account. The LOS has not yet been validated as a quantitative tool. However, the developed LC-EC method had been validated, and was used to quantitate the nitrite concentrations present in spiked basal dialysate in at the end of chapter 2 of this thesis. **Figure 4.8** shows the normalized responses for both methods, relative to the amount of nitrite present with respect to time during these experiments. Responses were normalized by dividing the response at each time point by the maximum response in the experiment. These values were then multiplied by 100 to convert to a percentage. An increase in nitrite levels within the first vial collection from the start of nitroglycerin perfusion was expected, as the environment of nitroglycerin action adjacent to the probe was monitored. A significant lag time of 50 minutes prior to an increase in response was observed with the 'LOS'-Pinnacle Board method, or the scatter-line plot. This lag time was calculated using the distance between the microdialysis probe and the "LOS"-Pinnacle system as well as the dimensions of tubing required. **Figure 4.9** shows the schematic of this system [5]. A lag time of 5 minutes prior to an increase in response was observed with the developed LC-EC system. This lag time was calculated using the distance between the microdialysis probe and the collection vial as well as the dimensions of tubing required. A comparison was made of the normalized response of the 'LOS'-Pinnacle system versus the normalized response of the developed LC-EC system for these experiments. When plotted, these values should be arranged in a linear fashion, and ideally, fitted with a line with R^2 coefficient of close to 1.

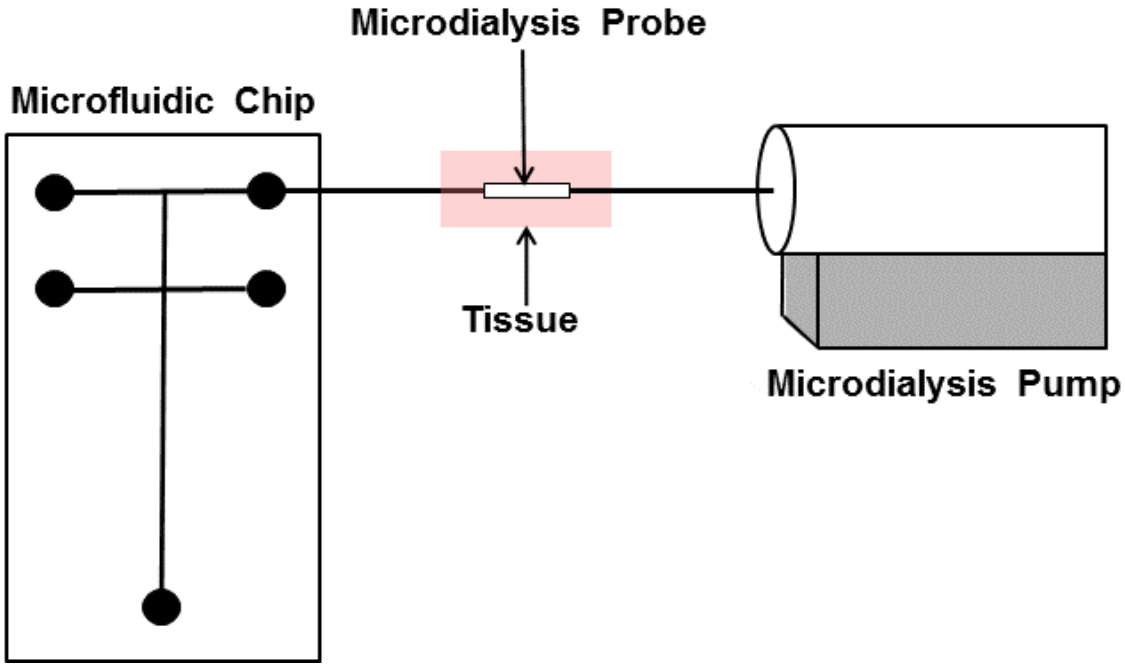

Figure 4.9: Schematic of the 'LOS'-Pinnacle Board system. Image reproduced with permission of DE Scott.

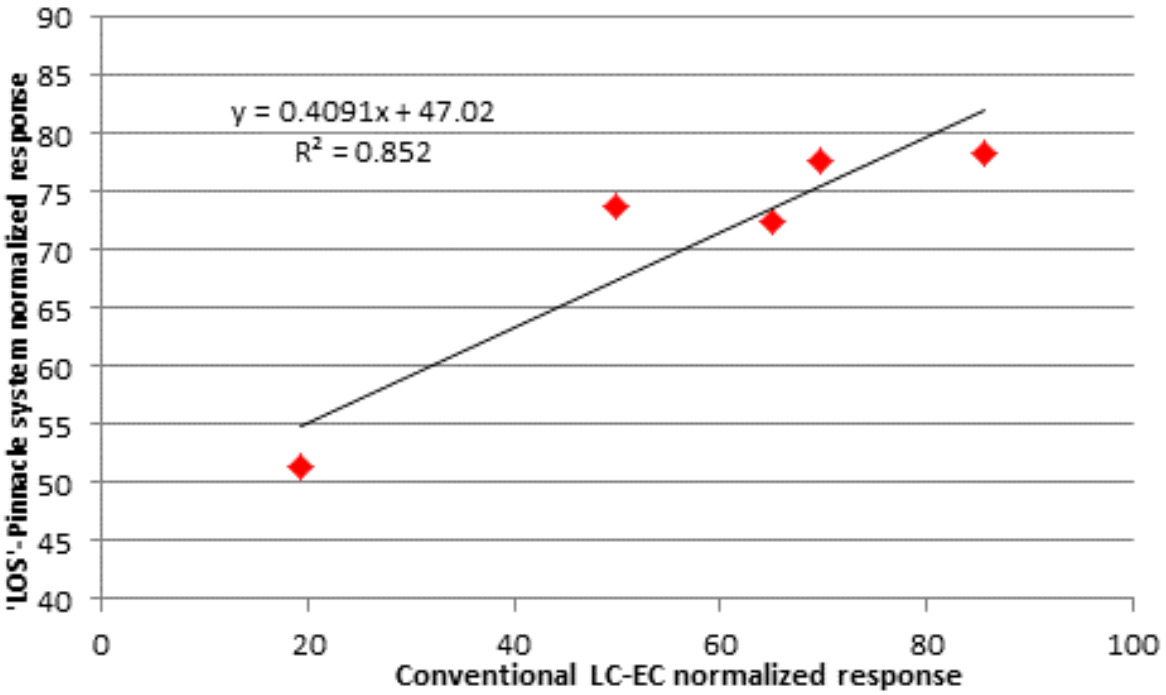

Figure 4.10: Comparison of normalized 'LOS'-Pinnacle Board and conventional LC-EC systems. The points plotted show linearity; however, the R^2 coefficient of 0.852 is far below that of a desired value of 1. Furthermore, the slope should be close to 1, ideally.

The plotted data points were linear but somewhat scattered with an R^2 coefficient of 0.852, as shown in **Figure 4.10**. Furthermore, the slope of this line was 0.409 and ideally should be close to 1. When the response of each system is normalized, if the response of one system doubles so too should that of the other. The LC-EC method developed was evaluated for linearity, and was determined to have an R^2 coefficient of 0.999. As a result of this validation, it is unlikely that the LC-EC system is problematic when evaluating nitrite within its linear range. The 'LOS-Pinnacle Board system has been able to qualitatively measure an increase in response as a result of elevated nitrite levels, however it has not been validated. The advantage of using the validated LC-EC method is that it is capable of quantitation.

4.7.3 Analysis of topical nitroglycerin cream subcutaneous dialysate

As an alternative method for the detection of nitric oxide products, nitroglycerin cream was evaluated. After a basal collection period of 60 minutes, nitroglycerin cream was applied to the epidermis over the area where the microdialysis probe was implanted subcutaneously. Two experiments involving the application of nitroglycerin cream occurred: the first was a circular application with a diameter of 1.27 cm; the second was a circular application of a 2.54 cm diameter. No substantial increase in nitrite levels was apparent throughout these experiments. It is believed that the epidermal application was too removed from

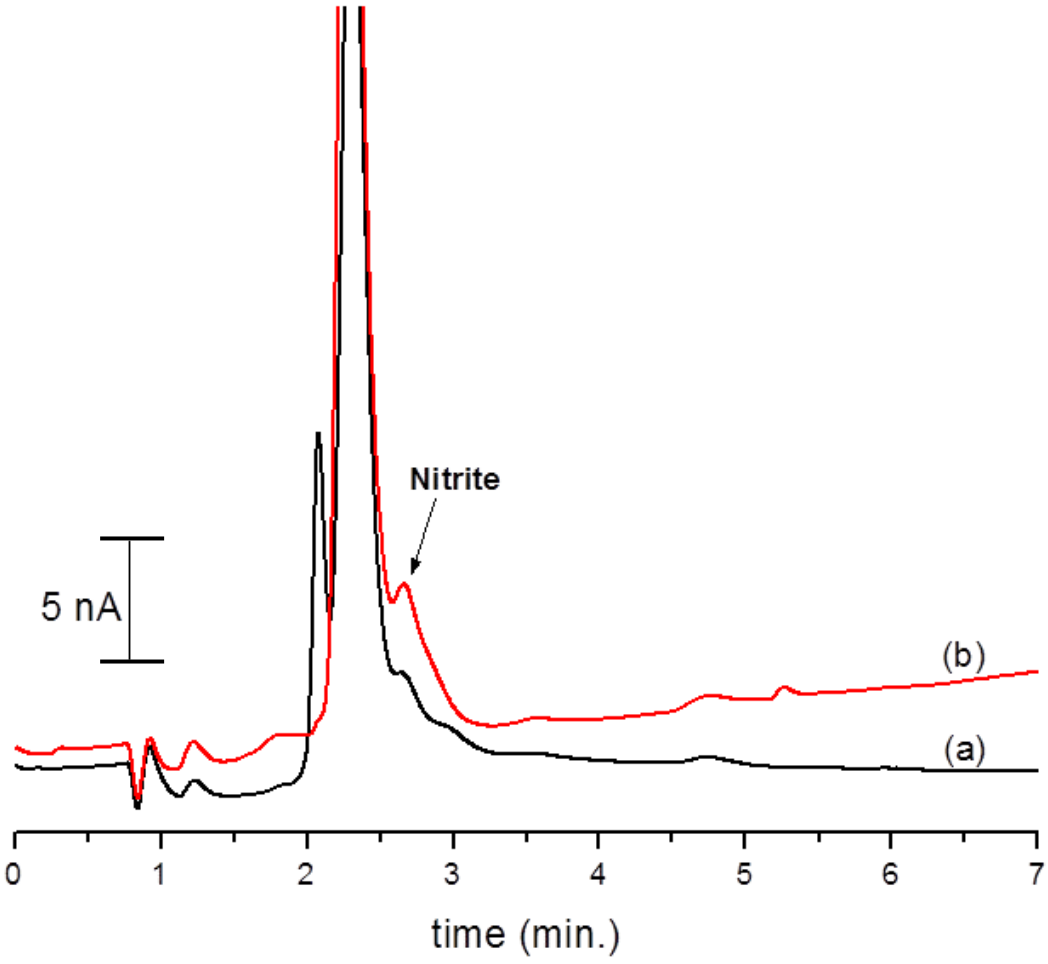

Figure 4.11: Overlay of chromatograms from the 0 time point of basal collection and 100 minutes after application of nitroglycerin cream (2%w/w). Nitrite increase is minimal as was expected. Trace (a) is under basal conditions and trace (b) is after nitroglycerin cream application. Mobile phase and detection conditions are the same as the previous chromatograms in this chapter.

the microdialysis probe implantation site and any nitric oxide and nitrite generated is too far away to diffuse into the microdialysis probe for collection. The epidermis is known for its vascularity; it could be possible that nitroglycerin is absorbed into the epidermis at the application site and is distributed into the vasculature in the epidermal tissue surrounding. Studies conducted with microdialysis probes implanted just below the surface of the skin with administration of nitroglycerin in a patch (Transderm Nitro Patches, Ciba) show an increase in nitrite production by a factor of 10 [9]. Figure **4.11** shows a comparison of a chromatogram under basal conditions with that after nitroglycerin cream application.

4.7.4 Analysis of NO in subcutaneous dialysate, produced by epidermal histamine injection

After a basal collection period of 60 minutes, 0.5 mL of a 0.1 mg/mL concentration of histamine was injected into the epidermis in the area over where the site of microdialysis probe implantation. No substantial increase in nitrite concentration was apparent from this injection throughout the experiment. It is again believed that the epidermal injection was too far away from the microdialysis probe implantation site, such that any nitric oxide and nitrite generated cannot diffuse into the microdialysis probe for collection. Studies conducted with microdialysis probes implanted just below the surface of the skin with administration of 15μL of histamine at a concentration of 1μM showed an increase in nitrite production by a factor of 3 [9]. **Figure 4.12** shows an overlay of

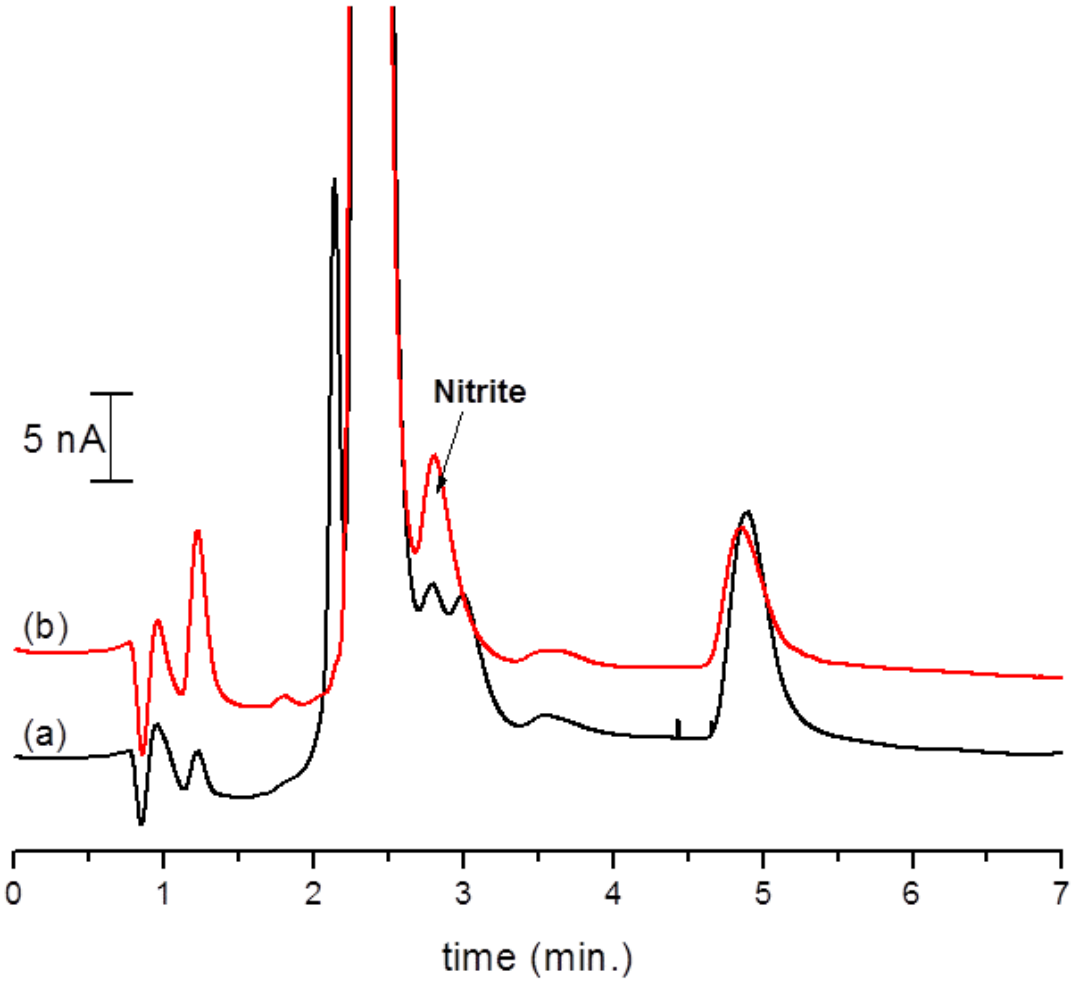

Figure 4.12: Overlay of chromatograms from the 0 time point of basal collection and 100 minutes after a 0.5 mL injection of histamine (0.1 mg/mL). Nitrite increase is minimal as was expected. Trace (a) is under basal conditions and trace (b) is after histamine injection. Mobile phase and detection conditions are the same as the in the previous figure.

chromatograms from two time points of the histamine injection experiment in sheep. From the graphs, a slight increase is noticed; however, it seems likely that the proximity of the probe to the injection site has an influence on nitrite production, as the concentration (0.1 mg/mL or 0.9 mM) and volume (0.5 mL) injected were significantly higher in comparison to those injected in the Clough study [9].

4.8 Summary

In the previous chapters, an LCLC-EC-UV/Vis system was developed to evaluate changes in nitrite and nitrate in dialysate from multiple locations in multiple animals. Chromatographic conditions were optimized for separation of nitrite and nitrate from many other compounds present in dialysate. In addition, detection parameters were optimized for EC and UV/Vis detection systems to obtain detection limits for nitrite and nitrate as low as possible and to reduce the likelihood of interferents. *In vitro* studies were conducted to evaluate the recovery of nitrite and nitrate from a microdialysis probe used in rat brain experiments. In addition, *in vitro* production of nitrite from the nitric oxide donor DEA NONOate was monitored as a proof of concept that the chromatographic and detection systems are capable of separating and identifying nitrite in a best case scenario in preparation for animal studies.

Experiments were conducted to determine whether or not damage occurring in the brain of the rat as a result of 3-MPA administration was influenced

by RNS formation and activity. It was determined that 3-MPA does not significantly increase nitric oxide production, and therefore, does not result in RNS generation. In addition, studies of nitric oxide production in sheep subcutaneous skin layers were conducted. First, *in vitro* nitroglycerin delivery studies were conducted to determine the % delivery to the probe sampling site. Then, in a proof of concept scenario, the formation of nitrite from nitric oxide production as a result of nitroglycerin perfusion at the microdialysis probe sampling site was investigated. Nitrite concentrations increased substantially from that present under basal conditions. This finding sheds light on the role of production of NO from nitroglycerin and its role in vasodilatation. Furthermore, comparison of levels of nitric oxide production detected and quantified by this method to that determined by the S. Lunte group method showed that these methods are complementary to one another. However, it is clear that further development of the 'Lab on a Sheep'-Pinnacle system is necessary for its application as a tool for nitrite quantitation.

Studies of nitrite formation as a result of epidermal application of nitroglycerin cream showed that a difference in distance of probe location from the application site minimized the collection of nitrite at the probe sampling site. Histamine injection studies had a similar outcome. Injection of histamine in the epidermal region allowed for minimal transfer to the probe implantation site in the subcutaneous region, minimizing the generation of nitric oxide and the formation of nitrite in the probe sampling area.

4.9 Future directions

Further animal studies need to be conducted. Further *in vitro* calibration studies are needed to validate the 'LOS'-Pinnacle Board system. Analysis of split *in vitro* microdialysis samples will allow for a better comparison between this system and the LC-EC method developed in this thesis. Further collaboration with the S. Lunte research group to examine the generation of NO in rats from nitroglycerin infusion are planned. The developed LC-EC method will be used to validate the 'LOS'-Pinnacle Board system. Implementation of these methods in studying nitroglycerin-based NO generation in rats will serve to validate their broad applicability.

As an independent project of the C. Lunte research group, it is desired to administer NO donors and NOS upregulators into the hippocampus brain regions of rats to study its influence on the production of RNS and to further evaluate the legitimacy of the rat as a model of oxidative stress in the brain. In addition, examination of RNS production in rats as a result of chemotherapeutics administration will commence. Increases in RNS as a result of chemotherapeutics administration will add additional support to GABA/glutamate studies in these models.

4.10 References

[1] Murad, F, Mittal, CK (1977). "Nitric oxide activates guanylate cyclase and increases guanosine 3':5'-cyclic monophosphate levels in various tissue preparation". *Proc. Natl. Acad. Sci. USA* **74** (8): 3203-3207.

[2] Hink, U, Alhamdani, MS (2008). "Nitroglycerin Hits the Nerve: Role for Mitochondrial Aldehyde Dehydrogenase"? *J Am. Coll. Cardiology.* **52** (11): 961-963.

[3] Chen, Z, Foster, MW (2005). "An essential role for mitochondrial aldehyde dehydrogenase in nitroglycerin bioactivation". *Proc. Natl. Acad. Sci.* USA **102**: 12159-12164.

[4] Lantoine, F, Iouzalen, L (1998). "Nitric oxide production in human endothelial cells stimulated by histamine requires Ca^{2+} influx". *Biochem. J.* **330**: 695-699.

[5] Kendrick, KM, De La Riva, C (1989). "Microdialysis measurement of monoamine and amino acid release from the medial preoptic region of the sheepin response to heat exposure". *Brain Res. Bulletin*. **22** (3): 541-544.

[6] Lunte, SM, Nandi, P (2010). "The Development of a Miniaturized Wireless Microdialysis-Microchip Electrophoresis System for In Vivo Monitoring of Drugs and Neurotransmitters in Awake and Freely Moving Sheep". *14th Intl. Conf on Miniaturized Sys. For Chem and Life Sci.* Groningen, Netherlands. 1535-1537.

[7] Ahmad, UK, Harun, SN (2011). "Forensic analysis of Nitroglycerin in Post Blast Samples. *Proc. Of 3rd Intl. Conference and Workshops on Basic and Applied Sciences.* Acacdemia.edu.

[8] Snyder, LR, Dolan, JW (2007). "A New Look at the Selectivity of Reversed-phase HPLC Columns". *Anal. Chem.* **79**: 3252-3262.

[9] Clough, GF, Bennett, AR (1998). "Measurement of Nitric Oxide Concentration in Human Skin In Vivo Using Dermal Microdialysis". *Exp. Phys.* **83**: 431-434.